# INVOLVEMENT OF TISSUE TRANSGLUTAMINASE (TG2) ISOFORMS IN THE DEVELOPMENT OF RENAL CELL CARCINOMA

by
Ayça Ece Nezir

Submitted to Graduate School of Natural and Applied Sciences
in Partial Fulfillment of the Requirements
for the Degree of Doctor of Philosophy in
Biotechnology

Yeditepe University
2023

INVOLVEMENT OF TISSUE TRANSGLUTAMINASE (TG2) ISOFORMS IN THE DEVELOPMENT OF RENAL CELL CARCINOMA

APPROVED BY:

Prof. Dr. Dilek Telci Temeltaş ……
(Thesis Supervisor)
(Yeditepe University)

Prof. Dr. Ömer Faruk Bayrak ……
(Yeditepe University)

Assoc. Prof. Dr. Ayşegül Doğan ……
(Yeditepe University)

Prof. Dr. Elif Damla Arısan ……
(Gebze Technical University)

Assoc. Prof. Dr. Gözde Korkmaz ……
(Koç University)

DATE OF APPROVAL: ..../..../20..

I hereby declare that this thesis is my own work and that all information in this thesis has been obtained and presented in accordance with academic rules and ethical conduct. I have fully cited and referenced all material and results as required by these rules and conduct, and this thesis study does not contain any plagiarism. If any material used in the thesis requires copyright, the necessary permissions have been obtained. No material from this thesis has been used for the award of another degree.

I accept all kinds of legal liability that may arise in case contrary to these situations.

Ayça Ece Nezir

Signature ……..



*To my family…*

# ACKNOWLEDGEMENTS

I am deeply indebted to my supervisor Prof. Dr. Dilek Telci Temeltaş, the most dependable and supportive person I met during my academic journey. I could hardly imagine that the first moment of our interaction—me reading Salinger and her showing an interest in my book—would become a milestone in my personal history. I have evolved into my best self in the last ten years, owing to her contributions to every aspect of my life. In this final hour of our collaboration, I must state that my opinion of us being the best and most efficient team will remain forever and always: let it be a project or bowling! My dear professor; for the last time, let us raise and point our wands to all darkness in the world and shout: LUMOS!

I am grateful to my co-advisor Prof. Dr. Asıf Yıldırım and the committee members Prof. Dr. Ömer Faruk Bayrak, Assoc. Prof. Dr. Ayşegül Doğan, Prof. Dr. Elif Damla Arısan, and Assist. Prof. Dr. Gözde Korkmaz for all their contributions in guiding my work. I also thank Ayla Burçin Asutay for her technical support in endless flow cytometry experiments.

I must extend my sincere gratitude to all the members and alumni of DT Lab. Foremost, I would like to thank İpek Bedir, an amazing partner with the most beautiful laugh, who constantly fails to deny support for anyone around her. I am still astonished that each time I felt like falling, I found myself leaning on her: Thank you for being the truest friend. I also thank Selen Tiryaki for her constant support, especially for not letting me starve! Special thanks to Hande Nayman for letting me take a journey into her incredible mind. Thanks to Zeynep Büşra Bolat and Enzim Substrat for their sincerity under any circumstances. Many thanks to Kaan Öztürk for always holding my hands from far lands.

I cannot begin to express my appreciation to Elif Everest, my intelligent, devoted, truthful, *fierce* friend. About two-thirds of my life, the most significant part, has been blessed by her presence, and this will never come to an end. Cheers to the purest of blood!

I must convey my endless love to my parents, Nihal and Semih Nezir, to whom I owe everything. Not to mention my not-so-little brother Uğur Nezir, the wittiest person on earth and the best human being a sister can wish to have in their life. You are my treasure.

This study was supported by the Scientific and Technological Research Council of Turkey (TUBITAK) with grant numbers 219Z216 and 222S296.

# ABSTRACT


## INVOLVEMENT OF TISSUE TRANSGLUTAMINASE (TG2) ISOFORMS IN THE DEVELOPMENT OF RENAL CELL CARCINOMA

Transglutaminase 2 (TG2) is a multifunctional protein that is ubiquitously expressed in all tissues. TG2-related events in the context of tumorigenesis placed TG2 in the center of cancer cell research, where it was recognized as an important mediator in cancer development and progression. Later studies showing the involvement of TG2 in cancer progression, drug resistance, epithelial-mesenchymal transition (EMT), metastasis, and the acquisition of cancer stem cell properties showed that these effects were tightly associated with the GTPase activity of TG2. Our group previously demonstrated the relationship of TG2 with RCC, whereby the increase in TG2 levels was associated with low survival time and a high risk of metastasis. Following studies have shown that increased TG2 expression tightly correlates with high nuclear grade and poor prognosis in patients with RCC. Thus, the TG2 protein is implicated in the progression of RCC and stands out as an important molecular target in cancer therapy. The TG2 protein has four isoforms hitherto identified. These C-terminally truncated isoforms produced by alternative splicing events have reduced GTP binding affinity and transamidase activity and display a high GTPase activity compared with the full-length TG2. A gene expression study examining intact kidney and tumor tissues revealed the presence of different TG2 transcripts in RCC. In light of this initial finding, the present thesis first focused on showing the upregulation of TG2 isoforms in a larger RCC patient population. Next, to understand the molecular basis of TG2 isoform-mediated cellular transformation, the effects of the expression of each TG2 isoform on the cellular transformation were investigated in renal proximal tubule epithelial cell (RPTEC) models. In this regard, we demonstrated that inducing the expressions of TG2 or its isoforms increased the proliferation rate, promoted cell cycle progression, contributed to the activation of EMT, and caused an increased invasion potential in RPTECs. Our findings demonstrate the importance of TG2 isoforms in cellular transformation in RCC and elucidate the importance of targeting TG2 and its isoforms in clinical practice.

# ÖZET


## DOKU TRANSGLUTAMİNAZ (TG2) İZOFORMLARININ BÖBREK HÜCRELİ KARSİNOM OLUŞUMU İLE İLİŞKİSİ

Transglutaminaz 2 (TG2) proteini çok fonksiyonlu bir enzim olarak tüm hücrelerde ifade edilir. TG2'nin epitelyal-mezenkimal geçiş (EMG), metastaz ve kanser kök hücre özelliği kazanımı gibi patolojik süreçler üzerindeki etkileri bu proteini kanser tedavisinde önemli bir hedef haline getirmiş olup söz konusu etkiler TG2'nin GTPaz aktivitesi ile ilişkilendirilmiştir. Literatürde ilk defa grubumuz tarafından yapılan çalışmalar TG2'nin RCC metastaz riski ve düşük hasta sağ kalımı ile ilişkisini ortaya koymuştur. Daha sonra yapılan çalışmalar verilerimizi doğrulamış ve TG2 proteinini RCC hastalığının ilerlemesi ile yakından ilişkilendirerek kanser tedavisinde önemli bir hedef molekül olarak öne çıkarmıştır. TG2 proteininin tanımlanmış protein kodlayan dört izoformu bulunmaktadır. Hücrelerde alternatif mRNA uç birleştirme sonucunda üretilen bu izoformlar tam uzunluktaki TG2 proteinine kıyasla düşük GTP ilginliği ve düşük transamidaz aktivitesi göstermekte olup yüksek GTPaz aktivitesine sahiptir. Son yıllarda normal böbrek ve RCC tümör dokularıyla yapılan bir gen ifade analizinde RCC olgularında ifade edilen farklı TG2 transkriptlerinin varlığı ortaya konmuştur. Bu çalışmadan hareketle mevcut tez kapsamında öncelikle daha büyük bir hasta popülasyonu incelenerek TG2 ve izoformlarının RCC hastalarında artış gösterdiği grubumuz tarafınca doğrulanmıştır. Daha sonra TG2 izoform ifadesine bağlı hücre transformasyonunun moleküler mekanizmalarını anlamak amacıyla her bir TG2 izoformunun renal proksimal tübül epitel hücre (RPTEC) modelinde ifade edilmesinin bu hücrelerdeki kanser transformasyonu üzerine etkisi incenmiştir. Bu bağlamda TG2 izoform ifadesi indüklenen RPTEC'lerin çoğalma/büyüme hızlarının arttığı, hücre döngüsünde ilerledikleri, EMG sürecinin aktive olduğu ve hücrelerin invaziv potansiyelinin arttığı gösterilmiştir. Elde edilen bulgularımız RCC gelişiminde hücre transformasyon ayağında TG2 izoformlarının önemini göstermekte ve böbrek kanseri tedavisinde TG2 ile izoformlarının hedeflenmesinin önemine işaret etmektedir.

# TABLE OF CONTENTS

ACKNOWLEDGEMENTS ..... v

ABSTRACT ..... vi

ÖZET ..... vii

LIST OF FIGURES ..... xi

LIST OF TABLES ..... xiv

LIST OF SYMBOLS/ABBREVIATIONS ..... xvi

1. INTRODUCTION ..... 1

1.1. TRANSGLUTAMINASE ENZYME FAMILY ..... 1

1.1.1. TG Mechanism of Action ..... 2

1.1.2. TGs in Physiology and Pathology ..... 4

1.2. TG2 STRUCTURE AND FUNCTION ..... 6

1.2.1. TG2 in a Nutshell ..... 6

1.2.2. Enzymatic and Non-Enzymatic Activities of TG2 ..... 7

1.2.3. Regulation of TG2 Activity ..... 9

1.2.4. Subcellular Localization of TG2 ..... 12

1.3. TG2 IN CANCER ..... 14

1.3.1. TG2 and Inflammation ..... 15

1.3.2. TG2, Epithelial-Mesenchymal Transition, and Invasion ..... 16

1.3.3. TG2 and Modulation of the Tumor Microenvironment ..... 18

1.4. ALTERNATIVELY SPLICED VARIANTS OF TG2 ..... 20

1.5. RENAL CELL CARCINOMA ..... 24

1.5.1. An Overview of RCC ..... 24

1.5.2. TG2 in the Propagation of RCC ..... 25

1.5.3. Grading Renal Cell Carcinoma ..... 27

2. AIM OF THE STUDY ..... 30

3. MATERIALS AND METHODS ..... 31

1.6. AMPLIFICATION AND CHARACTERIZATION OF PLASMID VECTORS ..... 31

1.6.1. Design of the Lentiviral Plasmid Vectors Coding for TG2 Isoforms ..... 31

1.6.2. Amplification of the Lentiviral Plasmid Vectors....36
1.6.3. Isolation of the Lentiviral Plasmid Vectors....36
1.6.4. Storage of the Transformant Bacteria....37
1.6.5. Confirmation of the Gene Sequences....38
1.7. CELL LINES AND HANDLING....39
1.8. ESTABLISHING RENAL EPITHELIAL CELLS EXPRESSING TG2 ISOFORMS....40
1.8.1. Lentiviral Particle Production in 293-FT cells....40
1.8.2. Transduction of RPTECs with the Lentiviral Particles....42
1.8.2.1. Optimization of Pre-Treatment and Gene Expression Parameters....42
1.8.2.2. Transduction of RPTECs with TG2 Isoforms....43
1.9. CHARACTERIZATION OF THE TRANSDUCED CELLS....43
1.9.1. Analysis of TG2 Isoform mRNA Expression Profiles....43
1.9.1.1. Optimization of the Melting Temperatures for TG2 Isoform Primers....43
1.9.1.1.1 Total RNA Isolation....44
1.9.1.1.2 cDNA Synthesis....44
1.9.1.1.3 Gradient PCR....45
1.9.1.2. Real-Time Quantitative PCR Analysis for TG2 Isoforms....45
1.9.2. Detection of TG2 Isoforms on RPTEC Membranes....46
1.10. ANALYSIS OF THE EFFECTS OF TG2 ISOFORMS ON CELLULAR PROCESSES....46
1.10.1. Analysis of Cell Proliferation....46
1.10.2. Analysis of the Cell Cycle....47
1.10.2.1. Cell Cycle Analysis with Cytell....47
1.10.2.2. Flow Cytometry Analysis of Cell Cycle....47
1.10.2.3. Western Blotting for Cell Cycle Proteins....47
1.10.2.3.1 Protein Isolation....47
1.10.2.3.2 Protein Content Assay....48
1.10.2.3.3 SDS-PAGE and Western Blotting....48
1.10.3. Analysis of the EMT and MMP Profiles....50
1.10.3.1. Analysis of EMT....50
1.10.3.2. Analysis of the MMP Profile....50
1.10.3.3. Analysis of Cell Mobility....51
1.11. ANALYSIS OF TG2 ISOFORM EXPRESSION IN PATIENTS WITH RCC....51

1.11.1. Bioinformatic Analysis of a Reported RCC Dataset....51
1.11.2. qPCR Analysis of TG2 Isoform Levels in Patients with RCC....51
1.12. STATISTICAL ANALYSIS....52
4. RESULTS....53
1.13. TG2 ISOFORM LEVELS IN PATIENTS WITH RCC....53
1.13.1. Altered Expression Profiles of TG2 Isoforms in ccRCC....53
1.13.2. Association of TG2 Isoforms with RCC Grade and Stage....54
1.14. CHARACTERIZATION OF LENTIVIRAL PLASMID VECTORS....57
1.15. TRANSFECTION EFFICIENCY....60
1.16. CHARACTERIZATION OF TRANSDUCED RENAL CELLS....61
1.16.1. Optimal RPTEC Transduction and Induction Conditions....61
1.16.2. Induced Gene Expression in RPTECs....65
1.16.3. Cell Surface Localization of TG2 Isoforms in RPTECs....68
1.17. EFFECTS of TG2 ISOFORMS ON CELLULAR PROCESSES....70
1.17.1. Growth Profiles of Transduced RPTECs....70
1.17.2. Cell Cycle Progression of Transduced RPTECs....72
1.17.3. EMT and MMP Profiles of Transduced RPTECs....77
1.17.4. Migration Potential of Transduced RPTECs....82
5. DISCUSSION....85
6. CONCLUSIONS AND FUTURE WORK....95
APPENDIX A....126

# LIST OF FIGURES

Figure 1.1. Transamidation and deamidation activities of TGs ..... 1

Figure 1.2. Amino acid sequences at the active site regions of TGs ..... 2

Figure 1.3. Two main steps of TGase reactions ..... 3

Figure 1.4. The functional domains of TG2 ..... 7

Figure 1.5. Diverse actions of TG2 ..... 8

Figure 1.6. Conformations of TG2 ..... 10

Figure 1.7. Reversible redox regulation of TG2 ..... 11

Figure 1.8. Functions of TG2 depending on its cellular distribution ..... 13

Figure 1.9. Mechanisms involved in the oncogenic functions of TG2 ..... 14

Figure 1.10. The relationship between TG2 and inflammation in normal and transformed cells ..... 16

Figure 1.11. The relationship between TG2 and EMT ..... 18

Figure 1.12. Regulation of HIF-1α-mediated responses to cellular oxygen levels ..... 19

Figure 1.13. Transglutaminase 2 isoforms ..... 21

Figure 1.14. Pathways associated with TG2 in RCC ..... 26

Figure 1.15. RCC survival rates based on TNM stages ..... 29

Figure 3.1. hTGM2 plasmid map ..... 32

Figure 3.2. TGH plasmid map ..... 32

Figure 3.3. TGH2 plasmid map ..... 33

Figure 3.4. tTGv1 plasmid map ..... 33

Figure 3.5. tTGv2 plasmid map ..... 34

Figure 3.6. EGFP plasmid map ..... 34

Figure 3.7. Mock plasmid map ..... 35

Figure 3.8. psPAX2 packaging plasmid map ..... 41

Figure 3.9. pMD2.G envelope plasmid map ..... 42

Figure 4.1. TG2 isoform expression levels in patients with ccRCC ..... 54

Figure 4.2. Differences in TG2 isoform mRNA expression levels between low (G1 and G2) and high Fuhrman grades (G3 and G4) ..... 56

Figure 4.3. Differences in TG2 mRNA expression levels between low (pT1-2) and high T grades (pT3) ..... 57

Figure 4.4. Bacterial colonies on LB agar plates ..... 58

Figure 4.6. tTGv1 regions (2696 bp) amplified from the vector by gradient PCR ..... 59

Figure 4.7. TG2 (2735 bp), TGH (2318 bp), TGH2 (1721 bp), tTGv1 (2696 bp), tTGv2 (2609 bp), EGFP (1391 bp), and stuffer DNA (Mock; 977 bp) regions amplified from the vectors by gradient PCR ..... 59

Figure 4.8. 293-FT cells transfected with the EGFP reporter plasmid ..... 61

Figure 4.9. Optimization of optimal transduction and gene expression conditions for RPTECs (24 hours) ..... 63

Figure 4.10. Optimization of optimal transduction and gene expression conditions for RPTECs (48 hours). ..... 63

Figure 4.11. Optimization of optimal transduction and gene expression conditions for RPTECs (72 hours) ..... 64

Figure 4.12. Optimization of optimal transduction and gene expression conditions for RPTECs (96 hours) ..... 64

Figure 4.13. (a) TG2, (b) TGH, (c) TGH2, (d) tTGv1, and (e) tTGv2 regions amplified from Dox-induced RPTEC cDNA by gradient PCR ..... 66

Figure 4.14. Isoform expression levels in transduced RPTECs ..... 67

Figure 4.15. Time-dependent isoform expression levels in transduced RPTECs ..... 68

Figure 4.16. TG2 isoform levels on RPTEC surface determined by flow cytometry ..... 69

Figure 4.17. Time-dependent growth of transduced RPTECs ..... 70

Figure 4.18. Time-dependent growth of transduced RPTECs during the 96 hours post-induction ..... 72

Figure 4.19. Cell cycle progression of transduced RPTECs at 96 hours upon Dox induction ..... 73

Figure 4.20. Cell cycle progression of transduced RPTECs at 96 hours upon Dox induction ..... 75

Figure 4.21. Protein levels of cyclins and CDKs in induced RPTECs determined by western blotting ..... 77

Figure 4.22. EMT marker levels in transduced RPTECs at 72 hours following Dox induction. ..... 79

Figure 4.23. EMT marker levels in transduced RPTECs at 96 hours following Dox induction. ..... 80

Figure 4.24. MMP levels in transduced RPTECs at (a) 72 and (b) 96 hours following Dox induction ..... 82

Figure 4.25. Wound healing capacities of transduced RPTECs ..... 83

Figure 4.26. Monitoring of the wound healing capacities of transduced RPTECs ..... 84

# LIST OF TABLES

Table 1.1. The Fuhrman grading system ..... 27

Table 1.2. The WHO/ISUP grading system ..... 28

Table 1.3. TNM staging for RCC ..... 28

Table 3.1. GoI residues and lengths on Tet-On lentiviral plasmid vectors ..... 36

Table 3.2. Components of 10X TAE buffer. ..... 37

Table 3.3. Primers used for the sequencing of GoI regions on lentiviral plasmid vectors .. 38

Table 3.4. Components of the AQ90 High Fidelity DNA Polymerase reaction mixture .... 38

Table 3.5. PCR program for AQ90 High Fidelity DNA Polymerase. ..... 39

Table 3.6. Expected PCR product sizes for each plasmid vector. ..... 39

Table 3.7. Components of the renal epithelial cell growth kit. ..... 40

Table 3.8. Transfection buffer components. ..... 41

Table 3.9. Forward and reverse primers specific for TG2 transcriptional variants. ..... 43

Table 3.10. Components of the Sensiscript reverse transcription kit reaction mixture. ..... 44

Table 3.11. QuantiTect SYBR Green PCR Kit reaction mixture. ..... 45

Table 3.12. Thermal cycle protocol for QuantiTect SYBR Green PCR Kit. ..... 45

Table 3.13. SDS-PA gel buffers. ..... 48

Table 3.14. SDS-PA gel compositions. ..... 49

Table 3.15. Running and transfer buffer recipes. ..... 49

Table 3.16. Preparation of 10X TBS (pH 7.6). ..... 50

Table 4.1. Demographic and clinical characteristics of the patients. ..... 55

Table 4.2. BLAST analysis results of the TG2 isoform sequences. ..... 60

Table 4.3. Experimental groups designed for the determination of optimal transduction conditions for RPTECs. ..... 62

Table 4.4. Calculated doubling time of TG2 isoform-transduced RPTECs. ..... 71

Table 4.5. Cell cycle profiles of transduced RPTECs based on Cytell imaging results. ..... 74

# LIST OF SYMBOLS/ABBREVIATIONS

| | |
|---|---|
| °C | Degree Celsius |
| kDa | Kilodalton |
| kHz | Kilohertz |
| mA | Milliampere |
| ml | Milliliter |
| mM | Millimolar |
| nm | Nanometer |
| V | Volt |
| v/v | Volume per volume |
| w/v | Weight per volume |
| xg | Times gravity |
| | |
| Amp | Ampicillin |
| APS | Ammonium persulfate |
| Asp | Aspartic acid |
| ATP | Adenosine triphosphate |
| BLAST | Basic Local Alignment Search Tool |
| BSA | Bovine serum albumin |
| Bsd | Blasticidin |
| Cys | Cysteine |
| DNA | Deoxyribonucleic acid |
| Dox | Doxycycline |
| ECM | Extracellular matrix |
| EF1A | Eukaryotic translation elongation factor 1-alpha |
| EGF | Epidermal growth factor |
| EMT | Epithelial-mesenchymal transition |
| ER | Endoplasmic reticulum |
| ERK | Extracellular signal-regulated kinase |
| ERp57 | Endoplasmic reticulum-resident protein 57 |
| EV | Extracellular vesicle |
| FAK | Focal adhesion kinase |

| | |
|---|---|
| FITC | Fluorescein |
| FN | Fibronectin |
| FXIIIa | Factor XIII-A |
| GDP | Guanosine diphosphate |
| GE | Gel electrophoresis |
| GoI | Gene of interest |
| GPCR | G protein-coupled receptor |
| GTP | Guanosine triphosphate |
| HIF | Hypoxia-inducible factor |
| His | Histidine |
| IKK | I kappa B kinase |
| IL | Interleukin |
| ISUP | International Society of Urological Pathology |
| ITG | Integrin |
| LB | Luria-Bertani |
| lncRNA | Long non-coding RNA |
| MMP | Matrix metalloprotease |
| mRNA | Messenger RNA |
| miRNA | Micro RNA |
| mTOR | Mechanistic target of rapamycin |
| NCBI | National Center for Biotechnology Information |
| NES | Nuclear export signal |
| NF-κB | Nuclear factor-kappa B |
| ORF | Open reading frame |
| PA | Polyacrylamide |
| PBS | Phosphate-buffered saline |
| PCR | Polymerase chain reaction |
| PDI | Protein disulfide isomerase |
| PDGFR | Platelet derived growth factor receptor |
| PI | Propidium iodide |
| PI3K | Phosphatidylinositol 3-kinase |
| PLA2 | Phospholipase A2 |
| PLCδ | Phospholipase C gamma |

| | |
|---|---|
| PS | Protamine sulfate |
| PTEN | Phosphatase and tensin homolog |
| qPCR | Quantitative PCR |
| RA | Retinoic acid |
| Rb | Retinoblastoma protein |
| RCC | Renal cell carcinoma |
| RhoA | Ras homolog family member A |
| RNA | Ribonucleic acid |
| RPTEC | Renal proximal tubule epithelial cell |
| SDC4 | Syndecan-4 |
| SDS | Sodium dodecyl sulfate |
| TEMED | Tetramethyl ethylenediamine |
| TG | Transglutaminase |
| TG2 | Tissue transglutaminase |
| TGase | Transamidase |
| TGF-β | Transforming growth factor-beta |
| TGH | Transglutaminase homolog |
| TGH2 | Transglutaminase homolog 2 |
| Tm | Melting temperature |
| TME | Tumor microenvironment |
| TNF-α | Tumor necrosis factor-alpha |
| TNM | Tumor-lymph node-metastasis |
| TRE | Tetracycline-responsive element |
| TRX | Thioredoxin-1 |
| tTGv1 | Tissue transglutaminase variant 1 |
| tTGv2 | Tissue transglutaminase variant 2 |
| VEGF | Vascular endothelial growth factor |
| VEGFR | VEGF receptor |
| VHL | Von Hippel-Lindau |
| WHO | World Health Organization |
| YAP | Yes-associated protein 1 |

# 1. INTRODUCTION

## 1.1. TRANSGLUTAMINASE ENZYME FAMILY

Transglutaminases (TGs), also known as protein-glutamine γ-glutamyltransferases (EC 2.3.2.13), constitute a suprafamily of calcium-dependent, structurally and functionally related enzymes. TGs are commonly recognized for catalyzing the formation of an isopeptide bond, leading to the crosslinking of a free amine group (acyl acceptor) and the γ-carboxamide group of a protein- or peptide-bound glutamine (acyl donor) [1–5]. This action, called transamidation, results in the formation of stable, insoluble macromolecular complexes, including protein aggregates resistant to degradation by chemicals, detergents, and proteases [6–9]. The multifunctional TG enzymes exert their effects mainly through their transamidation and deamidation activities (Figure 1.1).

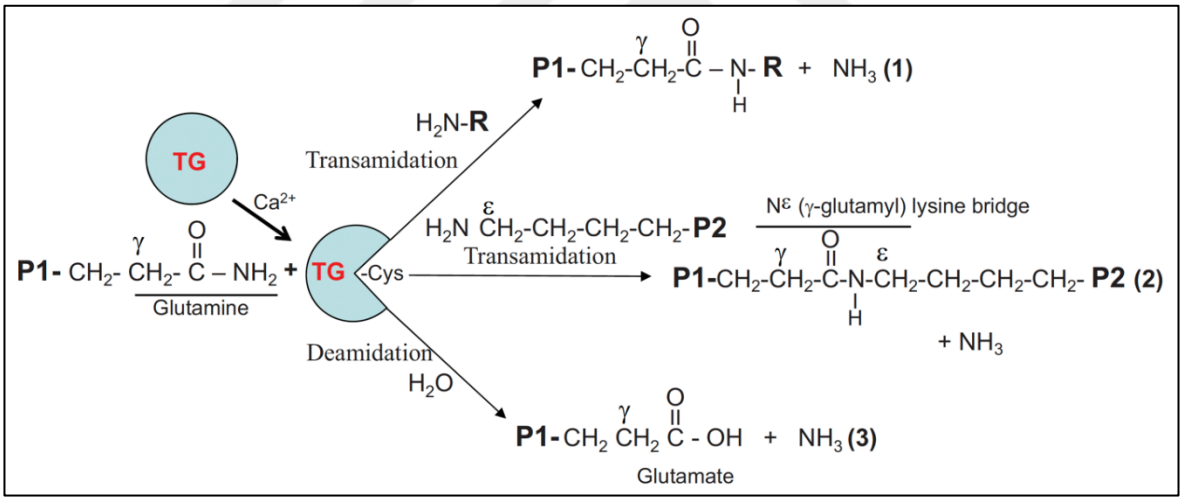



Figure 1.1. Transamidation and deamidation activities of TGs. The calcium-dependent transamidation (crosslinking) activity generates covalent links between primary amines (designated as P2) and glutamine residues of acceptor proteins (designated as P1). The resulting isopeptide bond can contribute to the formation of (1) polyamines or monoamines crosslinked with proteins or (2) protein-protein crosslinks. (3) Deamidation might occur by the utilization of $H_2O$ under slightly acidic conditions [4].

### 1.1.1. TG Mechanism of Action

The term “transglutaminase” was introduced for the first time in 1959 [10], in an attempt to define a newly discovered guinea pig liver enzyme showing transamidating properties [10, 11]. Later, this enzyme came to be known as tissue transglutaminase (TG2), and, to date, a total of nine TG family members have been described: TG1 to TG7, erythrocyte membrane protein band 4.2 or band 4.2, and factor XIII-A (FXIIIa) [4]. TGs are extensively and ubiquitously expressed in prokaryotes and eukaryotes, including all tissues of mammalian origin, invertebrates, plants, fungi, yeasts, and unicellular organisms [2].

From an evolutionary point of view, TGs seem to be related to papain-like cysteine proteases based on similarities in the catalytic triad, as well as the transamidation mechanism [1, 12]. The major difference of the TG family lies in their specificity for amine substrates and γ-carboxamides of glutamine side chains [13]. The catalytic mechanism depends on a Cys-His-Asp triad and a highly conserved active site region (GQCWVF); only band 4.2 does not show any enzyme activity due to a Cys → Ala substitution (GQAWVF) at the active site (Figure 1.2) [1].

```
GVSPMSWIGSVDILRRWKNHGCQRVKYGQCWVFAAVACTVLRCLGIPTRVVTNYNSAHDQ   TG1
GRDPRSWNGSVEILKNWKKSGFSPVRYGQCWVFAGTLNTALRSLGIPSRVITNFNSAHDT   TG2
GTSPLHWRGSVAILQKWLKGRYKPVKYGQCWVFAGVLCTVLRCLGIATRVVSNFNSAHDT   TG3
GANPAEWTGSVAILKQWNATGCQPVRYGQCWVFAAVMCTVMRCLGIPTRVITNFDSGHDT   TG4
GVSPLEWKGSVAILQQWSARGGQPVKYGQCWVFASVMCTVMRCLGVPTRVVSNFRSAHNV   TG5
GTNPSAWVGSVEILLSYLRTG-YSVPYGQCWVFAGVTTTVLRCLGLATRTVTNFNSAHDT   TG6
GVPPSAWTGSVDILLEYRSSE-NPVRYGQCWVFAGVFNTFLRCLGIPARIVTNYFSAHDN   TG7
GTAPYKWTGSAPILQQYYNTK-QAVCFGQCWVFAGILTTVLRALGIPARSVTGFDSAHDT  FXIIIa
GALLNKRRGSVPILRQWLTGRGRPVYDGQAWVLAAVACTVLRCLGIPARVVTTFASAQGT Band 4.2
```

Figure 1.2. Amino acid sequences at the active site regions of TGs [1].

The TG enzyme activity is a two-step reaction (Figure 1.3) that is apparently the reverse of proteolysis observed in the action of cysteine proteases [14, 15]. The first step is the nucleophilic attack on a glutamine side chain (carboxamide) of the protein substrate by the functional thiol group on the active site cysteine, which results in the formation of an acyl donor-enzyme intermediate complex and a concomitant ammonia release [16]. While this step is common for all TG reactions, the acyl acceptor in the second step can vary, determining the outcome of the enzyme activity. When the acyl acceptor is the ε-amino

group on a peptide-bound lysine residue, the outcome is the covalent crosslinking of peptides. This reaction can also result in intramolecular crosslinking if the acyl acceptor is on the same substrate protein. If a free primary amine acts as the acyl acceptor, the outcome is the post-translational modification of the protein substrate by amine incorporation. Alternatively, deamidation may occur when water acts as the acyl acceptor, causing a hydrolysis reaction [1, 17, 18]. Of note, a condition of optimal temperature and acidic pH is required for the occurrence of these reactions [2, 19].

Throughout this thesis, the transamidation and deamidation activities of TGs resulting in crosslinking, amine incorporation, or glutamate formation are collectively refferred to as the "TGase" activity.

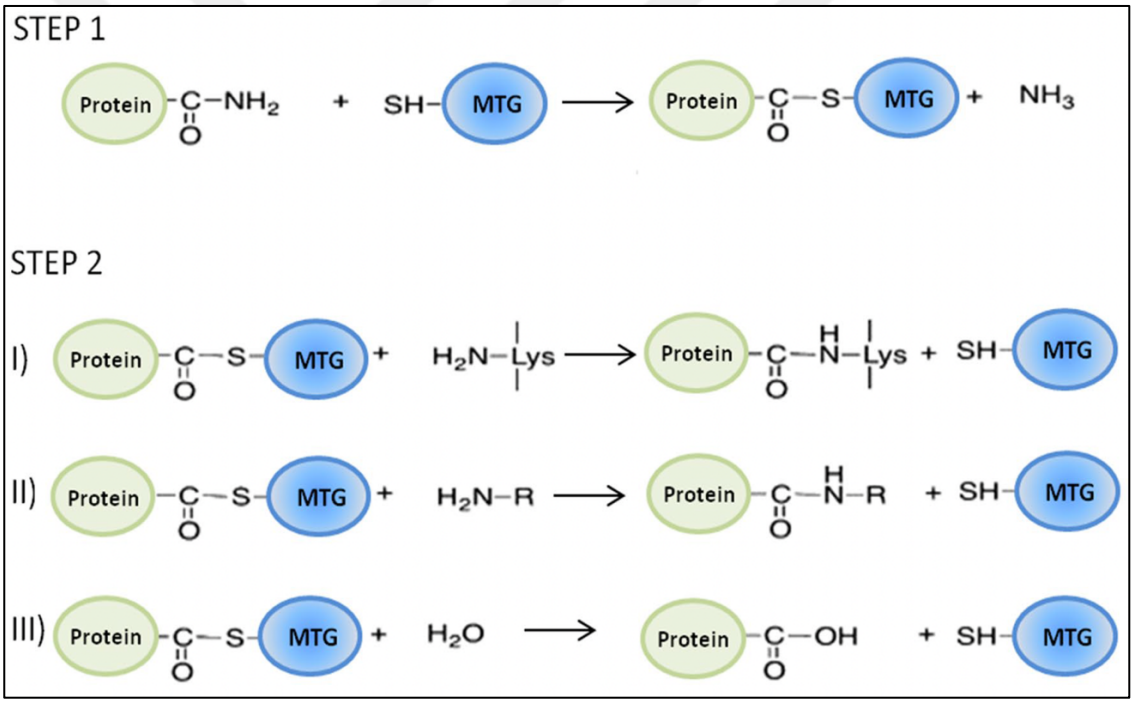



Figure 1.3. Two main steps of TGase reactions. Step 1: The thiol group on the active site cysteine attacks the acyl donor glutamine residue on the substrate protein. Step 2: (I) An ε-amino group on a peptide-bound lysine residue, (II) a primary amine, or (III) water acts as acyl acceptor, affecting the reaction outcome. MTG: mammalian TG [1].

### 1.1.2. TGs in Physiology and Pathology

TG1 (keratinocyte TG) expression has been found in the stratified squamous epithelia of the skin and upper digestive and lower female genital tracts. TG1 is responsible for the cornified envelope formation, preventing the skin from dehydration and pathogen invasion [20]. Lamellar ichthyosis, an autosomal recessive keratinization disorder characterized by abnormal cornification, is caused by TG1-encoding gene mutations [21, 22]. Congenital ichthyosis results in a severely compromised skin barrier in newborns, and individuals with this condition suffer long-term problems due to an excessive skin permeability. In mouse models, TG1 knockout was shown to cause serious dehydration and a lifespan limited to a few hours [23].

TG2, also known as tissue transglutaminase, is ubiquitously expressed in a wide variety of organisms [1]. The protein is predominantly cytosolic; however, it is also distributed in the nucleus, on the plasma membrane, endolysosomes, and extracellular vesicles [24–26]. Besides its main activity of transamidation, TG2 has been found to exert GTP hydrolase [27], protein kinase [28–30], protein disulfide isomerase (PDI) [31], and scaffolding actions [32]. TG2 is now well known for its altered expression or activity in several prevalent diseases, including celiac disease, Alzheimer's disease, Parkinson's disease, atherosclerosis, fibrosis, diabetes, and cancer [33]. According to a study, no abnormal phenotype emerged in TG2 knockout mice; however, the protein apparently played an important role in apoptotic clearance, as well as fibroblast adhesion capacity required in wound healing [34]. TG2 was also shown to be important in rat wound healing and angiogenesis functions [35]. In a follow-up study, besides delayed wound healing, TG2 knockout mice were characterized with a poor response to stress [36].

TG3 expression has been found to be expressed in the small intestine, brain, skin, mucosa, and hair follicles [4]. Also named as epidermal TG, this enzyme is another member of the family involved in cornified envelope formation [37]. TG3 also participates in the morphogenesis of hair fibers [38]. TG3 precursor mRNA is expressed in higher levels in response to calcium; the protein is produced as a zymogen and activated by proteolytic cleavage [39]. As a common trait with TG2, TG3 can bind and hydrolyze GTP molecules [39]. TG3 knockout in mice results in a compromised skin barrier function and hair

development [40, 41]. Additionally, an association has been found between TG3 and several cancers, including esophageal and oral squamous cell carcinoma [42, 43].

TG4 (prostate TG) is found in the prostate gland, prostatic fluids, and seminal plasma [44]. TG4 knockout results in reduced fertility [45], while the upregulation of TG4 promotes prostate cancer [44] by inducing epithelial-to-mesenchymal transition (EMT) [46].

TG5 is found in stratified squamous epithelia, with similar roles to that of TG1 and TG3 [47]. Another trait TG5 has in common with other TGs—namely TG2 and TG3—is regulation by GTP and ATP molecules. Binding of these nucleoside phosphates inhibits the crosslinking function of TG5, while this effect is reversed by $Ca^{2+}$ [48]. Inactivating mutations of TG5 in humans cause skin peeling syndrome [49]. However, the only TG5 knockout animal model established so far failed to mimic this pathology. Since TG1 was identified as the main TG responsible for the skin barrier formation, the pathological difference was attributed to the upregulation of TG1 in model mice but not the human skin. Nevertheless, in the absence of TG1, TG5 was able to maintain the skin barrier function during adult life [50].

Expression of TG6 is localized in the human testes and lungs, as well as in the central nervous system of mice [51, 52]. Human carcinoma cells displaying neuronal characteristics have also been found to exhibit TG6 expression [53]. TG6 is yet another TG family member that is regulated by guanine nucleotides and produced as a zymogen [53]. Spinocerebellar ataxia [54] and acute myeloid leukemia [55] have been associated with TG6 mutations. Moreover, TG6 knockout mice are prone to the development of tuberculosis, although they exhibit no phenotypic defects [56].

TG7 has been poorly characterized. This member is predominantly expressed in the testes, lungs, and brain (Mehta, 2005) but a more recent study reported TG7 expression in the kidney and the upregulation of its mRNA during renal fibrosis in mice [57]. The significance of TG7 knockout remains to be elucidated [13].

FXIIIa (plasma TG or fibrin-stabilizing factor) is mainly involved in blood coagulation, hence wound healing, and widely present in platelets, plasma, macrophages, dendritic cells, and the placenta. FXIIIa is produced as a zymogen (FXIII), activated upon proteolytic cleavage by thrombin, and crosslinks fibrin molecules in the presence of $Ca^{2+}$ [58]. FXIIIa is also present in chondrocytes and osteoblast lineage cells and has a role in bone synthesis

[59]. FXIIIa knockout mice have been shown to exhibit defects in clotting and several associated pathologies, such as miscarriage, diminished angiogenesis, and abnormal tissue remodeling [60–62].

Band 4.2, the transamidation-incompetent member of the TG family, is predominantly found in erythrocytes, bone marrow, fetal liver, and spleen [1]. Band 4.2 is a major component of the erythrocyte membrane cytoskeleton, with a crucial role in the maintenance of membrane integrity [4]. Absence of Band 4.2 causes alterations in red blood cell function of mice [63]. Japanese patients with Band 4.2 deficiency present with hemolytic anemia [64].

An interesting fact is that five members of the TG family (TG2, TG3, TG4, TG5, and FXIIIa) cause autoantibody production in TG-related immune diseases and have a significant prognostic value; however, the underlying mechanisms and the potential autoantigenic roles of the other TGs remain unexplored [13]. Identification of common sequence- or conformation-specific domains of TGs responsible for the emergence of autoantigenicity might help us better elucidate the major physiological and pathological events regulated by the TG family and the possibility of compensation for the loss of an individual family member [4].

## 1.2. TG2 STRUCTURE AND FUNCTION

### 1.2.1. TG2 in a Nutshell

TG2 is a ubiquitously expressed 76-kDa protein and a unique member of the TG family due to its multifunctional nature [65, 66]. TG2 has four functional domains: an N-terminal β-sandwich domain that contains fibronectin (FN)-binding sites and regulates cell adhesion; a catalytic domain possessing the catalytic triad that enables the TGase functions; a β-barrel-1 domain that forms a nucleotide binding site and takes part in signaling events; and a β-barrel-2 domain that is involved in phospholipase C gamma (PLCδ) binding and adrenergic signaling (Figure 1.4) [67]. Unlike other TG family members, all cells in the human body actively express TG2 to some extent, hence the name “tissue transglutaminase” [17]. To date, a diverse array of intracellular and extracellular TG2 substrates have been identified [6, 68, 69], and various post-translational modifications arise as a result of the TGase activity of TG2 in distinct cellular compartments and on numerous substrates.

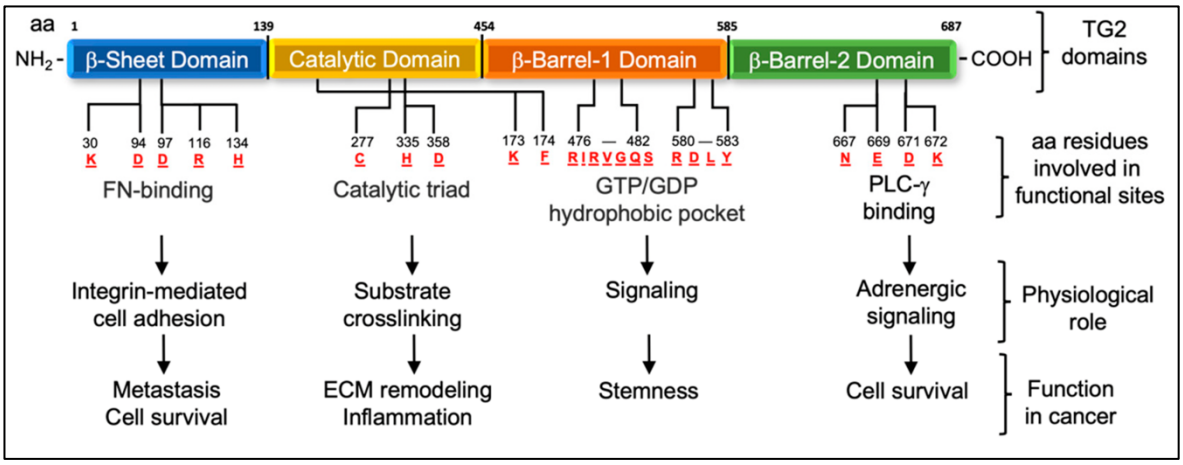



Figure 1.4. The functional domains of TG2. Amino acid residues involved in physiological and pathological events are shown. aa, amino acid; ECM, extracellular matrix; FN, fibronectin; PLC, phospholipase C [70].

### 1.2.2. Enzymatic and Non-Enzymatic Activities of TG2

During the initial structural studies, the nucleotide-binding pocket of TG2 pointed out the possibility of GTPase and kinase activities, which was confirmed for the first time when TG2 was found to mediate the interaction between the α1-adrenergic receptor and PLCδ in proliferating hepatocytes [27]. Accumulating studies have since reported various effects of the GTPase activity [71–73]. As reviewed elsewhere, the nucleotide-binding pocket of TG2 is vastly different from that of other G-proteins, hence the mechanism of signaling related to the nucleotide interaction remains unclear [74, 75].

The kinase activity was initially reported when insulin-like growth factor-binding protein-3 was identified as a substrate for the enzyme [76]. The study also showed that the kinase activity was inhibited by $Ca^{2+}$. To date, many additional kinase substrates for TG2 have been reported, including p53 [29], retinoblastoma protein (Rb) [30], histones [77], matrix metalloprotease (MMP)-3, and E-cadherin [78].

The PDI activity of TG2 was reported for the first time with the discovery where the denatured RNase A was converted to its active form by TG2, independently from the presence of either calcium or GTP [31]. Later, it was revealed that adenine nucleotide translocator 1, a protein involved in the formation of the mitochondrial membrane permeability transition pore, was a target of TG2 for PDI post-translational modification

[79]. This resulted in the release of pro-apoptotic proteins into the cytoplasm, implicating TG2 in the regulation of mitochondrial apoptosis. Additionally, the PDI activity of TG2 was shown to contribute to the correct assembly of several mitochondrial respiratory chain complexes, safeguarding ATP production [80]. A more recent study showed that heat-shock factor 1, a key transcriptional regulator of heat shock response, is trimerized by the PDI activity of TG2 through the formation of three intermolecular disulfide bridges, enabling the nuclear translocation of the substrate [81].

TG2 also has non-enzymatic scaffolding functions in the extracellular space; the protein acts as an adhesion co-receptor for FN and mediates integrin (ITG) signaling, realizing crucial functions in cell survival and propagation [32, 82]. The TG2/FN complex also recruits the platelet derived growth factor receptor (PDGFR)-β and leads to its activation [83, 84]. TG2 has also been found in extracellular vesicles (EVs); however, the actions of EV-associated TG2 and the functional outcomes remain relatively less explored [85].

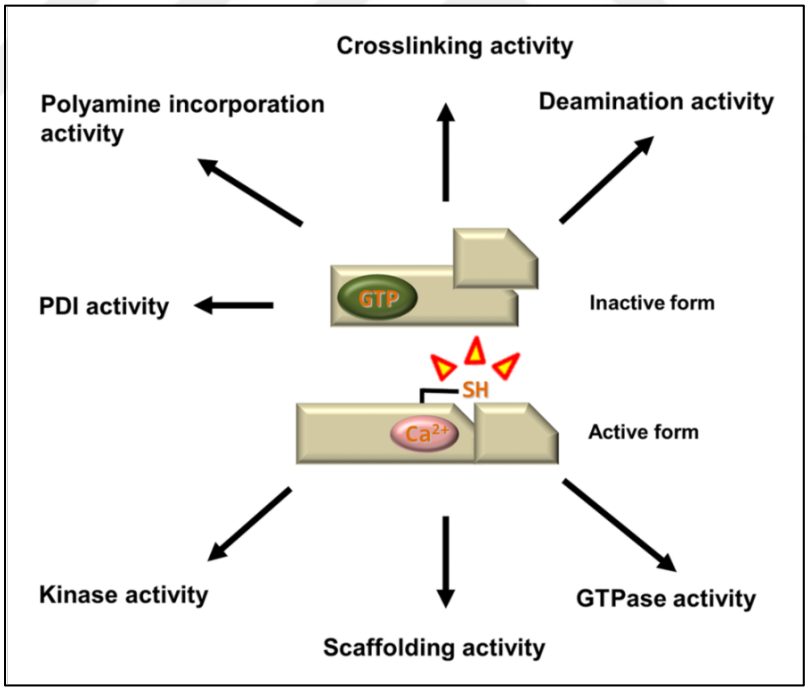



Figure 1.5. Diverse actions of TG2 [86].

The complex array of activities (Figure 1.5) and associated functions described above make TG2 a critical protein for the maintenance of homeostasis; therefore, TG2 needs to be tightly regulated. Particular microenvironmental conditions, including cellular cofactors, localization, as well as its post-transcriptional and post-translational modifications, are

involved in modulating the actions of TG2 [87]. Mechanisms involved in orchestrating TG2 functions are explained in more detail in the following sections.

### 1.2.3. Regulation of TG2 Activity

As described in Section 1.1.1, the Cys277-His335-Asp358 catalytic triad of TG2 is highly conserved and not only shared by all TG family members that possess the enzymatic activity but also by papain-like superfamily cysteine proteases [12]. The regulation of TG2 enzyme activity is highly dependent on reversible changes in the protein conformation, as revealed by the analysis of its crystal structure [67, 88, 89]. $Ca^{2+}$-binding stabilizes the TGase-active open conformation, while the inhibition of TGase activity is dependent on the binding of GTP, GDP, or ATP nucleotides, all of which withhold the protein in the closed (compact) form [67, 89–97] through the formation of hydrogen bonds between the active site cysteine and an adjacent tyrosine residue [98]. These two activities are mutually exclusive: TG2 bound with $Ca^{2+}$ does not exhibit GTPase activity, and the GTP-bound form cannot exhibit the TGase activity [99, 100]. However, unlike the case of GTP, the interaction between TG2 and ATP does not affect the TGase activity [101, 102].

Because the majority of intracellular TG2 is bound to GTP/GDP and concentration of $Ca^{2+}$ is low, TG2 inside the cells is usually in the crosslinking-inactive form. In the extracellular space, although the $Ca^{2+}$ level is high and GTP/GDP level is low, the oxidative environment is often not permissive for the crosslinking activity of the enzyme unless a mechanical or chemical stress is present [103, 104] (Figure 1.6).

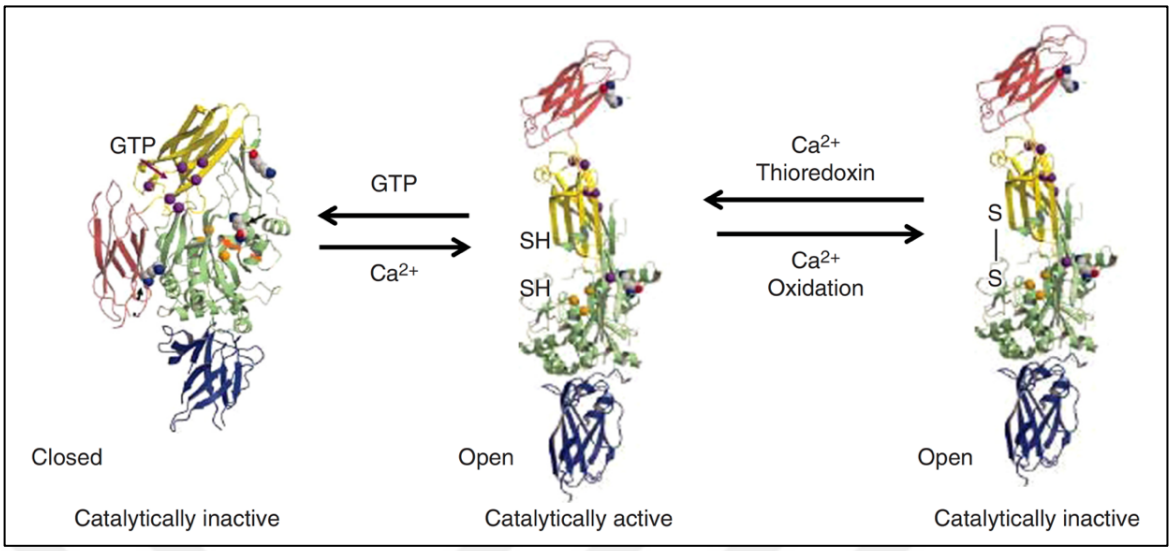



Figure 1.6. Conformations of TG2. The protein is in a closed and TGase-inactive state when bound with GTP/GDP. The TGase-active open conformation of TG2 is stabilized by Ca2+, rendering the active site accessible for substrates. Oxidation causes an open, TGase-inactive state, while this can be reversed by thioredoxin. Blue: C-terminal domain; red: N-terminal domain [4].

Although thioredoxin-1 (TRX) had long been associated with the activation of TGase activity by reduction in the extracellular environment, a key player enabling the inactivation—endoplasmic reticulum-resident protein 57 (ERp57)—was discovered several years later. As the name implies, ERp57 is a PDI chaperone that resides on the ER and mediates glycoprotein folding. Secreted ERp57 can be found in the extracellular space or on the cell membrane [105]. ERp57 was shown to oxidize TG2 with a much higher rate constant than other extracellular small molecule oxidants. Based on co-localization assays in human umbilical vein endothelial cells (HUVECs), ERp57 and TRX were suggested to reversibly and allosterically modulate the activation state of extracellular TG2 [106] (Figure 1.7).

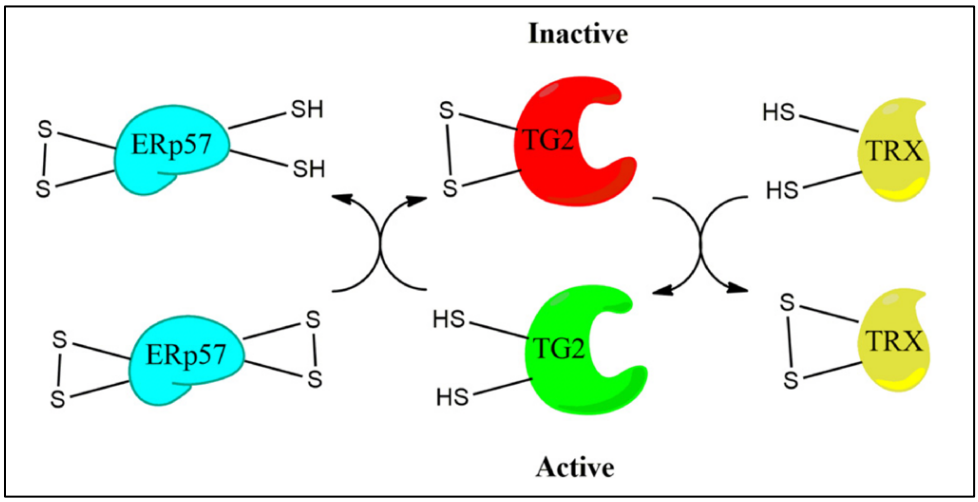



Figure 1.7. Reversible redox regulation of TG2: ERp57 oxidizes (inactivates), while TRX reduces (activates) extracellular TG2 through thiol-disulfide exchange TG2 [106].

TG2 activity is also regulated by $Mg^{2+}$ and nucleotide complexes [102, 107]. Recently, two newly identified glutamate residues were shown to be bound by $Ca^{2+}$ or $Mg^{2+}$ in a competitive manner, respectively enhancing the TGase or GTPase activity [108]. Another mechanism involved in regulating the activity of TG2 is the competitive inhibition, where endogenous amines can act as TG2 inhibitors by competing with the natural substrates or by directly modifying the enzyme's cysteine residues through disulfide bond formation [109–111]. Moreover, interferon-γ, the major cytokine released by gluten-reactive T cells in celiac disease, has been reported to take part in the activation of TG2 [112]. The level of TG2 can also be altered under certain conditions. For example, excess calcium levels during oxidative stress can lead to the ubiquitination and degradation of TG2 [113, 114]. TGF-β can also activate TG2 during oxidative stress, leading to the formation of intracellular aggregates.

Several other mechanisms are likely involved in regulating the enzyme activity, such as $Ca^{2+}$-binding to noncanonical sites on the protein [115], nitric oxide-mediated nitrosylation [116], binding of lipids [117, 118], small molecules, or other interaction partners [119], and proteolysis of the protein [120] have been reported in the literature. Expression of alternatively spliced TG2 variants also influence the activities of the protein: the C-terminally truncated TG2 isoforms generated by alternative RNA splicing are known to have a decreased GTP-binding affinity and transamidase activity [121–125].

### 1.2.4. Subcellular Localization of TG2

The functions of TG2 are vastly regulated by its subcellular localization due to distinct molecular interactions in the local microenvironment. Therefore, the dynamic localization of TG2 in response to the microenvironmental cues is crucial in understanding the exact behavior of the protein in diverse contexts.

Nuclear TG2 comprises approximately 5–7% of the total TG2 pool depending on the cell type, and the majority of nuclear TG2 was reported to associate with the chromatin [126]. In a follow-up study, TG2 was found to associate particularly with the euchromatin region in non-proliferating cells [127]. In line with this, TG2 mediates the expression of various transcription factors, such as nuclear factor-kappa B (NF-κB) and Sp1 [128, 129], upon its translocation to the nuclear compartment under stress. During proliferation, however, TG2 was tightly associated with the condensed chromatin [127]. Given that histone H3 is a substrate of TG2 kinase activity [77] and is known to be phosphorylated during proliferation at a key residue involved in chromatin condensation [130], TG2 is likely responsible for regulating the chromatin structure [126].

TG2 is also localized inside and on the outer membrane of mitochondria [126]. Under oxidative stress conditions, mitochondrial TG2 can be upregulated to push the cells in the direction of survival or death [131]. Furthermore, as described above, TG2 regulates the energy production process [80, 132] and mitochondrial membrane permeabilization [79]. Therefore, mitochondrial TG2 is an important player in the determination of cell fate under physiological and pathological conditions.

TG2 can also function in the endoplasmic reticulum (ER) [126]. TG2 has been implicated in calcium ion transport at the ER-mitochondria contact sites, and its interaction with several ER proteins has been reported [133]; however, the exact activities and functional significance of ER-associated TG2 remain to be clarified.

TG2 in the extracellular space crosslinks several matrix proteins, including FN, fibrin, collagen, and laminin [134–136], playing a key role in cell adhesion, migration, and extracellular matrix (ECM) remodeling, which will be discussed in detail in the following sections.

Another relatively unexplored area of research is the functions of TG2 present in extracellular vesicles. Since TG2 lacks the classical signal for secretion, its externalization from the cells has been of great interest. One possible route is its externalization via microparticles in a TG2 crosslinking-dependent manner [137]. In some cells, targeting of TG2 to the vesicles may be dependent on its association with syndecan-4 (SDC4), a heparan sulfate proteoglycan and a well-known interactor of TG2 [138, 139]. A particular sequence at the FN binding site of TG2 might also be involved; however, the externalization event was found to be independent of FN and dependent on the closed conformation of TG2 [138, 140]. Utilization of the endosomal recycling pathway through the interaction of TG2 and phosphoinositides on the endosomal membrane was also reported as an unconventional secretion mechanism [118]. P2X7R, a nucleotide-gated ion channel protein, was identified as a regulator of TG2 and TRX externalization as part of the innate immune response [141].

Diverse functions of TG2 in distinct cellular compartments are summarized in Figure 1.8.

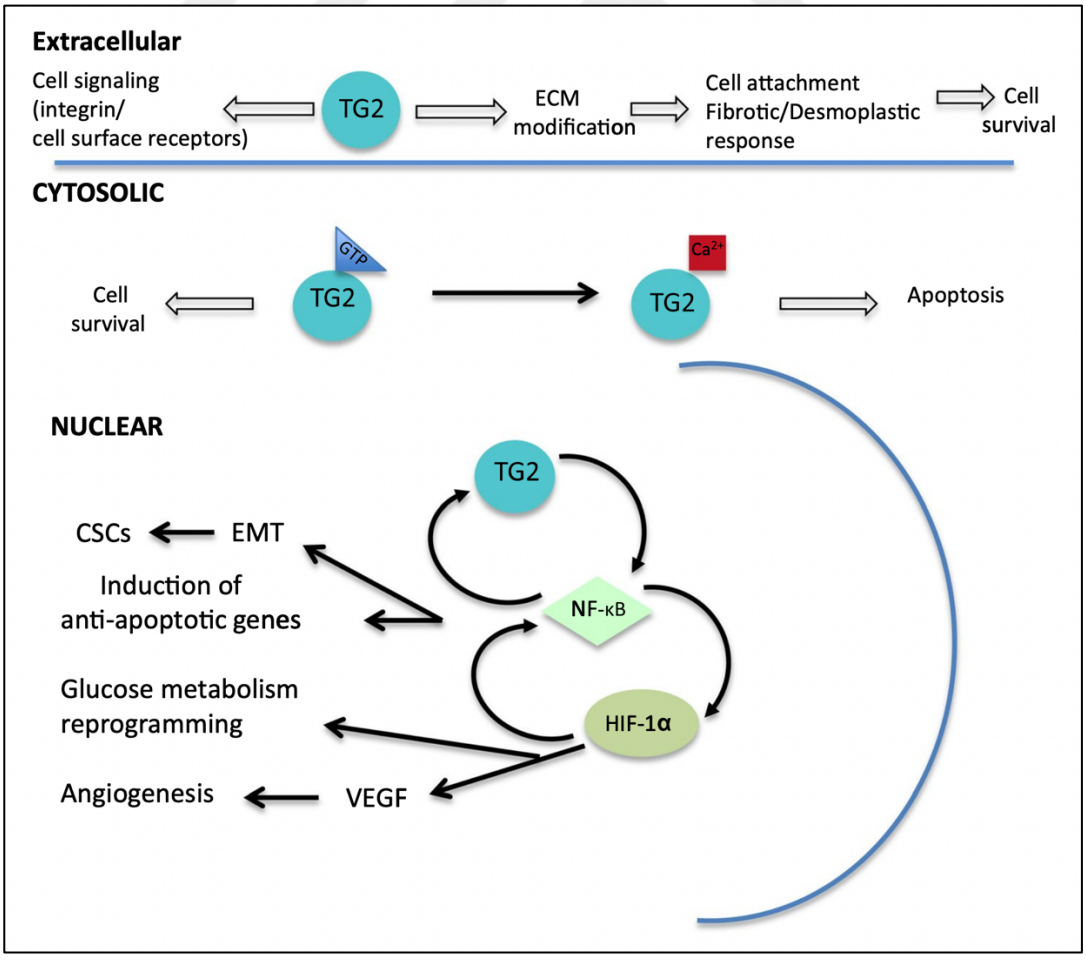



Figure 1.8. Functions of TG2 depending on its cellular distribution [142].

## 1.3. TG2 IN CANCER

A tumor-promoting effect was suggested for TG2 due to its upregulation and correlation with poor prognosis in numerous cancers, including glioblastoma [143], ovarian [144, 145], pancreatic [146], lung [147] and breast cancer [148]. Activation of oncogenic pathways by TG2 result in drug resistance, EMT, metastasis, and stemness (Figure 1.9). The TGase and GTPase activities of TG2, as well as its scaffolding interactions, have been implicated in the promotion of cancer in a cell type and context-dependent manner [70].

Many oncogenic pathways are activated directly or indirectly by TG2, including NF-κB, focal adhesion kinase (FAK), phosphatidylinositol 3-kinase (PI3K)/Akt, β-catenin, Ras homolog family member A (RhoA), and Yes-associated protein 1 (YAP) [129, 149–152]. Briefly, TG2 was shown to mediate resistance against chemotherapy through the activation of NF-κB or integrin outside-in signaling, resulting in cell-matrix adhesion [153]. A link between TG2 and EMT, as well as metastasis and stemness, has been suggested [144, 145, 154]. According to different reports, both the TGase and GTPase activities, as well as protein-protein interactions, have been implicated in the oncogenic functions of TG2 [70].

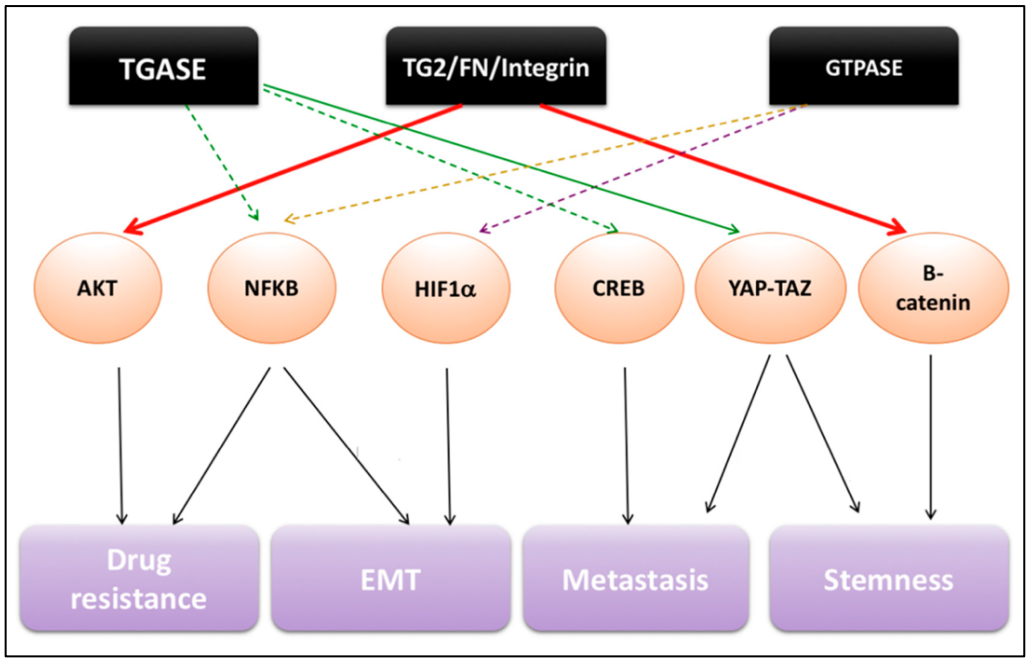



Figure 1.9. Mechanisms involved in the oncogenic functions of TG2. CREB, cAMP-response element-binding protein; FN, fibronectin; HIF, hypoxia-inducible factor; NF-κB, nuclear factor-kappa B; TGase, transamidase; YAP, Yes-associated protein 1 [70].

### 1.3.1. TG2 and Inflammation

In many ways, cancer progression is similar to inflammatory response, tissue injury, and remodeling [155, 156]. A possible link between cancer progression and inflammatory response was first identified in 1863, suggesting that chronic inflammation enhanced cell proliferation, thus leading to cancer progression [157]. In following studies throughout the years, chronic inflammation was shown to increase the metastatic potential of the cells in the tumor stroma, whereas a reduction in cancer development was achieved with anti-inflammatory drugs [158, 159]. The growth, survival, and progression of cancer cells can be regulated by immune cells that infiltrate tumors during inflammatory responses [155, 156].

TG2 has been described as a pro-inflammatory protein since increased TG2 expression and activity are related to many inflammatory diseases, including cancer [159, 160]. Several cytokines and GFs that contribute to the inflammatory signaling, including transforming growth factor (TGF)-β1, tumor necrosis factor (TNF)-α, interleukin (IL)-1, and IL-6, are potent TG2 inducers [161–163]. Particularly, the role of NF-κB as the driving force behind inflammation places TG2 at the center of pro-inflammatory response. NF-κB is activated by TG2 via the ubiquitination and proteasomal degradation of the inhibitory protein IκB or the phosphorylation of NF-κB. The inflammatory transcription factor NF-κB then translocates to the nucleus to activate the transcription of numerous pro-inflammatory cytokines, including those involved in the transcriptional regulation of TG2 [164]. This interplay between NF-κB and TG2 generates a condition of sustained inflammation, which is crucial in cancer progression (Figure 1.10).

An intertwining mechanism in TG2-related inflammation is the post-translational modification of phospholipase A2 (PLA2), another enzyme with a central role in inflammation. TGase-dependent polyamine incorporation and crosslinking actions of TG2 activate PLA2, which then takes part in arachidonic acid release from cell membrane glycerophospholipids, resulting in the synthesis of eicosanoids [165]. In the extracellular space, eicosanoids activate GPCRs and the downstream cytokines TNF-α and ILs, which eventually activate NF-κB. Finally, NF-κB activates the transcription of PLA2, generating yet another positive feedback loop that initiates a strong inflammatory signaling cascade [166].

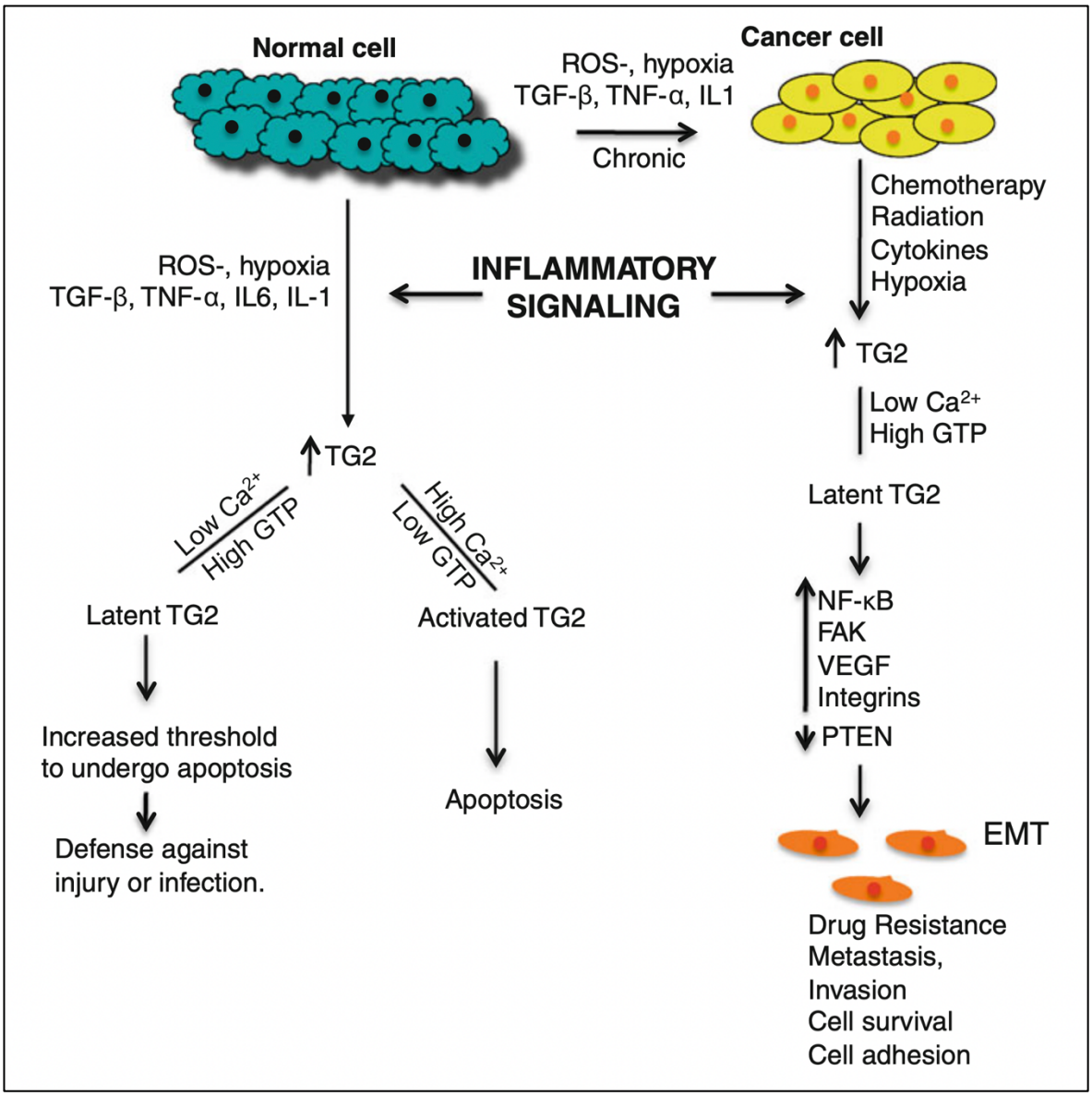



Figure 1.10. The relationship between TG2 and inflammation in normal and transformed cells [167].

### 1.3.2. TG2, Epithelial-Mesenchymal Transition, and Invasion

EMT is an essential processes for the reprogramming of cells during embryonic development [168, 169]. During adulthood, mesenchymal-like fibroblast cells existing in many tissues usually respond to conditions such as wound formation and contribute to the repair processes [170]. Although EMT is responsible for repairing tissues during inflammation, it also

accounts for the damage in pathological tissues, leading to metastasis and the acquisition of stem cell-like characteristics [145, 154, 171].

The malignant characteristic of tumor cells relies on their ability to survive and colonize in distant sites, which depends on the acquisition of a mesenchymal profile through EMT [172]. EMT is characterized by the loss of E-cadherin and a concomitant increase in the transcriptional factors Snail, Slug, Zeb 1/2, and Twist 1/2 [173]. Expression of these EMT transcription factors heavily relies on the transcriptional regulation by NF-κB, which is non-canonically activated by TG2. Hypoxia-inducible factor (HIF)-1α is another key player in this process since both NF-κB and TG2 can activate the expression of HIF-1α, which, in turn, activates the TG2 gene promoter.

Another autostimulatory loop in the process of EMT exists between TG2 and TGF-β. TG2-mediated crosslinking of the latent TGF-β results in the release of its active form, which is a potent inducer of EMT [174]. Activated TGF-β also induces the expression of TG2, further contributing to the cellular transformation [175].

EMT in cancer cells is usually followed by the increase in cell invasion potential. In this regard, cancer cells are reliant on the degradation of the basement membrane by MMPs, enzymes that digest virtually all ECM components. Particularly, MMP-1, MMP-2, MMP-3, and MMP-9 are involved in uncontrolled ECM degradation during metastatic initiation [176]. Degradation of TGase-active TG2 on the cell surface by certain types of MMPs results in a reduced ECM crosslinking, as well as the disruption of the TG2/FN/ITGB1 complexes involved in adhesion [136]. In several other cancers, including ovarian cancer [177] and squamous carcinoma [178], reduced TG2 expression was associated with reduced MMP expression and the suppression of metastasis. In addition, recently, TG2-dependent activation was also tied to the biosynthesis of MMP-2 and MMP-9, the main enzymes responsible from the degradation of basement membrane that facilitates intra/extravasation [179].

Taken together, TG2 orchestrates the complex processes and phases involved in the spreading of aggressive cancer cells through its multiple functions (Figure 1.11).

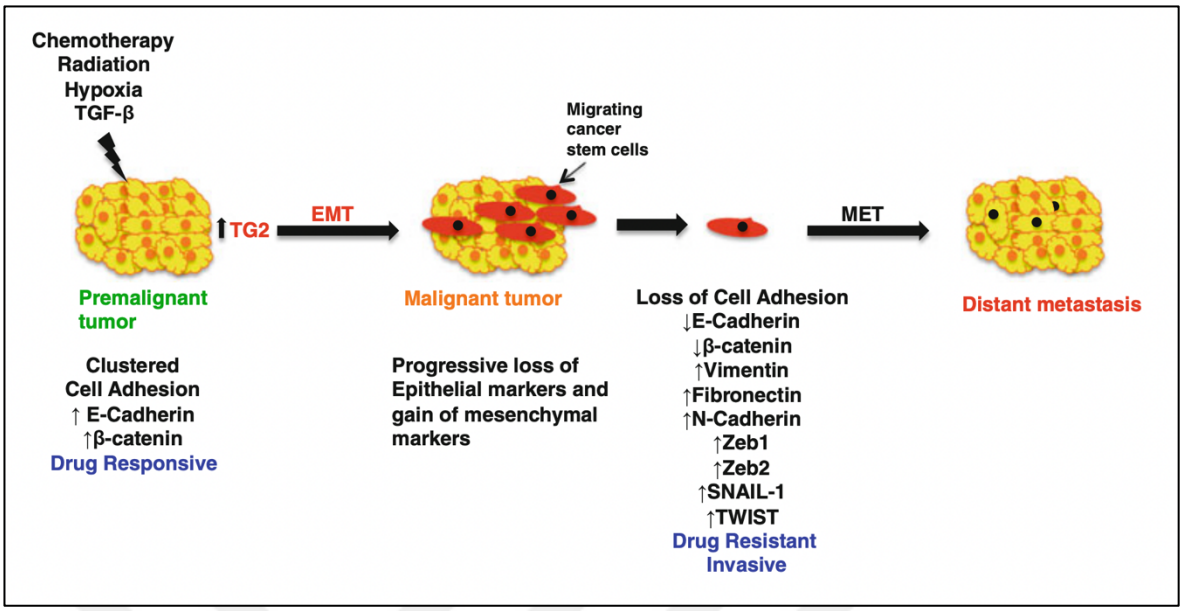



Figure 1.11. The relationship between TG2 and EMT [167].

### 1.3.3. TG2 and Modulation of the Tumor Microenvironment

Cancer cells undergo a metabolic switch to aerobic glycolysis even when their mitochondria are completely functional, causing the formation of lactate as an end product. This "Warburg effect" causes a reduction in pH, and the TME becomes acidic [180]. In this context, an interesting feature of TG2 in the TME is the release of ammonia as a byproduct of the TGase activity, which might enable cancer cells to tolerate the acidic conditions and survive [181].

Another common event in the TME is the creation of a hypoxic environment by rapidly expanding cancer cells due to the inadequate blood supply. Angiogenesis can be induced under hypoxic conditions through the activation of HIF-1. TG2 can downregulate the physiological inhibitor of HIF-1α, called von Hippel-Lindau (VHL). HIF-1α then translocates to the nucleus and, associating with its subunit HIF-1β, induces the expression of its target genes containing hypoxia response element (HRE) in their promoter (Figure 1.12). The direct stimulatory loop between TG2 and HIF-1α contributes to the accumulation of this angiogenesis-promoting protein. TG2 further contributes to the angiogenic events by inducing the expression and release of vascular endothelial growth factor (VEGF) into the tumor microenvironment (TME), resulting in the activation of VEGF receptor (VEGFR2).

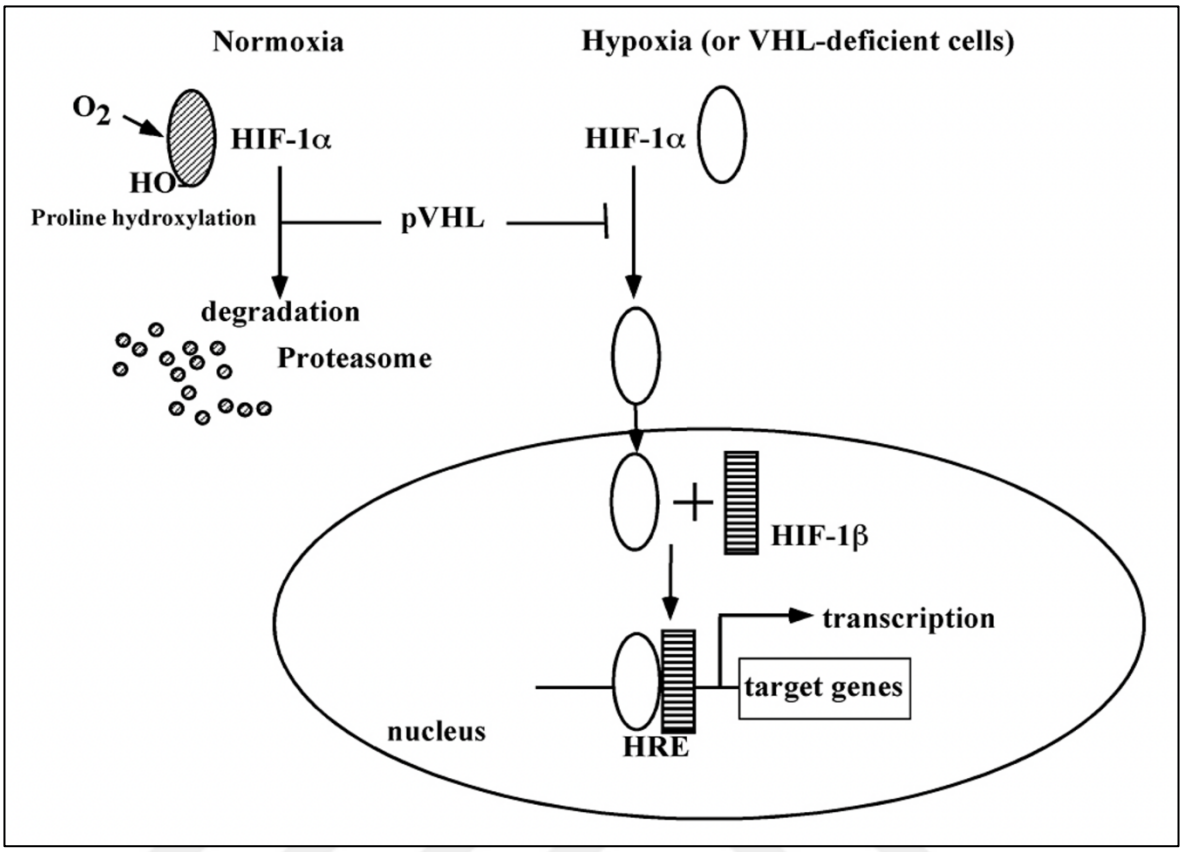



Figure 1.12. Regulation of HIF-1α-mediated responses to cellular oxygen levels [182].

A crucial activity in the TME is the spreading of the oncogenic potential of tumor cells via proteins [183] or nucleic acids carried in EVs [184, 185]. Alteration of gene expression in EV-recipient cells has been reported for both tumor and stem cells [186–188]. The "seed and soil" theory states that metastasis does not occur by chance but certain tumor cells show a preference for the growth-promoting microenvironment of specific organs [189]. This phenomenon, called metastatic organotropism, was observed when exosomes derived from tumor cells were found to fuse preferentially with recipient cells resident at the predicted destinations [190]. Proteomic profiling of exosomes provided evidence that specific integrin expression patterns were predictive of certain sites of metastasis, and the exosomes contributed to the formation of the pre-metastatic niche [190].

Investigation of cancer cell communication via microvesicles in breast and glioma cells revealed TG2 as a crucial protein in conferring transforming characteristics to the normal fibroblast and epithelial cells within the tumor microenvironment [25]. Anchorage-independent growth and enhanced survival capacity were observed in the cells that received

TG2-bearing microvesicles, and these effects were found to be dependent on the enzyme's crosslinking activity. Furthermore, TG2 alone was insufficient for this kind of transformation but its collaboration with FN, the binding partner and crosslinking substrate of TG2, was necessary for the activation of mitogenic signaling in recipient cells. TG2-crosslinked FN aggregates were able to activate integrin signaling and the downstream effectors FAK and extracellular signal-regulated kinase (ERK) [25].

Recently, TG2 was found to be distributed in exosomes upon proteasome blockade, interacting with key proteins involved in exosome biogenesis [24]. TG2 enabled the selective recruitment of proteins into the exosomes, implicating a potential important role for TG2 in the intercellular communication in the tumor stroma.

## 1.4. ALTERNATIVELY SPLICED VARIANTS OF TG2

To date, four alternatively spliced variants of TG2 have been identified. The splice variants, as presented in Figure 1.13, include 63-kDa transglutaminase homolog (TGH), 37-kDa transglutaminase homolog 2 (TGH2), 75-kDa tissue transglutaminase variant 1 (tTGv1), and 70-kDa tissue transglutaminase variant 2 (tTGv2) [123, 124, 191]. The shortest two isoforms TGH and TGH2 were identified in human erythroleukemia cells [123], while two additional isoforms, tTGv1 and tTGv2, were found in human aortic vascular smooth muscle cells [124]. Two putative isoforms have also been revealed by RNA sequencing [192]. All isoforms of TG2 are truncated to some extent at their C-terminus, which is known to have an impact on protein stability and GTP/ATP binding. Whether the unique structures of the isoforms could implicate distinct effects on TG2-mediated physiological and pathological events remains to be explored [175].

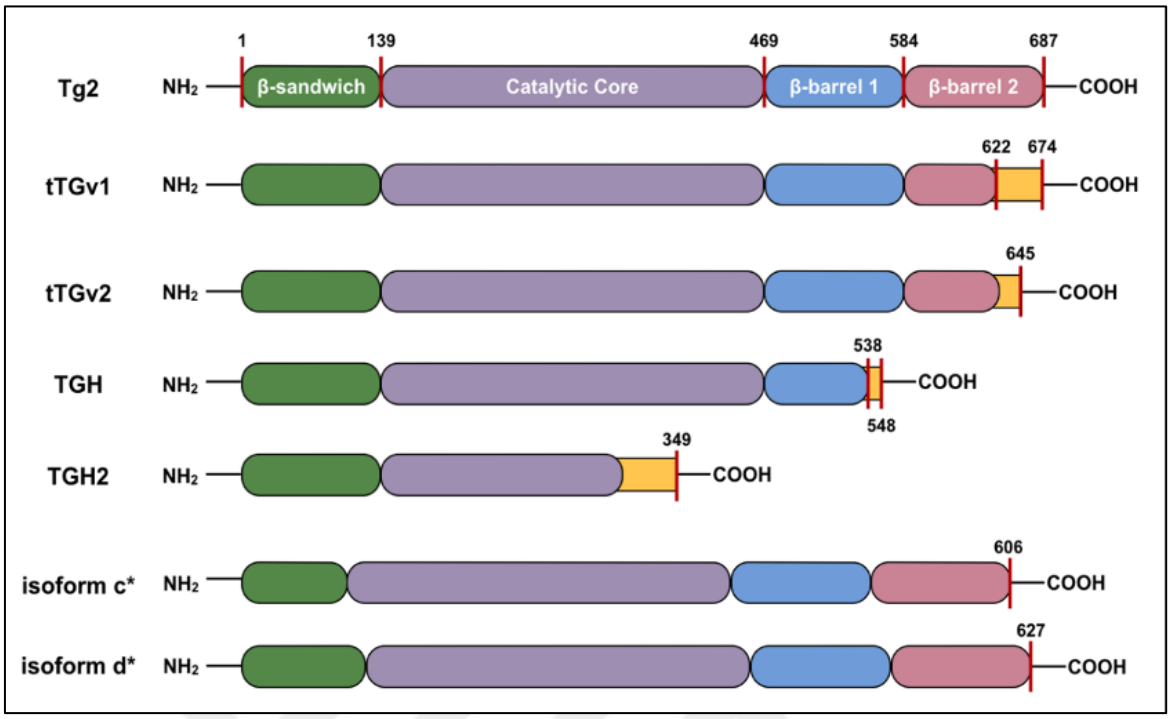



Figure 1.13. Transglutaminase 2 isoforms. Each domain is represented in different colors. Green, β-sandwich; purple, the catalytic core; blue, β-barrel 1; pink, β-barrel 2. Yellow regions represent the altered sequences in the truncated C-terminal ends of tTGv1, tTGv2, TGH, and TGH2. Two putative isoforms (isoform c and isoform d) are also given according to the sequence database from the NCBI website [192, 193].

A TG2 variant was identified for the first time through the analysis of a cDNA library from human erythroleukemia cells. This variant, named TGH, showed a 98% sequence similarity to the full-length TG2. A non-homologous nucleotide sequence started at position 1748 (exon 10), where a known intron-exon boundary existed. Therefore, this isoform was presumed to be the product of an alternative splicing event [123]. While the full-length TG2 is in a TGase-inactive and protease-resistant state when bound with guanine nucleotides, three out of four variants (TGH, tTGv1, and tTGv2) are insensitive to this regulation, possibly due to the loss of several C-terminal GTP-binding residues [124]. The insensitivity of the isoforms to GTP-mediated inhibition led to the speculation that intracellular crosslinked aggregates might accumulate over a long period due to the constitutive crosslinking activity, causing injury in several pathologies such as Huntington's disease. The late onset of such diseases could be explained in part by this low but continuous isoform-dependent process [124]. Moreover, these isoforms are more susceptible to rapid activation

by local transient increases in $Ca^{2+}$ concentration, which might affect the crosslinking-dependent functions of TG2, including the NF-κB activation. Hence, recent studies focused on the role of four isoforms, namely TGH, TGH2, tTGv1, and tTGv2, on the development of diseases, including neurodegenerative diseases and cancer.

TGH retains the catalytic domain present in the canonical isoform, as well as the high-affinity GTP-binding site positioned between amino acid residues 520–540 [194]. Although the exact structure is yet to be elucidated, the similarity of the isoelectric points of TGH and TG2 indicated that the tertiary structure of TGH might not be drastically altered by its unique C-terminal end [123].

Both TG2 and TGH were at detectable levels in retinoic acid (RA)-induced normal and erythroleukemia cells; however, the TGH/TG2 ratio was higher in the latter, implicating a distinct regulation under pathological conditions [123]. To date, several studies reported the expression of TGH in different disease states. For example, TGH expression was induced in the rat spinal cord upon injury, and the timing of induction was different compared to TG2. Interestingly, the initial point of TGH detection and the timing of apoptosis in the cells of injured spinal cord overlapped [195]. Therefore, TGH might be responsible for post-injury neuronal loss [122]. In fact, in a follow-up study, TNF-α-induced TGH caused cell death in fibroblast cells. This effect was found to be dependent on the formation of TGH aggregates rather than the TGase activity [121]. More recently, accumulation of TGH in hepatic cell nuclei was reported, as expected from the lack of a nuclear export signal (NES) on TGH [196]. TGH was also shown to induce neuroblastoma cell differentiation [197]. Additionally, TGH was reported to be upregulated in patients with Alzheimer's disease [198] but absent in vascular endothelial and smooth muscle cells [124]; this is an example to the notion that not all isoforms are always expressed in the same cell types, indicating distinct roles for the isoforms under certain pathological conditions [124].

TGH2, the shortest isoform of TG2, was identified using the same RA-induced erythroleukemia cells that allowed the discovery of TGH. TGH2 is produced by a splicing event in exon 6 and remains as the least characterized variant of the *TGM2* transcript. Similar to TGH, this variant preserved the active site cysteine required for the TGase activity of TG2; however, a known $Ca^{2+}$-binding site was lost. Amino acid residues between 204–227, which are known to be involved in GTP binding, are present in TGH2; however, other GTP-binding regions located through the C-terminal end are lost [191]. The isoelectric point of

TGH2 was also similar to those of TGH and TG2, and the protein product was detected in the normal human kidney, liver, and heart [191].

tTGv1 and tTGv2 are produced by splicing of an alternative site on exon 12 [94]. They were predominantly found in the cytosolic fractions of human umbilical vein endothelial cells (HUVECs) and the nuclei of vascular smooth muscle cells (VSMCs). The protein product of tTGv1 was more abundant than TG2 in RA-induced leukocytes, but tTGv2 was absent [124].

TG2, tTGv1, and tTGv2 all require the same amount of $Ca^{2+}$ to exhibit the TGase activity; although both variants display a residual TGase activity. The guanine-binding pockets of tTGv1 and tTGv2 are altered compared with that of TG2; however, these alterations do not affect the hydrolysis domain of tTGv1 and tTGv2, as revealed by their ability to catalyze GTP hydrolysis in the presence of $Mg^{2+}$ [94].

Expression studies of tTGv1 and tTGv2 in human embryonic kidney cells revealed a 28-fold and 9-fold reduction in transcript and protein levels compared to TG2, leading to the speculation that the C-terminal regions might affect the half-life of these proteins [124]. tTGv1 and tTGv2 were also found to show different localization patterns compared to TG2, which may indicate alternative functions for the isoforms in the cell [124]. Although TGH was previously reported to confer cytotoxicity [121], tTGv1 or tTGv2 did not induce apoptotic or necrotic cell death [124].

tTGv1 and tTGv2 levels were found to be significantly higher compared with the level of TG2 in peripheral blood mononuclear cells of patients with multiple sclerosis [199]. Importantly, PLA2 activation is closely related to the pathophysiology of multiple sclerosis, and TG2 is known to activate PLA2 in a TGase activity-dependent manner [200]. Since these isoforms are insensitive to GTP inhibition, and can rapidly exhibit TGase activity during a transient increase in $Ca^{2+}$, there is a possibility that tTGv1 and tTGv2 have a significant impact on the progression of multiple sclerosis [201].

Protein-protein interactions may also be altered as a result of the C-terminal truncation. For example, tTGv1 and tTGv2 are likely unable to bind GPR56, a G protein-coupled receptor (GPCR) acting as a suppressor of tumor growth and metastasis, due to the alterations in the C-terminal β-barrel domain involved in this interaction. These isoforms are also unlikely to bind PLCδ1, possibly affecting their subcellular localization, as well as the cellular events.

On the other hand, the N-terminal FN-binding domain is preserved, meaning that these isoforms can be externalized to the cell surface through an association with FN [32]. The loss of C-terminal amino acids may also cause the splice variants of TG2 to abrogate the C-terminally located nuclear export signal [175]. These may result in the loss of some canonical functions of TG2 or at least differences in the activity levels, or explain differential localization of the truncated isoforms and give rise to noncanonical functions for these isoforms, potentially playing important roles in different disease pathologies.

As alternative splicing is a rather active process in malignant neoplasms [202], a gene expression study for TG2 variants was performed in various cancer cell lines, revealing the expression patterns for all TG2 isoforms [203]. The expression levels of the splice variants were in correlation with the full-length form in normal cells, while distinct expression patterns were observed in cancer cells. TGH and TGH2, in particular, were found to be preferentially expressed in melanoma and prostate cancer. This unique pattern may be due to the cancer-promoting properties of the truncated variants. For example, GTP-binding/GTPase, but not transamidase activity, was found to be important for the induction of EMT and cancer stemness in mammary epithelial cells [204]. In addition, a novel cell-impermeable inhibitor specifically designed to target extracellular TG2 has been developed and tested recently, supporting the notion that the intracellular, GTPase-TG2 carries transforming properties [205]. Splice variants of TG2 may also influence inflammatory processes. Since the TGase activity of the full-length TG2 is involved in the inflammatory responses [206], the constituent but residual transamidase activity of the isoforms may have a decreased ability to contribute in this signaling [175].

## 1.5. RENAL CELL CARCINOMA

### 1.5.1. An Overview of RCC

Kidney cancer accounts for approximately 2.2% of the cancer diagnoses and cancer-related mortality. A total of 81,800 new cases and 14,890 estimated deaths were reported in the US in 2023, and the incidence of kidney cancer increased by 1% for both men and women [207]. Over 90% of kidney cancer cases are classified as renal cell carcinoma (RCC) [208]. RCC derives from renal tubular epithelial cells and comprises of a heterogeneous group of cancers

[209, 210]. The three major subtypes of RCC are clear cell RCC (ccRCC), papillary RCC (pRCC), and suspicious cell carcinoma (chRCC) [211]. ccRCC accounts for over 80% of all RCC cases and the majority of kidney cancer-related death [212]. Heterogeneity of these cancers result in a variety of clinical outcomes [213], and 30% of patients eventually develop metastases, leading to a high rate of mortality [214].

A marked increase in RCC incidence is observed with age, and the risk is about two times higher for men than woman [207]. Among the most frequent risk factors for the development of RCC are excess body weight, hypertension, and smoking, as well as medical conditions related to kidney [215]. Moreover, the risk for patients with a family history of RCC is two-fold higher due to the predisposing genetic mutations [216, 217]. A major gene underlying the predisposition of these patients to RCC is the tumor suppressor VHL, mutation of which causes von Hippel-Lindau disease. Inactivation of the VHL protein product leads to uncontrolled expression of HIF-1 and -2, highly oncogenic proteins related to vascularization and thus progression of aggressive cancers [218]. VHL is known to be the most frequently mutated gene in ccRCC. Accordingly, ccRCC tumors are highly vascular and prone to metastasis [219]. Mechanistic target of rapamycin (mTOR) pathway is another tumor-promoting signaling axis in the pathology of RCC; activation of mTOR signaling increases the cellular levels of HIF-1α, contributing to the angiogenic events [212, 220].

### 1.5.2. TG2 in the Propagation of RCC

VEGF and mTOR signaling activities are the main events in RCC pathology. Numerous kinase inhibitors, including the VEGF inhibitors sunitinib, pazopanib, and sorafenib, and mTOR inhibitors temsirolimus and everolimus have significantly improved disease outcomes in metastatic RCC; however, more effective therapies are still needed since complete tumor remission has not been achieved [212].

A previous miRNA profiling study identified 103 downregulated miRNAs in RCC, and the gain-of-function experiments in primary and metastatic RCC cell lines revealed that miR-1285 strongly inhibited RCC cell proliferation, invasion, and migration potential [221]. When the putative targets of miR-1285 were analyzed, TG2 was found as the only target significantly upregulated in clinical specimens. Moreover, knockdown of TG2 in RCC cell

lines resulted in diminished proliferative, invasive, and migratory properties, supporting the evidence that TG2 is a center molecule in the pathological events of RCC [221].

TG2 contributes to the highly hypoxic state in RCC: (i) TG2 constitutively activates the expression of HIF-1α, causing the activation of VEGF and angiogenesis; (ii) TG2 inhibits phosphatase and tensin homolog (PTEN), the suppressor of the PI3K/Akt axis, resulting in the activation of mTOR; and (iii) TG2 activates NF-κB, the central transcriptional regulator of inflammation [193]. Importantly, the last two actions of TG2 further promote HIF-1α accumulation (Figure 1.14). Taken together, TG2-dependent cellular events make this protein a prominent target in RCC treatment.

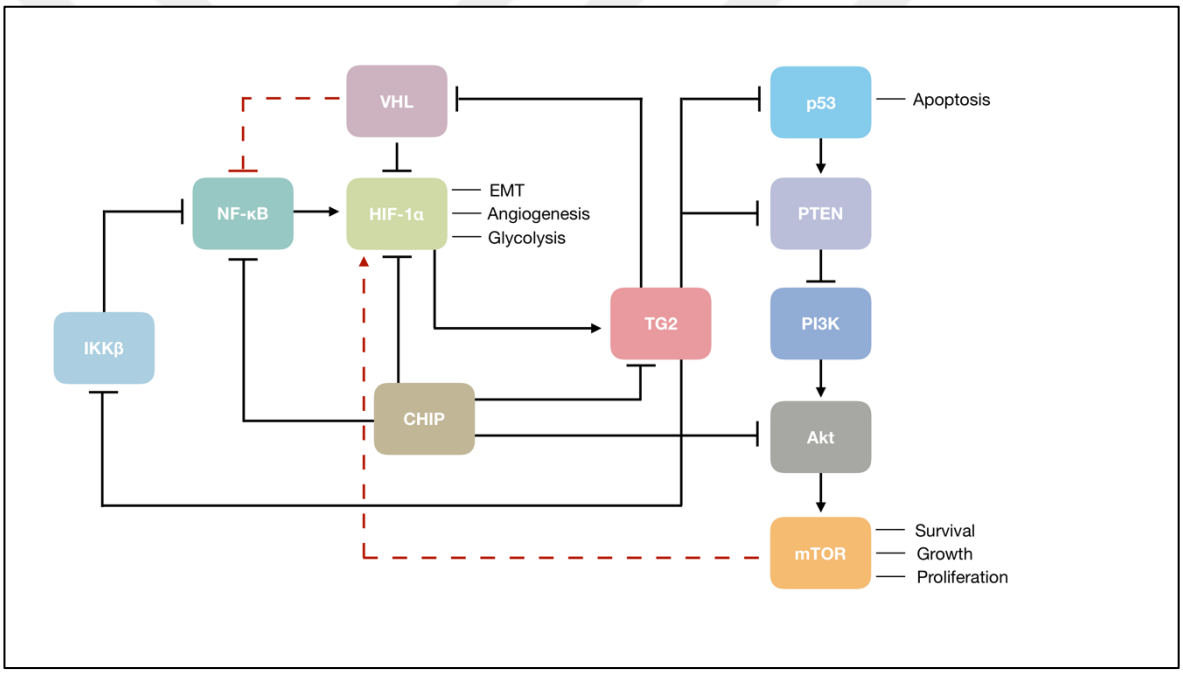



Figure 1.14. Pathways associated with TG2 in RCC. CHIP, carboxyl-terminus of Hsp70-interacting protein; HIF, hypoxia-inducible factor; IKK, I kappa B kinase; mTOR, mechanistic target of rapamycin; NF-κB, nuclear factor-kappa B; PI3K, phosphatidylinositol 3-kinase; PTEN, phosphatase and tensin homolog [193].

A study involving gene expression analysis in primary RCC specimens have linked TG2 with the development and progression of metastatic RCC [222]. According to a following research, increased TG2 expression was paralleled with the high nuclear grade and poor patient prognosis observed in RCC [223]. The molecular aspects of TG2-mediated progression were reported in a recent study, where the silencing of TG2 was found to impair

cellular adhesion, migration, invasiveness, and stemness potential of RCC cells [224]. Moreover, TG2 rescues RCC cells from p53-induced apoptosis [225]. Thus, TG2 expression and activation status is tightly related to the outcomes of the RCC disease.

### 1.5.3. Grading Renal Cell Carcinoma

The Fuhrman grading system has been widely employed for the grading of RCC since 1982. The system is based on the nuclear features, including the nuclear size, shape, and nucleolar prominence of tumors [226] (Table 1.1). The initial results in the application of this grading system were promising, showing a significant difference in the metastatic potential and survival rates between grade 1 and grade 2-4 tumors, and the method quickly found widespread application. However, issues with the initial study design that led to the adoption of Fuhrman grading, including the retrospective nature, low number of enrolled patients with adequate follow-up data, treatment heterogeneity, and no distinction between the clinical subtypes of RCC, continue to raise criticism [227]. Additionally, the Fuhrman system cannot be applied in cases that show discordance between the three nuclear features considered, which accounts for as high as 21% of all cases [228].

Table 1.1. The Fuhrman grading system [229].

| Grade | Nuclear diameter | Nuclear shape | Nucleoli |
|---|---|---|---|
| 1 | Small (~10 µm) | Round, uniform | Absent, inconspicuous |
| 2 | Larger (~15 µm) | Irregularities in outline | Visible at ×400 |
| 3 | Even larger (~20 µm) | Obvious irregular outline | Prominent at ×400 |
| 4 | As for grade 3 + bizarre multilobed nuclei spindle cells | | |

Over the years, with the increasing understanding of the diverse unique features of each tumor, the absence of a grading system considering the distinct natures of RCC subtypes became an issue. Analyses focusing on the individual association of each parameter with prognostic outcomes revealed the nucleolar features as the most dominant parameter in characterizing the clear cell and papillary RCC subtypes, and a modified four-grade system for these tumors where grades 1-3 would be defined based solely on the nucleolar features

was proposed [230–232]. Following a few updates, the final version of the World Health Organization/International Society of Urological Pathology (WHO/ISUP) grading system was published [233, 234] (Table 1.2). The predictive power of this grading system was significantly increased when necrosis was incorporated as an important parameter in RCC [235]. Nevertheless, both systems currently find their use in clinical practice, and the Fuhrman grading system continues to be the method of choice in many cases.

Table 1.2. The WHO/ISUP grading system [227].

| Grade | Features |
|---|---|
| 1 | Tumor cell nucleoli absent or inconspicuous and basophilic at 400× magnification |
| 2 | Tumor cell nucleoli conspicuous and eosinophilic at 400× magnification and visible but not prominent at 100× magnification |
| 3 | Tumor cell nucleoli conspicuous and eosinophilic at 100× magnification |
| 4 | Tumors showing extreme nuclear pleomorphism, tumor giant cells and/or the presence of any proportion of tumor showing sarcomatoid and/or rhabdoid dedifferentiation |

The tumor-lymph node-metastasis (TNM) system is the most widely used cancer staging system, defining the size and spreading profile of tumors [236]. The T1 and T2 stages and their subclasses—1a, 1b, 2a, and 2b—define the tumor size, while the T3 and T4 stages define the locoregional extensions. The N stages imply the presence (N1) or absence (N0) of regional lymph node metastasis, and the M stages imply the presence (M1) or absence (M0) of distant site metastasis [237] (Table 1.3).

Table 1.3. TNM staging for RCC [237].

| Stage | Definition | Subdivision |
|---|---|---|
| T0 | No evidence of primary tumor | |
| T1 | < 7 cm in greatest dimension, confined to the kidney | 1a: <4 cm<br>1b: >4 cm and <7 cm |
| T2 | > 7 cm in greatest dimension, confined to the kidney | 2a: >7 cm <10 cm<br>2b: >10 cm |
| T3 | Extends into major veins or perinephric tissues but not into the ipsilateral adrenal gland or beyond Gerota fascia | 3a: Tumor extends into renal vein branches, or invades perirenal and/or renal sinus fat<br>3b: Tumor extends into the subdiaphragmatic inferior vena cava |

| | | |
|---|---|---|
| | | 3c: Tumor extends into the supradiaphragmatic inferior vena cava |
| T4 | Tumor invades beyond the Gerota fascia and/or contiguous extension into the ipsilateral adrenal gland | |
| N0 | No regional lymph node metastasis | |
| N1 | Metastasis to regional lymph nodes | |
| M0 | No distant metastasis | |
| M1 | Distant metastasis | |

The TNM stage was shown to be significantly different between patients with low-grade (Fuhrman grade 1-2) and high-grade (grade 3-4) RCC [238]. Characteristics of the different stages of RCC are summarized in Figure 1.15.

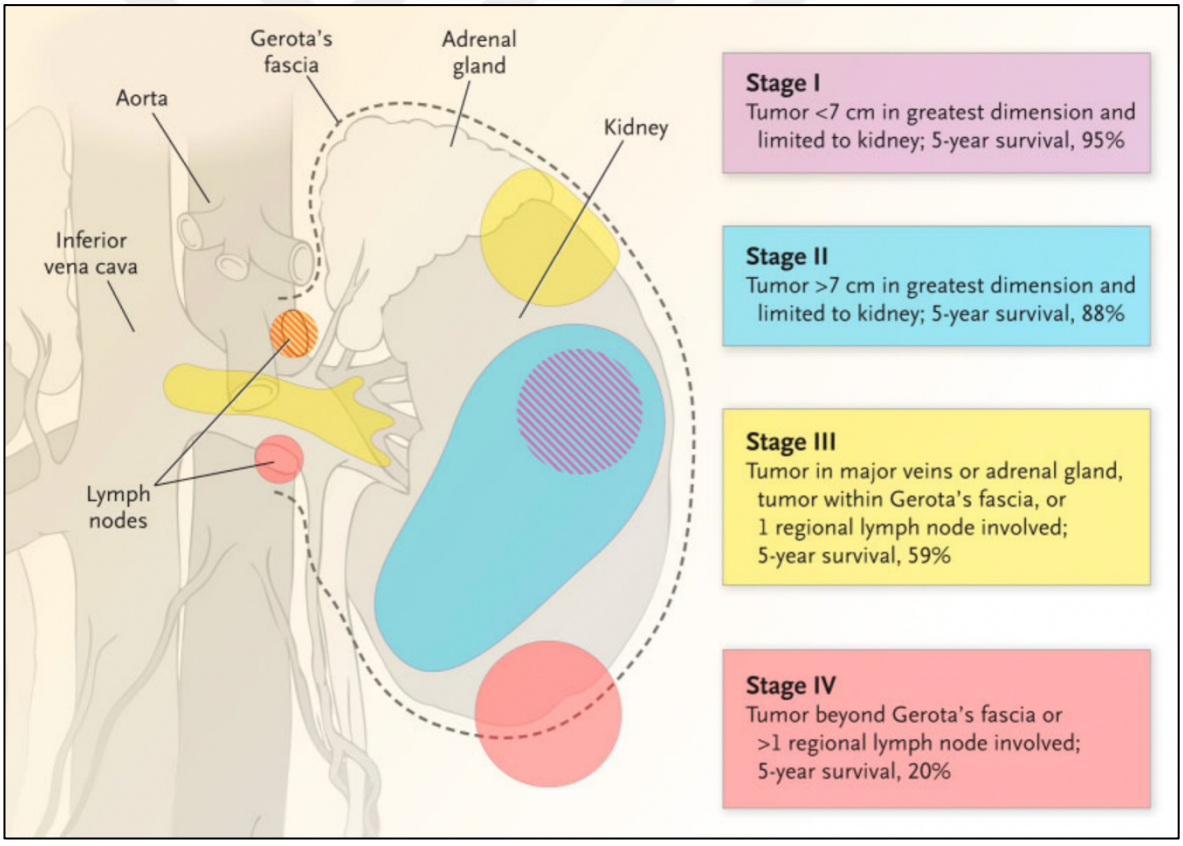



Figure 1.15. RCC survival rates based on TNM stages [239].

# 2. AIM OF THE STUDY

TG2 is a ubiquitously expressed, multifunctional protein with diverse roles in cellular processes. It has a calcium-dependent transamidase activity enabling the post-translational modification of proteins in its catalytically active form, and is a GTP-binding/GTPase enzyme with roles in the cellular signaling pathways. TG2 has been shown to strongly correlate with malignant transformation. During tumor initiation and progression, TG2 is downregulated in many cancers, due to its pro-apoptotic roles depending on its transamidase activity. On the contrary, tumors in a more aggressive state, bearing properties of invasion, metastasis, and stemness, tend to overexpress TG2 and display an enhanced survival. Because of its relevance in this aggressive cancer phenotype and drug resistance, TG2 has been of great interest as a potential molecular target. Yet, cellular responses against the modulation of TG2 levels show diversity depending on the cell type and context. An emerging realization is that epigenetic alterations might be a potential reason underlying the diverse responses under different physiological and pathological settings. Studies have reported the presence of alternatively spliced variants of TG2 and their altered expression levels in a variety of cancer cells. Given that the GTP binding/GTPase ability of TG2 has been associated with the survival, migration, and stemness of RCC, and the splice isoforms exhibit a higher GTPase activity than the canonical full-length TG2, we propose that the TG2 isoforms might contribute to the cellular transformation in RCC. Therefore, the first objective of this study was to investigate the clinical significance of TG2 isoform expression in patients with non-metastatic RCC. Then, we aimed to determine the potential effects of the alternatively spliced TG2 isoforms on cell proliferation, cell cycle, EMT, and invasion and migration potential of renal tubular epithelial cells, promoting cellular transformation.

# 3. MATERIALS AND METHODS

## 1.6. AMPLIFICATION AND CHARACTERIZATION OF PLASMID VECTORS

### 1.6.1. Design of the Lentiviral Plasmid Vectors Coding for TG2 Isoforms

Lentiviral plasmid vectors expressing human TG2 (12548 bp), TGH (12131 bp), TGH2 (11534 bp), tTGv1 (12509 bp), tTGv2 (12422 bp), and EGFP (11204 bp) and a mock vector (10790 bp) were purchased from Vector Builder GmbH (Neu-Isenburg, Germany) as transformant *Escherichia coli* (*E. coli*) stocks. An 'all-in-one' vector design, where all components (the promoter, transcription factors, suppressors) required for an inducible Tet-On expression system were expressed on the same plasmid, was employed. The maps of the seven plasmids carrying the genes of interest (GoI) are given in Figure 3.1 to

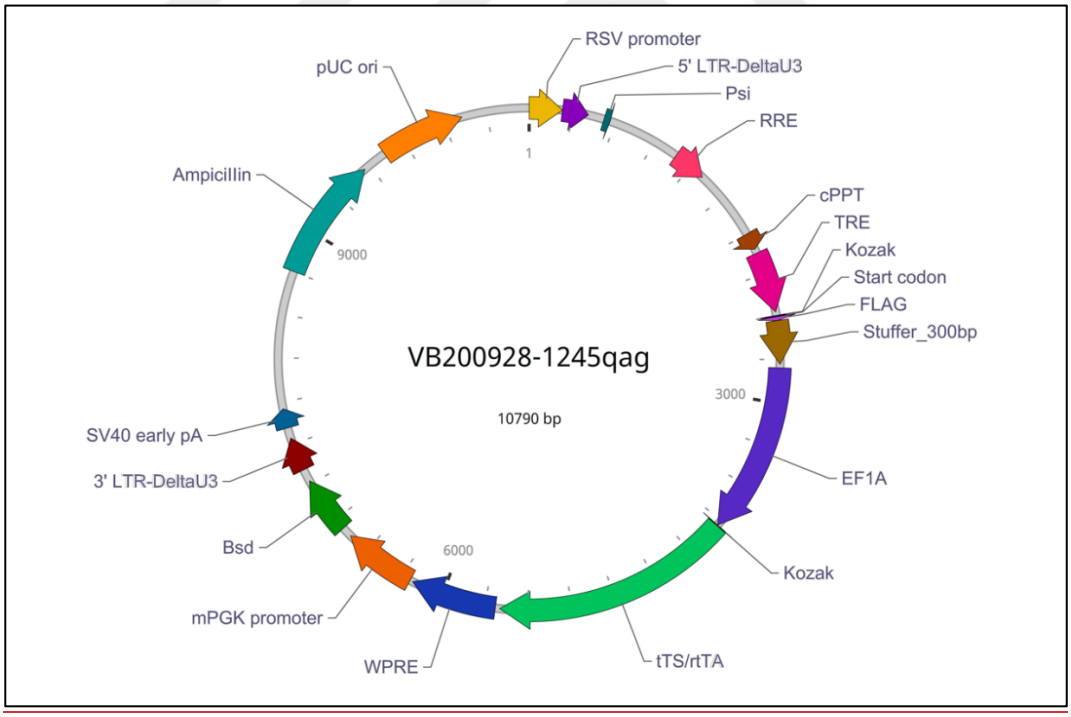



Figure 3.7. The open reading frames (ORFs) of hTGM2, TGH, TGH2, EGFP, and the Flag tag were automatically selected on the supplier's website (en.vectorbuilder.com) using the linked National Center for Biotechnology Information (NCBI) database. For tTGv1 and tTGv2, sequences were obtained from a previous study (Phatak et al., 2013) and added to the vectors manually.

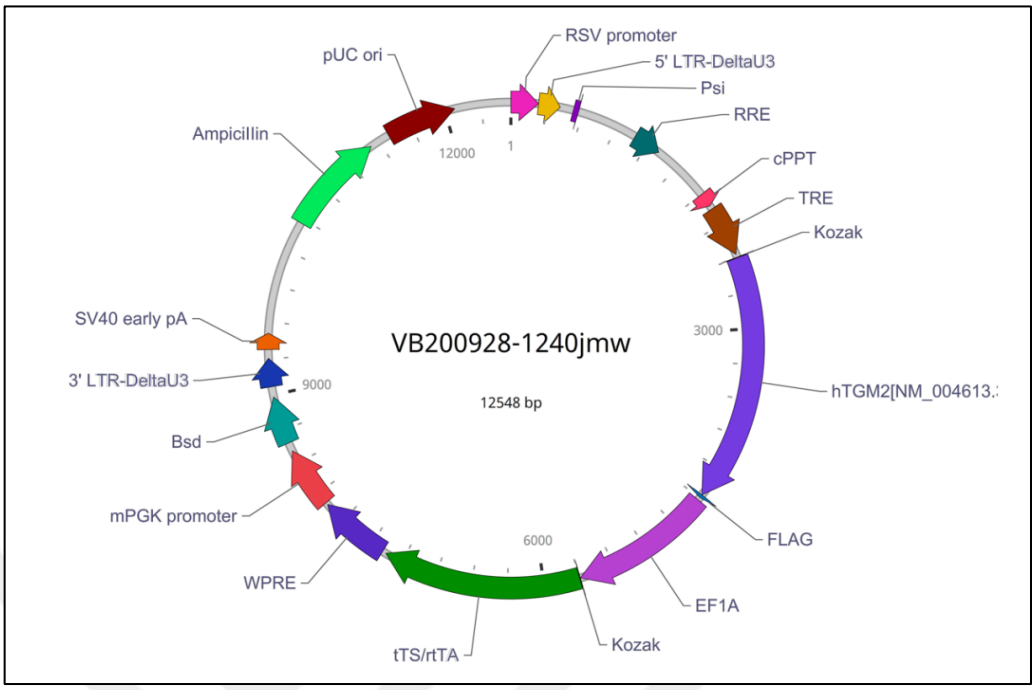



Figure 3.1. hTGM2 plasmid map.

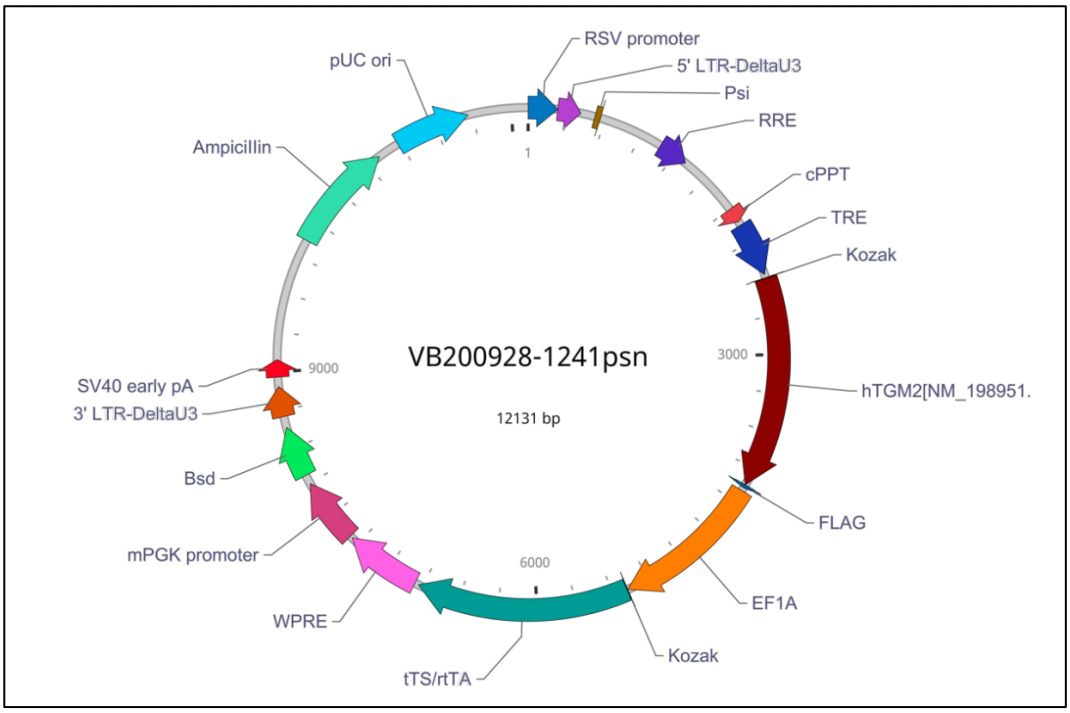



Figure 3.2. TGH plasmid map.

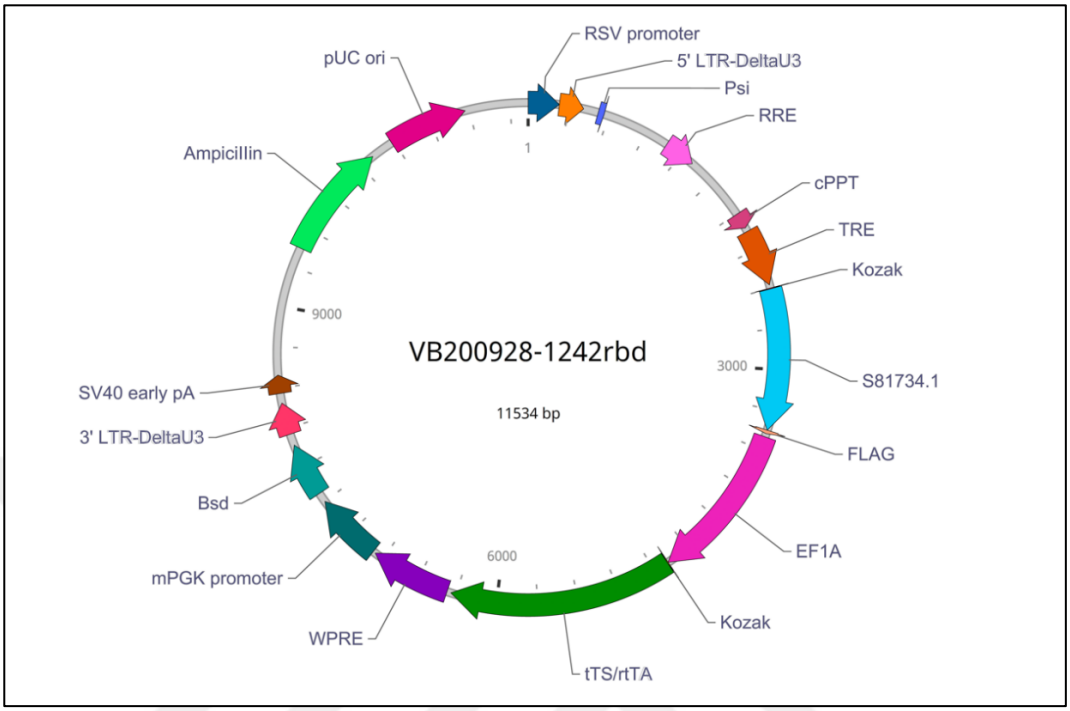



Figure 3.3. TGH2 plasmid map.

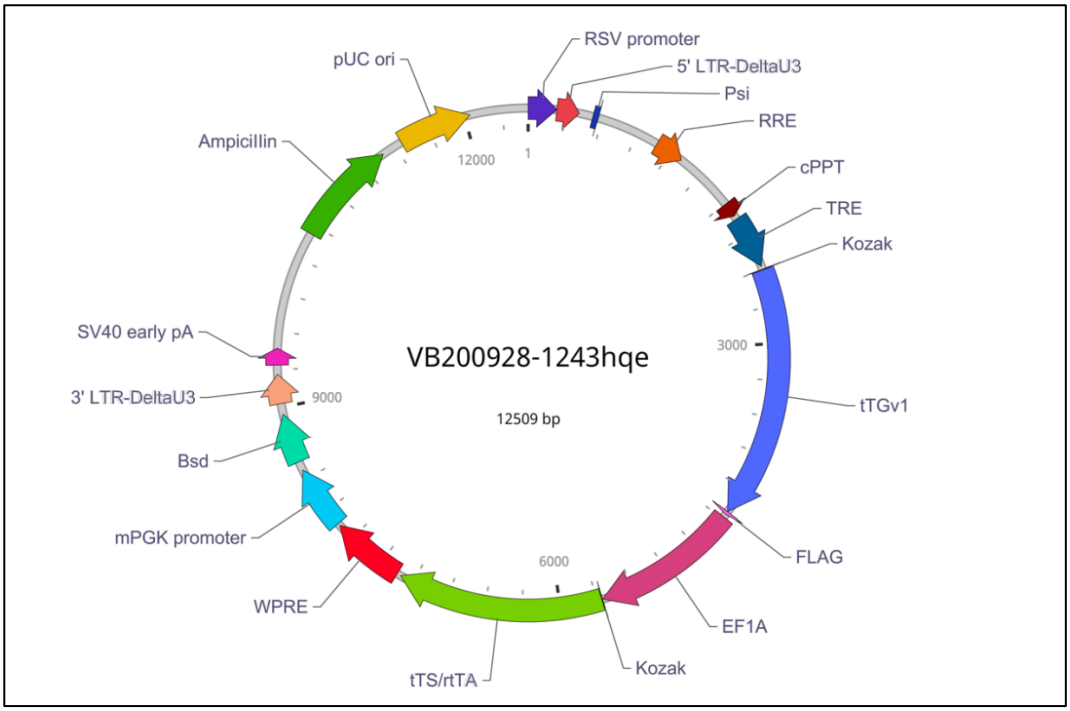



Figure 3.4. tTGv1 plasmid map.

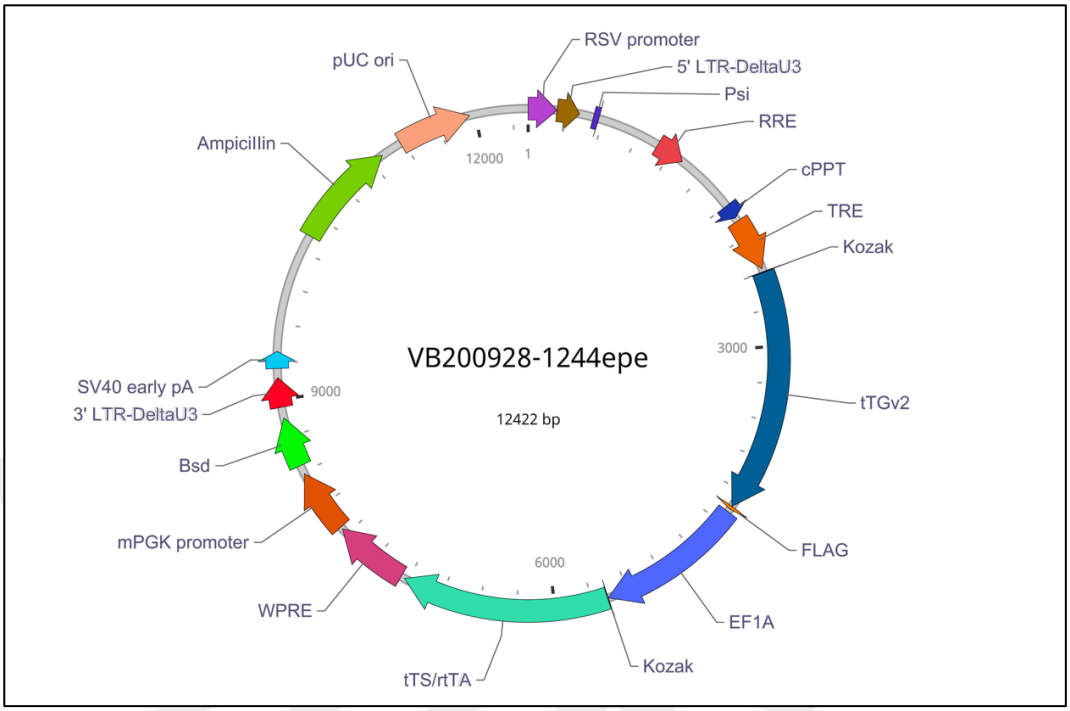



Figure 3.5. tTGv2 plasmid map.

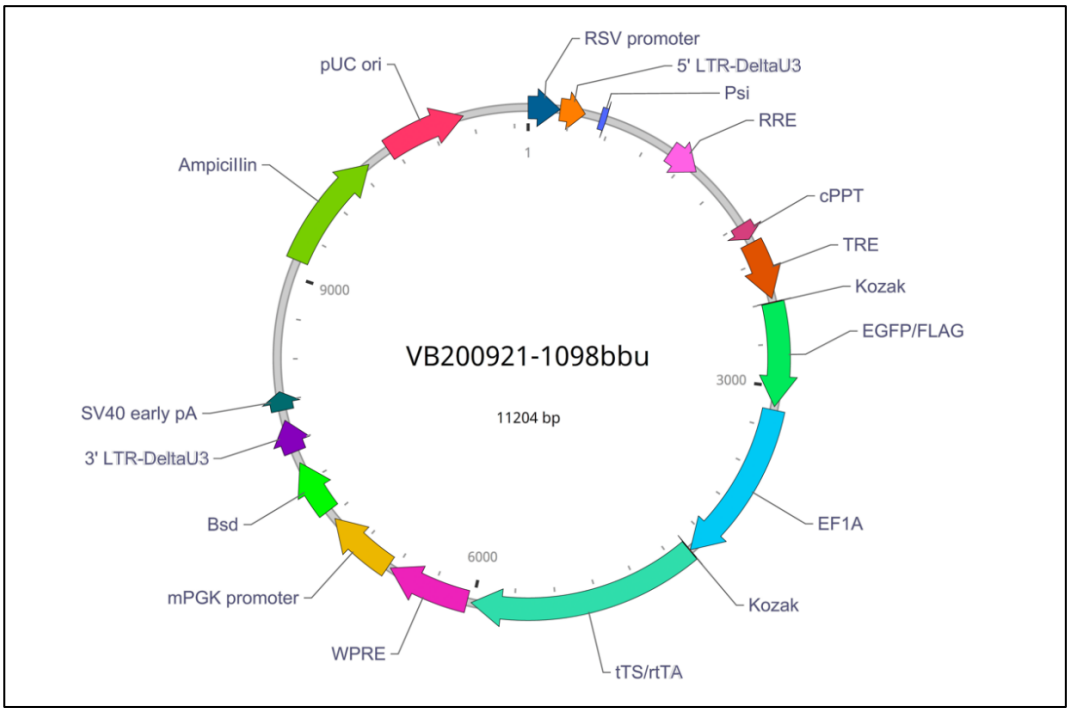



Figure 3.6. EGFP plasmid map.

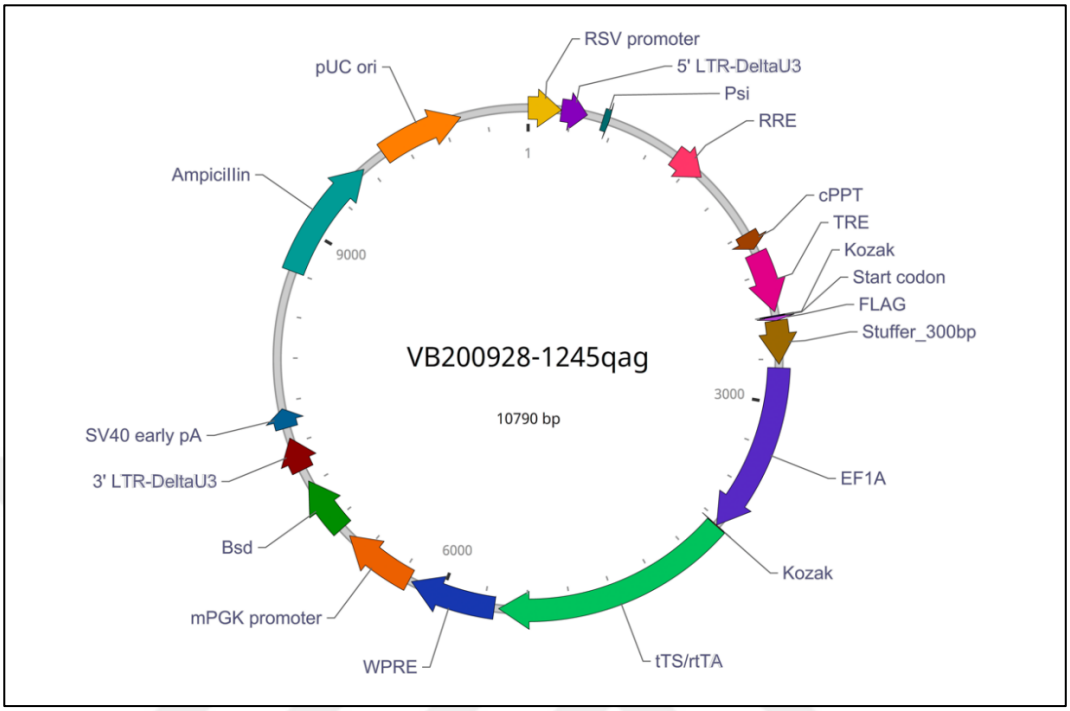



Figure 3.7. Mock plasmid map.

All vectors contained the Rous sarcoma virus (RSV) promoter to drive the transcription of viral RNA in 293-FT cells. Truncated HIV-1 5' long terminal repeat (5' LTR-DeltaU3), HIV-1 Rev response element (RRE), and HIV-1 packaging signal (Psi) were used to enable viral RNA transcription, nuclear export, and packaging, respectively. Central polypurine tract (cPPT) was used to facilitate the nuclear import of HIV-1 cDNA. A 2$^{nd}$ generation tetracycline-responsive element (TRE) promoter was used for the expression of the GoI. All GoI had an N-terminal Flag tag to facilitate antibody binding. T2A-linked tTS and rtTA_M2 (tTS/rtTA) transcription factors were present as regulators of the TRE promoter. In the absence of tetracycline analogs, such as doxycycline (Dox), tTS binds to TRE promoter to enable active suppression of gene transcription, whereas rtTA_M2 is unable to bind to TRE promoter. Conversely, when the inducing antibiotic is present, tTS dissociates and rtTA_M2 binds to the TRE promoter to activate gene transcription. Since rtTA_M2 alone does not provide active transcriptional repression, this system has lower leaky expression in the absence of the inducing agent. Expression of these transcription factors were under the control of the mammalian ubiquitous EF1A promoter, and Kozak translation initiation sequence was used to facilitate translation initiation from the ATG start codon. Woodchuck

hepatitis virus post-transcriptional regulatory element (WPRE) was used to enhance virus stability in packaging cells (HEK-FT), ensuring a higher titer of the packaged virus. Blasticidin (Bsd) resistance gene was added to allow mammalian selection, which was preceded by the mouse phosphoglycerate kinase 1 (mPGK) promoter. Truncated HIV-1 3' long terminal repeat (3' LTR-DeltaU3) was present to self-inactivate the 5' LTR during viral genome integration. The Simian virus 40 early polyadenylation signal (SV40 early pA) is used to terminate transcription and induce the polyadenylation of mRNAs. Ampicillin (Amp) resistance gene was used for bacterial selection, and the pUC origin of replication (ori) to facilitate the replication of plasmids in *E. coli*, regulating high-copy plasmid number. GoI residues on vectors and their length are given in Table 3.1.

Table 3.1. GoI residues and lengths on Tet-On lentiviral plasmid vectors.

| GoI | hTGM2 | TGH | TGH2 | tTGv1 | tTGv2 | EGFP |
|---|---|---|---|---|---|---|
| **Residues** | 2404-4464 | 2404-4047 | 2404-3450 | 2404-4425 | 2404-4338 | 2404-3147 |
| **Length (bp)** | 2061 | 1644 | 1047 | 2022 | 1935 | 744 |

bp, base pairs; EGFP, enhanced green fluorescent protein.

### 1.6.2. Amplification of the Lentiviral Plasmid Vectors

Transformant bacteria carrying the plasmid vectors (obtained from Vector Builder) were streaked on Luria-Bertani (LB) agar plates and incubated overnight at 37°C to allow colony growth. The next day, a single bacterial colony was picked with the aid of a sterile pipette tip and inoculated into 5 ml of LB broth to be grown at 37°C and 180 rpm for 3 hours. Finally, 150 µl of the liquid bacterial cultures were transferred into 150 ml of LB broth, and the bacteria were cultured overnight at 37°C and 180 rpm until an optical density (OD) of 0.2-0.4 was reached at λ=595 nm. All LB agar and broth preparations used to grow the bacteria contained a final concentration of 100 µg/ml Amp to allow bacterial selection.

### 1.6.3. Isolation of the Lentiviral Plasmid Vectors

Plasmid isolation was performed using HiPure MidiPrep Kit (Cat#: K210005; Invitrogen) as per the manufacturer's instructions. First, bacteria were harvested from 100 ml of the

cultures by centrifugation at 4,000 x*g* for 10 minutes, and then the cell pellets were resuspended in 4 ml of resuspension buffer. To lyse the bacterial cells, 4 ml of lysis buffer was added to the mixture, and the samples were incubated at room temperature for 5 minutes. Next, 4 ml of precipitation buffer was added onto the slurry and centrifuged at 10,000 x*g* for 15 minutes. The supernatants were then transferred into filter columns and drained. The columns were washed twice with 10 ml of wash buffer prior to the placement of fresh 15 ml collection tubes beneath the columns. Next, 5 ml of elution buffer was loaded into each column, and the flow-through from each column was collected by the gravity flow. To precipitate the DNA, 3.5 ml isopropanol was added to the tubes, which were then centrifuged at 4°C and 10,000 x*g* for 45 minutes. After washing with 3 ml of 70% ethanol at 10,000 x*g* and 4°C for 10 minutes, the pellets were air-dried for 15 minutes and dissolved in 200 µl TE buffer. Plasmid DNA concentrations were measured using NanoDrop™ (Cat#: ND-2000; Thermo Scientific).

The plasmid vectors were run on 0.8% (w/v) agarose gel prepared with the SYBR Safe DNA gel stain (Thermo Fisher #S33102; final concentration: 0.5X) and 1X tris-acetate-EDTA (TAE) buffer (Table 3.2; diluted 1:10 with $dH_2O$). After the completion of agarose gel electrophoresis (GE) at 100 V for 40 minutes, the bands were visualized using the ultraviolet (UV) illumination mode of the ChemiDoc XRS+ system (Bio-Rad).

Table 3.2. Components of 10X TAE buffer.

| Component | Amount |
|---|---|
| Tris | 48.5 g |
| Glacial acetic acid | 11.4 ml |
| 0.5 M EDTA solution (pH 8.0) | 20 ml |
| Ultrapure water | Up to 1 L |

EDTA, ethylenediaminetetraacetic acid.

### 1.6.4. Storage of the Transformant Bacteria

To store the transformant bacteria, the OD of grown cultures was measured every 30 minutes until it reached 0.4 at λ=595 nm. The bacterial culture and 50% (v/v) glycerol in $dH_2O$ were mixed at a ratio of 1:1, and 1 ml of the mixture (final glycerol concentration: 25%) was transferred into cryovials. The bacteria were stored at -80°C until further use.

### 1.6.5. Confirmation of the Gene Sequences

Polymerase chain reaction (PCR) was performed to confirm the sequence identity of all GoI. To this end, we designed PCR forward and reverse primers (Table 3.3) specific to the TRE and EF1A promoter regions, respectively, using the online Primer3 software. Following the analysis of designed primers for potential cross-dimer, self-dimer, and hairpin formations using the NetPrimer analysis tool, they were purchased from Sentebiolab (Ankara, Turkey).

Table 3.3. Primers used for the sequencing of GoI regions on lentiviral plasmid vectors.

| Primer | Sequence |
|---|---|
| Forward | 5'-TCTTCCATTTCAGGTGTCGTG-3' |
| Reverse | 5'-GGCATTAAAGCAGCGTATCC-3' |

Gradient PCR was performed using the isolated DNA to determine the optimal melting temperature ($T_m$) for the primers. tTGv1 plasmid (due to its high concentration following the isolation) was selected as the template DNA for this procedure. A temperature range of 59.0-59.5°C was tested. PCR was performed on Veriti Thermal Cycler (Applied Biosystems) using AQ90 High Fidelity DNA Polymerase (Ampliqon #A457403) according to the manufacturer's instructions (Table 3.4 and Table 3.5).

Table 3.4. Components of the AQ90 High Fidelity DNA Polymerase reaction mixture.

| Component | Amount |
|---|---|
| AQ Buffer (10X) | 2.5 µl |
| dNTP (10 mM) | 0.5 µl |
| Forward Primer (10 µM) | 0.5 µl |
| Reverse Primer (10 µM) | 0.5 µl |
| AQ Polymerase | 0.25 µl |
| Template DNA | 500 ng |
| NFW | Up to a total of 25 µl |

dNTP, deoxynucleotide triphosphate; NFW, nuclease-free water

Table 3.5. PCR program for AQ90 High Fidelity DNA Polymerase.

| Number of cycles | Duration of cycle | Temperature |
|---|---|---|
| 1 | 2 min | 95°C |
| | 20 sec | 95°C |
| 25 | 30 sec | $T_m$* |
| | 30 sec | 72°C |
| 1 | 5 min | 72°C |

*$T_m$: 59.0-59.5°C was tested to find the optimal temperature in gradient PCR experiments.

The primers were designed so that the GoI region present between the TRE and EF1A promoters on all plasmid vectors would be included in the product; thus, the sizes of the products would vary according to the particular GoI on each vector. Expected PCR product lengths for each vector are given in Table 3.6. Following the determination of the optimal $T_m$, PCR was performed using all vectors as a template. The PCR products were run on 2% (w/v) agarose gel and visualized as described above in this section. After confirming the specific amplifications based on the expected product sizes, the same PCR products and primers were used for Sanger sequencing (Triogen Biyoteknoloji, Istanbul, Turkey). The Basic Local Alignment Search Tool (BLAST) and ClustalW multiple alignment tool from the NCBI website were used to confirm sequence identities.

Table 3.6. Expected PCR product sizes for each plasmid vector.

| Vector | Product size (bp) |
|---|---|
| TG2 | 2735 |
| TGH | 2318 |
| TGH2 | 1721 |
| tTGv1 | 2696 |
| tTGv2 | 2609 |
| EGFP | 1391 |
| Mock | 977 |

EGFP, enhanced green fluorescent protein.

## 1.7. CELL LINES AND HANDLING

Renal proximal tubule epithelial cells (RPTECs) were obtained from ATCC (#PCS-400-010) and cultured in renal epithelial cell basal medium (RECBM; ATCC #PCS-400-030)

supplied with a renal epithelial cell growth kit (ATCC #PCS-400-040; Table 3.7). For subculturing, the cells were collected with trypsin-EDTA (0.05% trypsin and 0.02% EDTA), centrifuged at 150 x*g* for 5 minutes, seeded at a minimum density of 5000 cells/cm$^2$, and placed in an incubator at 37°C, 5% $CO_2$, with humidified air. The cells were not detached unless a 95% confluency was reached.

Table 3.7. Components of the renal epithelial cell growth kit.

| Component | Volume | Final Concentration |
|---|---|---|
| FBS | 2.5 ml | 0.5% |
| Triiodothyronine | 0.5 ml | 10 nM |
| rh EGF | 1.0 ml | 10 ng/ml |
| Hydrocortisone hemisuccinate | 0.5 ml | 100 ng/ml |
| rh insulin | 0.5 ml | 5 µg/ml |
| Epinephrine | 0.5 ml | 1 µM |
| Transferrin | 0.5 ml | 5 µg/ml |
| L-alanyl-L-glutamine | 6.0 ml | 2.4 mM |

293-FT cells were obtained from Invitrogen (#R70007) and routinely cultured in Dulbecco's Modified Eagle's Medium (DMEM, high glucose; Gibco #11965092) supplied with 10% (v/v) fetal bovine serum (FBS; Gibco #16000044), 100 U/ml penicillin/streptomycin, and 1 µg/ml gentamycin; during transfection, DMEM without gentamycin was used.

## 1.8. ESTABLISHING RENAL EPITHELIAL CELLS EXPRESSING TG2 ISOFORMS

### 1.8.1. Lentiviral Particle Production in 293-FT cells

In order to produce lentiviral particles for the transduction of RPTECs with TG2 isoforms, plasmid vectors were transfected to 293-FT cells using the calcium chloride method. For this purpose, 293-FT cells were seeded into 10-cm cell culture dishes at a concentration of 1x10$^6$ cells/dish in DMEM and allowed to attach overnight. Fresh culture medium was supplied to the cells 2 h prior to transfection. 293-FT cells were then treated with the transfection mixture (Table 3.8) prepared using 0.1X tris-EDTA (TE), 2.5 mM CaCl2, 2X HEPES-buffered saline (HBS) containing the plasmid vectors carrying the GoI (Tet-On vectors), Gag, Pol, Rev

packaging genes (psPAX2; Figure 3.8), and the VSV-G envelope gene (pMD2.G; Figure 3.9). Following a 30-minute incubation, the transfection mixture was added dropwise onto the culture medium by gently shaking the dishes to ensure the spreading of the transfection mixture. Following a 14 h incubation, the cells were finally washed with 1X PBS and supplied with fresh culture media.

Table 3.8. Transfection buffer components.

| Buffer | Components |
|---|---|
| 2X HBS<br>(7.11 ≤ pH ≤ 7.13) | 280 mM NaCl<br>100 mM HEPES<br>1.5 mM $Na_2HPO_4$ |
| 0.1X TE | 1 mM tris (ultra-pure)<br>0.1 mM EDTA (pH 8.8) |

EDTA, ethylenediaminetetraacetic acid; HBS, HEPES-buffered saline; HEPES, 4-(2-hydroxyethyl)-1-piperazineethanesulfonic acid; TE, tris-EDTA.

The viral particles produced and released into the cell culture media were collected at 24 and 48 hours following the medium change. All collected media were pooled, filtered using 0.22 mm polyethersulfone (PES) membrane filters, and stored at -80°C until further use. Excess transfection buffers were stored at -20°C for up to one month.

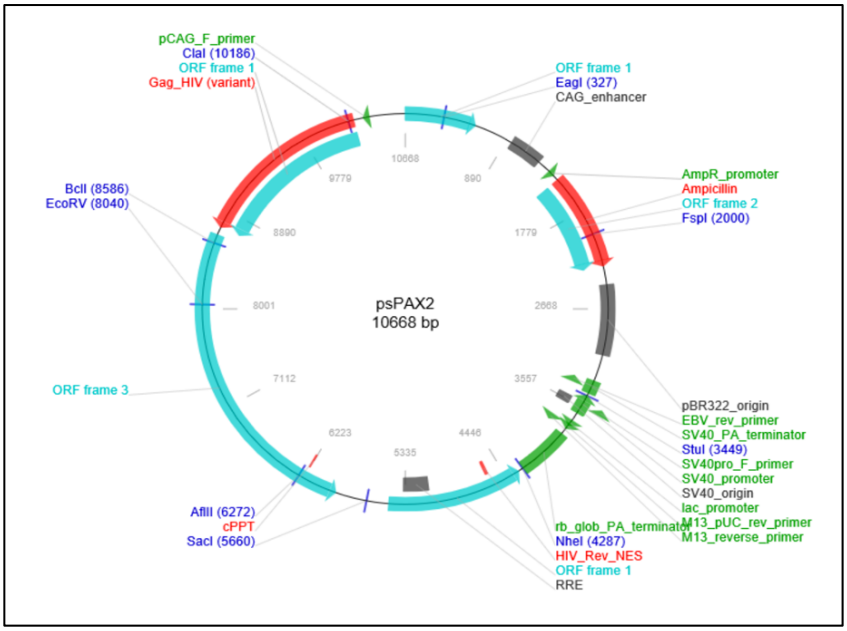



Figure 3.8. psPAX2 packaging plasmid map.

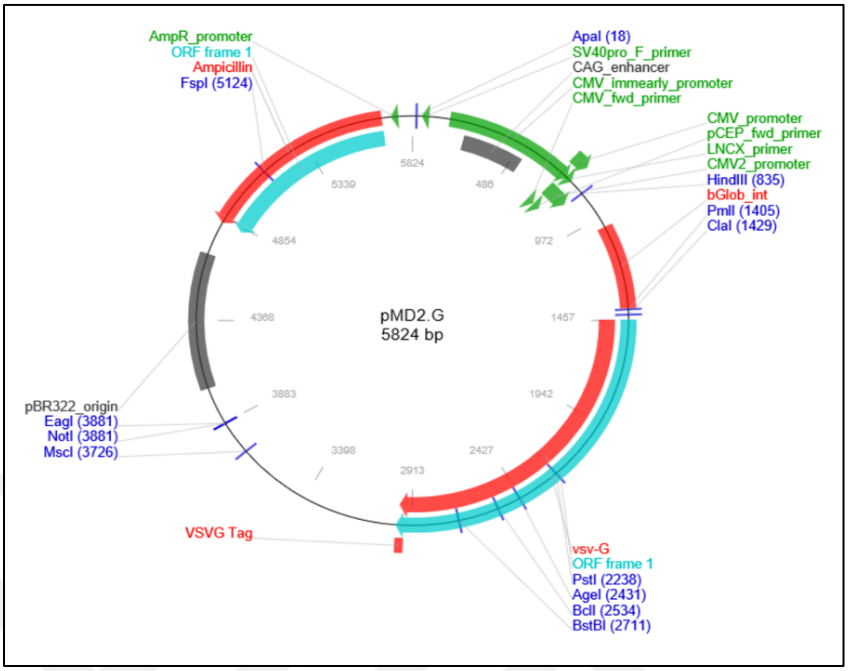



Figure 3.9. pMD2.G envelope plasmid map.

### 1.8.2. Transduction of RPTECs with the Lentiviral Particles

#### *1.8.2.1. Optimization of Pre-Treatment and Gene Expression Parameters*

To generate cell lines expressing various isoforms of TG2, RPTECs were transduced with lentiviral particles produced using HEK293-FT cells. Two important phases of the experiment required optimization: (i) pre-treatment with the polycation protamine sulfate and (ii) induction of gene expression.

To optimize the pre-treatment conditions for lentivirus delivery, different concentrations of protamine sulfate were tested. For this purpose, RPTECs were seeded in 6-well plates at a density of $3x10^5$ cells/well and allowed to attach. The next day, RPTECs were treated with 10, 25, and 50 µg/ml protamine sulfate in complete RECBM. After 2 hours of protamine sulfate pre-treatment, the cells were subjected to the EGFP lentiviral particle-containing media. Following 14 hours of incubation, the cells were washed with 1X PBS and allowed to recover in fresh culture media for another 24 hours. Transduced RPTECs were selected by treatment with 2.5 µg/ml Bsd. The selection proceeded until non-transformed control RPTECs were completely deceased due to the antibiotic treatment. For the optimal induction of gene expression, Dox treatment was tested at different time points. To induce gene

expression, the cells were subjected to 1 µg/ml Dox for 96 h. The cells were monitored for EGFP expression at each 24 h interval using the fluorescence imaging module of Cytell Cell Imaging System (GE Healthcare), and the optimal conditions for the most efficient transduction and gene expression were selected for the following experiments.

#### *1.8.2.2. Transduction of RPTECs with TG2 Isoforms*

Following the selection of optimal conditions, RPTECs were transduced with all lentiviral particles. As described in Section 3.2.2.1, RPTECs were seeded in 6-well plates at a density of $3x10^5$ cells/well, allowed to attach overnight, and then pre-treated with 10 µg/ml protamine sulfate for 2 h. The cells were then transduced with lentiviral particles carrying the TG2 isoforms for 14 h. Following the selection of transduced cells with 1 µg/ml Bsd, gene expression was induced by treatment with 1 µg/ml Dox for 48 to 96 hours. This procedure was followed for all experiments performed within the scope of this thesis.

## 1.9. CHARACTERIZATION OF THE TRANSDUCED CELLS

### 1.9.1. Analysis of TG2 Isoform mRNA Expression Profiles

#### *1.9.1.1. Optimization of the Melting Temperatures for TG2 Isoform Primers*

Primers specific for each TG2 isoform were designed and analyzed using the Primer3 NetPrimer tools, respectively, as defined in Section 3.1.5. Primer specificity was confirmed using the online alignment tool BLAST, available on the NCBI website. Primer sequences and the corresponding product sizes are shown in Table 3.9.

Table 3.9. Forward and reverse primers specific for TG2 transcriptional variants.

| Variant | Primer | Sequence | Product size (bp) |
|---|---|---|---|
| TG2 | Forward | 5'-CCCAAGCAGAAACGCAAG-3' | 246 |
| | Reverse | 5'-AGCCCTTCACAGCCTTCA-3' | |
| TGH | Forward | 5'-CCACATCACCAACAACACC-3' | 156 |
| | Reverse | 5'-CAGGAACACAGGGCTTTACC-3' | |
| TGH2 | Forward | 5'-CGAAGAGCACTGGAGTAGGAA-3' | 73 |
| | Reverse | 5'-CGCATTGAGAGTGTTGGTG-3' | |
| tTGv1 | Forward | 5'-GCTGGTGGCTGAGGTGTC-3' | 71 |

| | | | |
|---|---|---|---|
| | Reverse | 5’-GCTGGGATGTGGAGGTGC-3’ | |
| tTGv2 | Forward | 5’-GCTGGTGGCTGAGGTGTC-3’ | 70 |
| | Reverse | 5’-CACTGGTGTGGAGGTGCAG-3’ | |

bp, base pairs.

#### 1.9.1.1.1 Total RNA Isolation

For total RNA isolation, RPTECs were seeded in 6-well plates at a concentration of $3x10^5$ cells/well. Following attachment, the cells were homogenized in 250 µl of the TRIzol™ (Thermo Fisher) reagent and mixed with 50 µl of chloroform. After 15 minutes of incubation at room temperature, the cell homogenates were centrifuged at 12,000 x*g* for 15 minutes. RNA phase from each sample was transferred to a fresh 1.5 ml tube and mixed with an equal amount of isopropanol. After 10 minutes of incubation on ice, the samples were centrifuged at 12,000 x*g* and 4°C for 10 minutes. The pellets were then washed with 500 µl of 75% ethanol and centrifuged at 7,500 x*g* and 4°C for 10 minutes. The pellets were air-dried and then resuspended in 20 µl of RNase-free water. The RNA content was measured using NanoDrop™.

#### 1.9.1.1.2 cDNA Synthesis

cDNA was synthesized using the Sensiscript® reverse transcription kit (QIAGEN #205213) according to the manufacturer's instructions. The components required to prepare the reaction mixture are given in Table 3.10. The samples were incubated at 37°C for 1 hour using Veriti Thermal Cycler. cDNA concentrations were measured using NanoDrop™.

Table 3.10. Components of the Sensiscript reverse transcription kit reaction mixture.

| Component | Amount |
|---|---|
| Template RNA | 1000 ng |
| 10 µM Primer | 2 µl |
| 10X Reaction Buffer | 2 µl |
| Sensiscript Reverse Transcriptase | 1 µl |
| 5 µM dNTP | 2 µl |
| NFW | Up to 20 µl |

dNTP, deoxynucleotide phosphate; NFW, nuclease-free water.

1.9.1.1.3 Gradient PCR

Gradient PCR was performed as described in Section 3.1.5. Temperatures between 52 and 55°C were tested to determine the optimal $T_m$, and the bands were visualized using ChemiDoc XRS+.

### *1.9.1.2. Real-Time Quantitative PCR Analysis for TG2 Isoforms*

To analyze the TG2 isoform mRNA levels in transduced RPTECs, the cells were seeded in 6-well plates at a density of $3x10^5$ cells/well, and gene expression was induced with 1 µg/ml Dox for 96 h. Following total RNA isolation at every 24 h intervals and cDNA synthesis as described in section 3.4.1.1., quantitative PCR (qPCR) reaction mixtures were prepared using QuantiTect SYBR Green PCR Kit (QIAGEN #204143; Table 3.11). qPCR reactions were carried out using the Step One Plus Real Time PCR instrument (Applied Biosciences) according to the thermal cycle protocol in Table 3.12. The data was analyzed using the standard curve method. 18s rRNA was used as the internal control.

Table 3.11. QuantiTect SYBR Green PCR Kit reaction mixture.

| Component | Final Concentration |
|---|---|
| 2X QuantiTect SYBR Green PCR Master Mix | 1X |
| Forward primer | 1 µM |
| Reverse primer | 1 µM |
| cDNA Template | 500 ng |
| NFW | Up to 12.5 µl |

NFW, nuclease-free water.

Table 3.12. Thermal cycle protocol for QuantiTect SYBR Green PCR Kit.

| Step | Temperature | Duration | Cycle |
|---|---|---|---|
| Activation | 94°C | 15 minutes | 1 |
| Initial denaturation | 95°C | 5 minutes | 1 |
| Denaturation | 95°C | 60 seconds | |
| Annealing | $T_m^*$ | 60 seconds | 40 |
| Extension | 72°C | 60 seconds | |
| Final extension | 72°C | 10 minutes | 1 |
| Melt curve | 65-80°C | +0.5°C/12 sec | 1 |

### 1.9.2. Detection of TG2 Isoforms on RPTEC Membranes

The localization of TG2 isoforms on RPTEC outer membranes was assessed by flow cytometry. To this end, following the transduction and induction of RPTECs in 6-well plates as described in Section 3.2.2.2., the cells were detached with 2 mM EDTA in PBS (pH 7.4). After incubation at 37°C for 5 minutes, the cells were gently collected and centrifuged at 150 x*g* for 5 minutes. The cell pellets were resuspended in PBS-BSA (0.5% [w/v] heat-inactivated BSA in PBS; pH 7.4) and centrifuged at 150 x*g* for 5 minutes. Meanwhile, the fluorescein (FITC)-conjugated anti-Flag antibody (Sigma #F4049; final concentration: 5 µg/ml) was prepared in PBS-BSA. The cell pellets were resuspended in 500 µl of the antibody solution, and the sample tubes were placed on a rotator. The cells were incubated at 4°C for 1 hour and an additional 30 minutes at 37°C. An equal concentration of mouse IgG was used as a negative control. Finally, the cells were washed twice in PBS (150 x*g* for 5 min) and resuspended in 500 µl of 0.05% (w/v) formaldehyde. The cells were analyzed for cell surface expression of TG2 isoforms using the FACSCalibur™ flow cytometer (BD Biosciences) and CellQuest Pro Software.

## 1.10. ANALYSIS OF THE EFFECTS OF TG2 ISOFORMS ON CELLULAR PROCESSES

### 1.10.1. Analysis of Cell Proliferation

Transduced RPTECs were seeded in 96-well plates at a density of 2000 cells/well and allowed to attach. Next, gene expression was induced with 1 µg/ml Dox for 96 hours. At every 24-hour interval, the cells were subjected to WST-1 (ROCHE #11644807001) cell proliferation reagent (diluted 1:10 in RECBM) at 37°C for 1 hour. At the same time, for the analysis of cell numbers, RPTECs transduced with the mock vector (RPTEC-Mock) were seeded into 96-well plates at a density of 1000, 2000, 3000, 4000, and 5000 cells/well. These cells were treated with the WST-1 reagent after cell attachment, and a standard curve was plotted using the absorbance values obtained at 420 and 480 nm wavelength. Cell numbers

of all transduced RPTECs were calculated using the absorbance values obtained at each time point. To observe the long-term effects of TG2 isoforms on cell proliferation, transduced RPTECs were also observed for the 96 hours after the completion of Dox induction.

### 1.10.2. Analysis of the Cell Cycle

#### *1.10.2.1. Cell Cycle Analysis with Cytell*

The effect of TG2 isoforms on the cell cycle was first assessed using the Cytell cell imaging system. For this purpose, transduced RPTECs in 6-well plates were induced with Dox for 48 hours. Then, the cells were seeded in 96-well plates at a density of 2000 cells/well and allowed to attach overnight. As a control of cell cycle arrest at the early S phase, RPTEC-Mock cells were treated with 3 µg/ml aphidicolin for 24 hours. On the day of the experiment, the cells were washed with 1X PBS and fixed with 4% (w/v) paraformaldehyde for 15 minutes at room temperature. The cells were then permeabilized in 0.05% Triton X-100 in PBS for 5 minutes at room temperature and treated with 50 µg/ml RNase A at 37°C for 30 minutes to degrade RNA and eliminate the background signal. Following the treatment with propidium iodide (PI) at a concentration of 5 µg/ml for 5 minutes, cell monolayers were washed once with 1X PBS. Finally, 200 µl of PBS was placed into each well, and the signal intensity was analyzed using the orange filter of the Cytell imaging device.

#### *1.10.2.2. Flow Cytometry Analysis of Cell Cycle*

Similar to the analysis with Cytell (Section 3.5.2.1.), RPTECs were induced with Dox for 48 hours. The cells were then seeded into 6-well plates at a density of $3x10^5$ cells/well. After attachment, the cells were collected with trypsin, centrifuged at 150 x*g* for 5 minutes, and fixed in 500 µl of 70% ethanol (in PBS) for 2 hours at room temperature. The cell membranes were then permeabilized with 0.05% Triton X-100 (in PBS) for 5 minutes at room temperature and treated with PI (5 µg/ml, 5 minutes) immediately before flow cytometry analysis.

#### *1.10.2.3. Western Blotting for Cell Cycle Proteins*

1.10.2.3.1 Protein Isolation

RPTECs were induced as described in previous sections and seeded into 6-well plates at $3x10^5$ cells/well. Proteins were isolated at 96 hours following the first Dox treatment. After

washing the cells and completely draining PBS, 30 µl RIPA buffer was added to each well. The cells were then collected using scrapers and transferred into 1.5 ml tubes. Sonication was performed at 60 kHz (three cycles), and the samples were centrifuged at 1000 xg for 1 minute. The supernatants were transferred into clean 1.5 ml tubes and stored at -80°C until use.

1.10.2.3.2 Protein Content Assay

A detergent-compatible protein assay was performed to assess the protein content. First, a 500 µg/ml bovine serum albumin (BSA) working stock was prepared. The stock solution was subjected to heat inactivation at 57°C for 1 h. Next, protein standards of 10, 25, 50, 75, and 100 µg/ml were prepared by serial dilution. Meanwhile, all protein samples obtained from RPTECs were diluted in $dH_2O$ at a ratio of 1:10.

Using a 96-well plate, 5 µl of the standards and protein samples were mixed with 25 µl of Protein Assay Reagent A (Bio-Rad #5000113) and 200 µl of Protein Assay Reagent A (Bio-Rad #5000114) in triplicates. Absorbance values were obtained at 750 nm wavelength using a microplate reader (SpectraMax Paradigm Multi-Mode Microplate Reader, Molecular Devices), and protein concentrations were calculated using the BSA calibration curve.

1.10.2.3.3 SDS-PAGE and Western Blotting

Protein lysates denatured in Laemmli buffer at 95°C for 5 minutes were loaded into 12% sodium dodecyl sulfate-polyacrylamide (SDS-PA) gels prepared according to Table 3.13 and Table 3.14 and subjected to GE at 75 V for approximately 3 h. A Mini-PROTEAN Tetra Handcast System and PowerPac™ Basic Power Supply (BioRad) were used for gel preparation and running.

Table 3.13. SDS-PA gel buffers.

| | **4X Tris-SDS (lower gel buffer)** | **4X Tris-SDS (upper gel buffer)** |
|---|---|---|
| Tris Base | 1.5 M | 0.5 M |
| SDS | 0.4% (w/v) | 0.4% (w/v) |
| pH | 8.8 | 6.8 |

SDS, sodium dodecyl sulfate.

Table 3.14. SDS-PA gel compositions.

| | Separating Gel | Stacking Gel |
|---|---|---|
| Acrylamide/bis-acrylamide | 6 ml | 0.65 ml |
| Lower buffer | 3.75 ml | - |
| Upper buffer | - | 1.25 ml |
| APS | 50 µl | 25 µl |
| TEMED | 10 µl | 5 µl |
| $dH_2O$ | 5.20 ml | 3.25 ml |

APS, ammonium persulfate; TEMED, tetramethyl ethylenediamine.

Using a Mini Trans-Blot Module (Bio-Rad), the proteins were transferred onto nitrocellulose membranes of 0.22 or 0.45 mm pore size, depending on the molecular weight of the target proteins. Wet transfer was performed at 175 mA for 1.5 h for proteins of approximately 30-150 kDa.

Running and transfer buffers (10X) were prepared according to Table 3.15. The running buffer was diluted to 1X in $dH_2O$. The transfer buffer was diluted to 1X in $dH_2O$ with 20% (v/v) methanol. Both buffers were cooled at 4°C before use.

Table 3.15. Running and transfer buffer recipes.

| | 10X Running buffer | 10X Transfer buffer |
|---|---|---|
| Tris base | 0.25 M | 0.25 M |
| Glycine | 1.92 M | 1.92 M |
| SDS | 1% (w/v) | - |
| pH | 8.5 | 8.3 |

SDS, sodium dodecyl sulfate.

Blocking of the membranes was performed for 1 hour in 5% (w/v) non-fat milk prepared in 1X tris-buffered saline with Tween 20 (TBS-T; 1:1000). The membranes were incubated overnight with the primary antibodies for cyclin D1 (Cell Signaling Technology; CST #2978), cyclin D3 (CST #2936), cyclin E1 (CST #4129), CDK2 (CST #2546), CDK4 (CST #12790), and β-Actin (CST #4967) at a dilution of 1:1000 in 5% milk solution overnight at 4°C. HRP-linked anti-rabbit (CST #7074) or anti-mouse secondary antibodies were used depending on the source organism for each antibody (1:3000 in 5% milk; 2 hours at room temperature). The membranes were washed thrice in TBS-T for 10 minutes between each

step starting from blocking until the imaging, with an exception in the final wash step, which was performed using 1X TBS (Table 3.16).

Table 3.16. Preparation of 10X TBS (pH 7.6).

| Component | Concentration |
|---|---|
| Tris base | 0.2 M |
| NaCl | 0.15 M |

NaCl, sodium chloride.

Clarity Western ECL Substrate (Bio-Rad, #1705061) or WesternBright Sirius (Advansta, #K-12043-D20) was used to obtain luminescence. The chemiluminescence module of the ChemiDoc XRS+ imaging system and ImageLab software were used to visualize the bands.

### 1.10.3. Analysis of the EMT and MMP Profiles

#### *1.10.3.1. Analysis of EMT*

To analyze the effect of TG2 isoforms on EMT, mRNA expressions of specific markers were analyzed by qPCR. Transduced RPTECs were seeded in 12-well plates at a density of $1x10^5$ cells/well and subjected to Dox treatment. Total RNA was extracted, and cDNA was synthesized as described in Section 3.4.1. PCR primers for E-cadherin (*CDH1*), N-cadherin (*CDH2*), Snail 1 (*SNAI1*), Snail 2 (*SNAI2*), Zeb 1 (*ZEB1*), Zeb 2 (*ZEB2*), Twist 1 (*TWIST1*), Twist 2 (*TWIST2*), and vimentin (*VIM*) were obtained from QIAGEN (QuantiTect Primer Assay; #249900). qPCR was performed according to Table 3.12. No prior optimization was required since these primers are compatible with the QuantiTect SYBR Green PCR Kit for a $T_m$ of 55°C. Quantification was based on a standard curve, and 18s rRNA was used as an internal control.

#### *1.10.3.2. Analysis of the MMP Profile*

To investigate the invasion profile of transduced RPTECs, RNA was extracted as described in the previous section. QuantiTect Primer Assays for MMPs (1, 2, 9, and 13) were obtained from QIAGEN, and qPCR was performed according to Table 3.12. Quantification of MMPs in transduced RPTECs was based on the standard curve method, and 18s rRNA was used as an internal control.

#### *1.10.3.3. Analysis of Cell Mobility*

Transduced RPTECs were seeded into 24-well plates at a concentration of 300,000 cells/well and allowed to attach for 24 hours. Straight lines were drawn on cells using a six-comb Scratcher. The scratched zones were recorded immediately (at 0 h), for each well using the Cytell imaging module. The migration of RPTECs to the scratched area was captured at every 24 h interval until the end of 72 h, and the percentage of wound closure was calculated using ImageJ.

## 1.11. ANALYSIS OF TG2 ISOFORM EXPRESSION IN PATIENTS WITH RCC

### 1.11.1. Bioinformatic Analysis of a Reported RCC Dataset

Using the previously reported GSE47032 microarray dataset [240, 241], we accessed the characteristics of ten patients with ccRCC and analyzed the signal intensities of TG2 isoform-specific probes in normal and tumor tissue samples of each patient. Specific detection of TG2 isoforms by different probes of the Affymetrix GeneChip Human Exon 1.0 ST array was reported as follows: probe 3905188 for the full-length TG2, probe 3905161 for TGH, probes 3905171 and 3905172 for TGH2, probe 3905147 for tTGv1, and probe 3905148 for tTGv2 [240]. The CFL file containing the chip coordinates of the Affymetrix GeneChip Human Exon 1.0 ST Array was downloaded from the manufacturer's website, and the CEL files containing the signal intensity information were downloaded from the GEO database. The signal intensities from each sample corresponding to the isoform-specific probes were recorded to generate heat maps and bar graphs using MATLAB and GraphPad, respectively.

### 1.11.2. qPCR Analysis of TG2 Isoform Levels in Patients with RCC

In order to determine TG2 isoform expression levels in patients with RCC, tissue biopsies were obtained from a total of 55 patients and histopathologically analyzed at Istanbul Goztepe Prof. Dr. Suleyman Yalcin City Hospital. The institutional review board approved the study protocol (#2020/0423). Tissue samples were dried and stored at -80°C until use. Tumor samples and normal counterparts were homogenized in TRIzol™ using a teflon

homogenizer. The rest of the procedure was the same as described in Section 1.9.1. qPCR was performed using the isoform-specific primers in Table 3.9 and protocol in Table 3.12.

## 1.12. STATISTICAL ANALYSIS

Data obtained from three independent experiments were represented as means ± standard deviation (SD). Differences between group means were analyzed using the Student t-test. Multiple comparisons were performed using one-way analysis of variance (ANOVA), followed by Dunnett's Test. A p-value of less than 0.05 was considered statistically significant. Microsoft Excel (2019) was used for the analyses, and the graphs were generated using GraphPad Prism (version 8.4.3; GraphPad Software, USA; free trial downloaded from www.graphpad.com).

# 4. RESULTS

## 1.13. TG2 ISOFORM LEVELS IN PATIENTS WITH RCC

### 1.13.1. Altered Expression Profiles of TG2 Isoforms in ccRCC

In 2013, a study identified 2,462 differentially expressed genes between ccRCC tumor tissue samples and adjacent normal tissues by carrying out expression analyses both at the gene and exon levels [241]. Based on their microarray results obtained using the Affymetrix GeneChip Human Exon 1.0 ST Array, the authors reported a number of novel potential markers for the diagnosis of RCC and shared their database on Gene Expression Omnibus (GEO) with accession number GSE47032. In 2018, another study analyzed the levels of TG2 isoforms in ten patients with ccRCC in the GSE47032 dataset. The authors reported the specific detection of TG2 isoforms by different probes of the Affymetrix GeneChip Human Exon 1.0 ST array [240]; however, the study did not focus on the direct comparison of TG2 isoform levels in normal renal and RCC tumor tissues.

Using the GSE47032 dataset, we accessed the characteristics of the ten ccRCC patients and analyzed the signal intensities obtained from the reported isoform-specific probes in cancerous and non-cancerous tissue samples of each patient. The heat maps and relative expression levels of TG2 isoforms are provided in Figure 4.1. Based on our analysis, at least one TG2 isoform was upregulated along with the full-length TG2 in four out of ten tumor tissues (patients 5, 8, 9, and 10) compared with the levels in normal counterparts from the same patients.

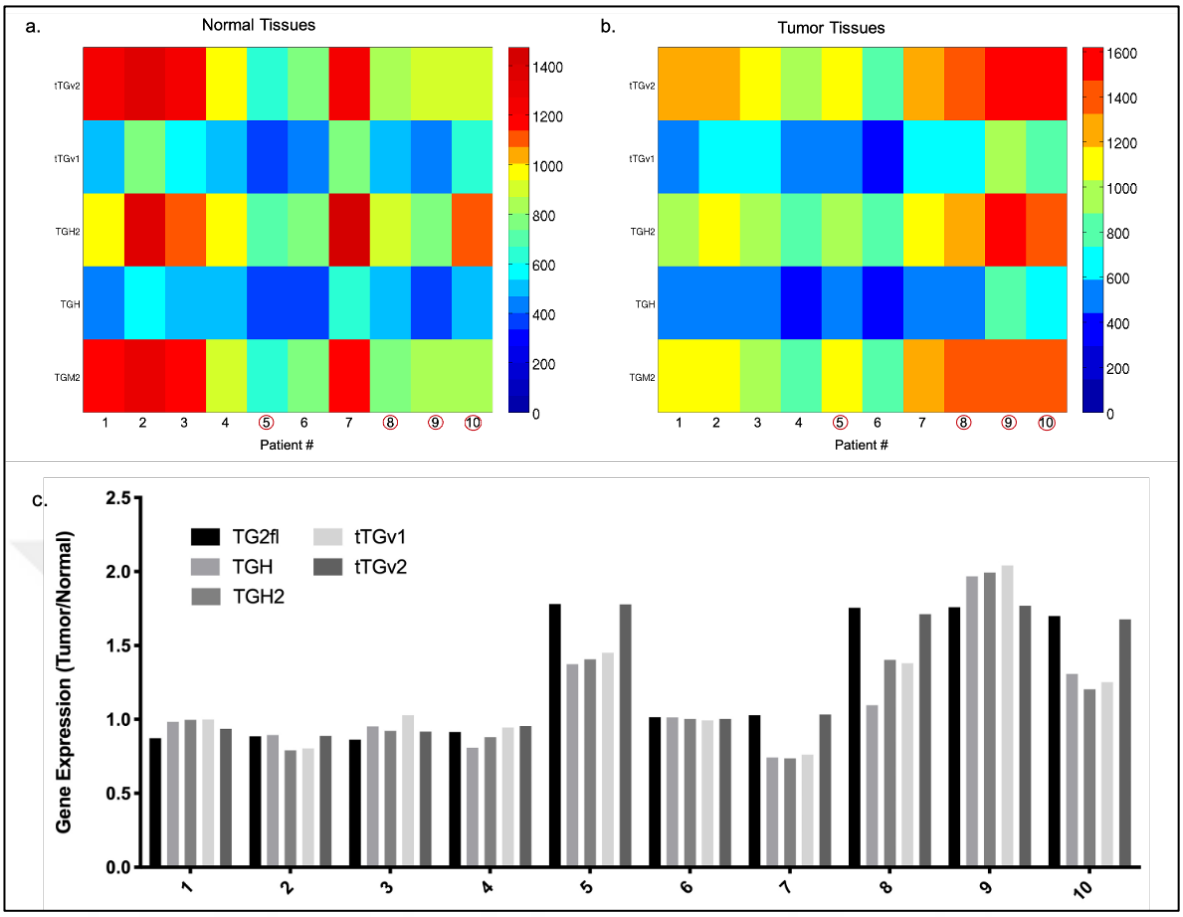



Figure 4.1. TG2 isoform expression levels in patients with ccRCC accessed from the GSE47032 dataset and analyzed using the signal intensities of probes specific to each isoform (TG2, 3905188; TGH, 3905161; TGH2, 3905171 and 3905172; tTGv1, 3905147; tTGv2, 3905148).

### 1.13.2. Association of TG2 Isoforms with RCC Grade and Stage

In order to elaborate on the differential expression of TG2 isoforms in ccRCC patients (Figure 4.1), we analyzed TG2 and TG2 isoform mRNA levels in control and tumor tissues of partial nephrectomy samples from a larger patient population with non-metastatic ccRCC. TG2 and TG2 isoform mRNA expression levels in normal and tumor tissue samples of the patients with RCC were analyzed by qPCR, and the results were expressed as relative expression levels ("Tumor/Normal") to study the changes in mRNA levels. The association of expression levels with the Fuhrman grade and T stage were investigated. The demographic data of enrolled patients are summarized in Table 4.1. Sex at birth and BMI

were not correlated with TG2 or TG2 isoform mRNA levels. Only a weak negative correlation (R=-0.2785, p=0.04) was found between TGH mRNA levels and age (at the time of surgery).

Table 4.1. Demographic and clinical characteristics of the patients.

| | **Study Population (N=40)** |
|---|---|
| **Sex at birth, N (%)** | |
| Female | 15 (37.5) |
| Male | 25 (62.5) |
| **Age at the time of surgery, mean (SD)** | 57.1 (12.4) |
| **BMI (kg/m$^2$), mean (SD)** | 28.9 (5.0) |
| **T Grade, N (%)** | |
| pT1a | 7 (17.5) |
| pT1b | 8 (20.0) |
| pT2a | 7 (17.5) |
| pT2b | 2 (5.0) |
| pT3a | 16 (40.0) |
| **Fuhrman Grade, N (%)** | |
| G1 | 10 (25.0) |
| G2 | 18 (45.0) |
| G3 | 9 (22.5) |
| G4 | 3 (7.5) |

The patients were grouped based on Fuhrman grades to identify potential associations with isoform levels (Figure 4.2). Our analyses showed that high TG2 expression was significantly associated with high Fuhrman grades (G3 and G4; p<0.001). High tTGv1 and tTGv2 mRNA levels in tumor tissues were also significantly associated with high Fuhrman grades (p=0.021 and p=0.028, respectively). No association was found between the mRNA expression levels of TGH or TGH2 and Fuhrman grade.

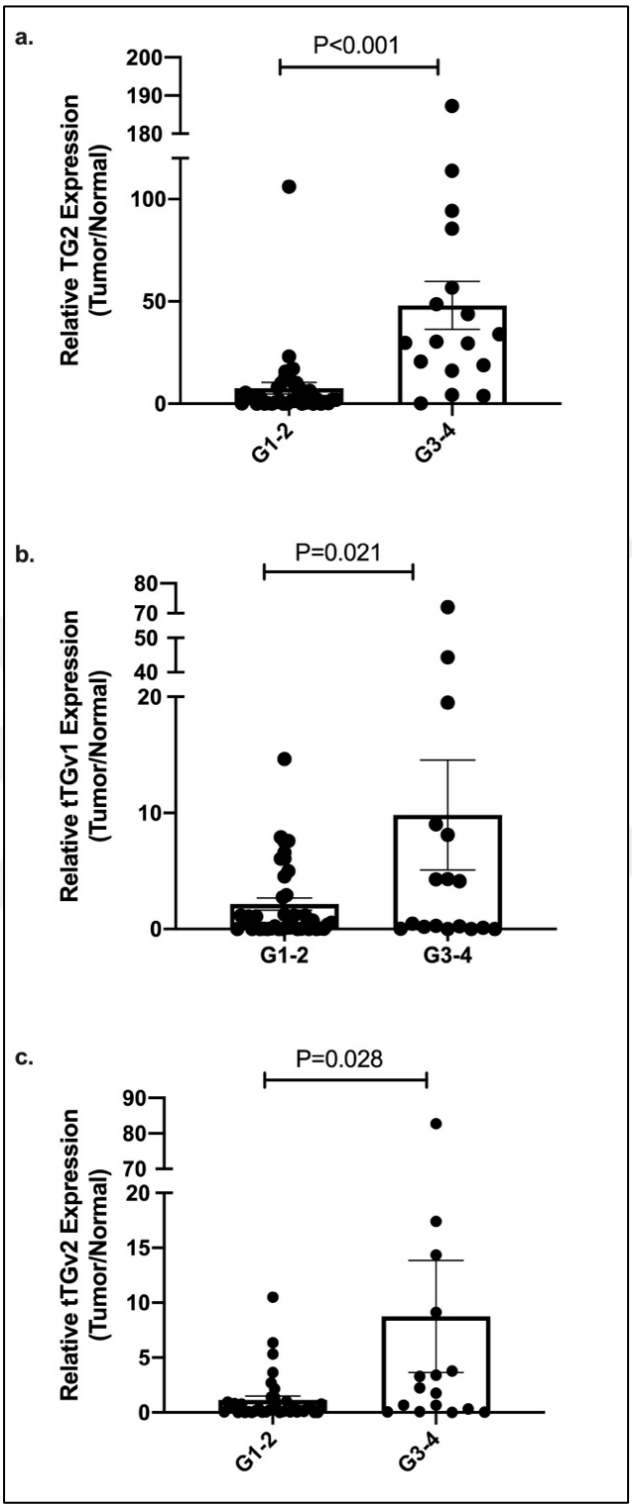



Figure 4.2. Differences in TG2 isoform mRNA expression levels between low (G1 and G2) and high Fuhrman grades (G3 and G4). High levels of (a) the full-length TG2, (b) tTGv1, and (c) tTGv2 were significantly associated with high Fuhrman grades. Two-tailed Student's t-test was used to compare the group means. Scatter plots represent the data as the mean ± SEM.

The potential association of tumor size with TG2 isoform mRNA expression levels was analyzed in subgroups of patients categorized based on the pT grade (Figure 4.3). According to the analyses, only TG2 was significantly associated with high pT grade (pT3; p=0.028). No significant association was found between TG2 isoform levels and tumor size when the patients were sub-divided into two groups as “pT1” and “pT>2.”

In an additional analysis, the association between the full-length TG2 levels and those of the isoforms was studied. The patients were subdivided into two groups based on the changes in TG2 mRNA levels: Patients with higher TG2 mRNA levels in their tumor tissues compared with the normal counterparts (TG2>1) and those with decreased TG2 mRNA levels (TG2<1). No significant association was found between an increase in TG2 and increased alternatively spliced isoform (p>0.5 for all).

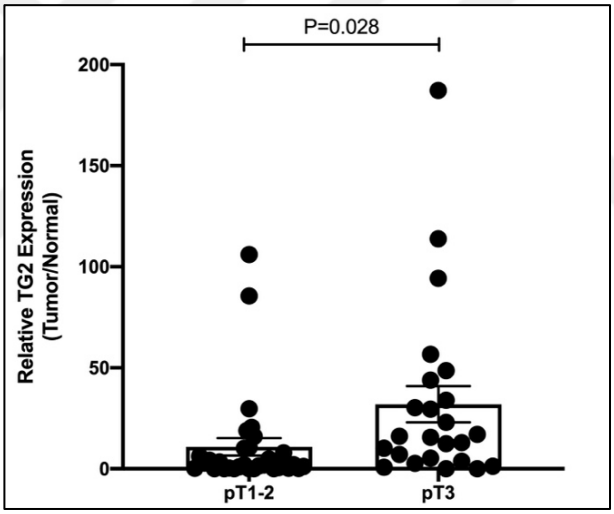



Figure 4.3. Differences in TG2 mRNA expression levels between low (pT1-2) and high T grades (pT3). A high level of TG2 was significantly associated with a high tumor size. Two-tailed Student’s t-test was used to compare the group means. Scatter plots represent the data as the mean ± SEM.

## 1.14. CHARACTERIZATION OF LENTIVIRAL PLASMID VECTORS

As described in Section 3.1, transformant bacterial colonies carrying the TG2, TGH, TGH2, tTGv1, tTGv2, EGFP, and Mock plasmids were grown on LB agar plates prior to the plasmid

isolation. Colony formation was observed in each plate streaked with the respective Amp-resistant bacteria (Figure 4.4).

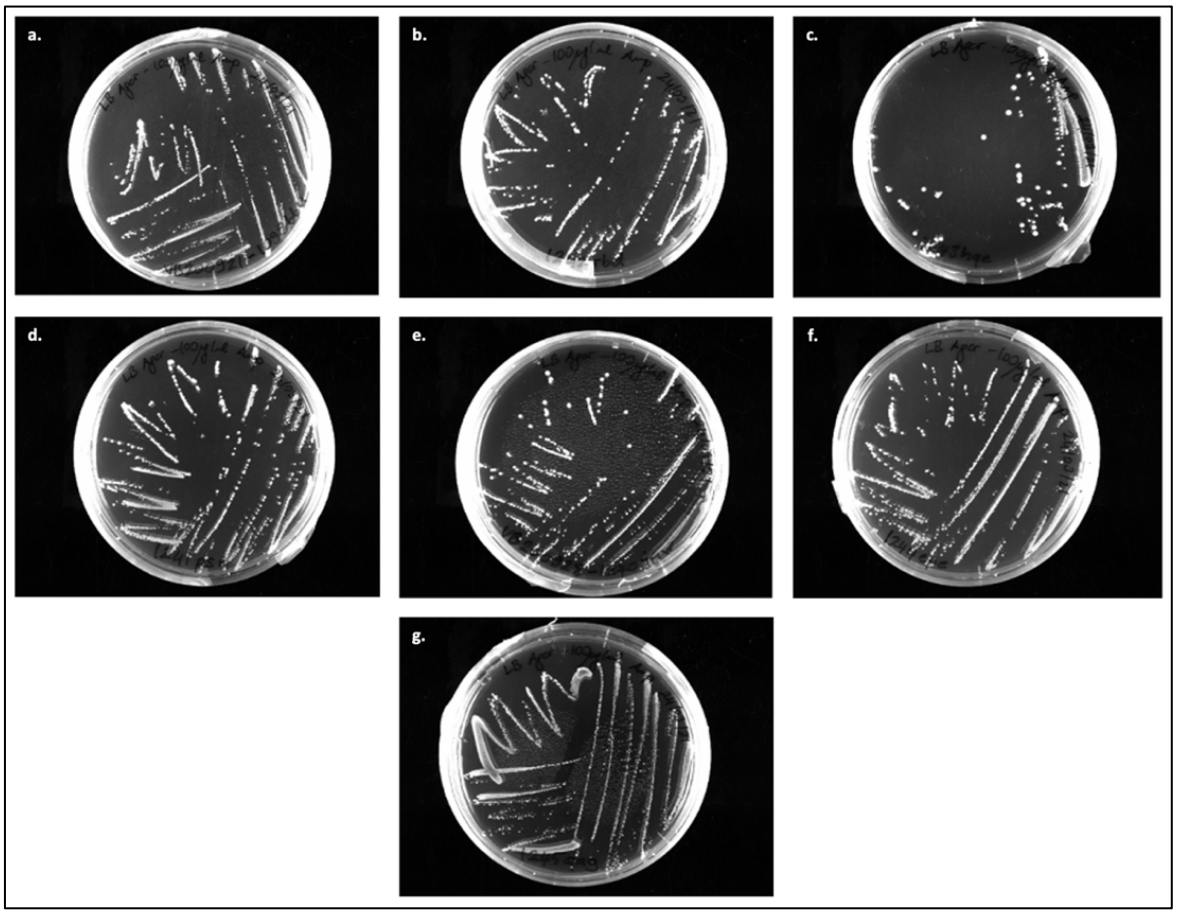



Figure 4.4. Bacterial colonies on LB agar plates. Transformant bacteria carrying (a) TG2, (b) TGH, (c) TGH2, (d) tTGv1, (e) tTGv2, (f) EGFP, and (g) Mock (vehicle control) plasmids were grown on LB agar containing 100 µg/ml Amp. The colonies were visualized using the Epi-white illumination source of the ChemiDoc XRS+ system.

Following the growth of selected colonies in LB broth and isolation of the plasmid DNA, gradient PCR was performed using the tTGv1 plasmid as a template DNA, which was selected as it possessed the highest concentration among other plasmids after the isolation. Forward and revers primers were designed to be universal for each TG2 isoform as they target the sequences specific to the TRE and EF1A promoters present on the vector backbone (Table 3.3). The region including the tTGv1 ORF was amplified at temperatures between 59.0–59.5°C using this universal primer pair. The optimum $T_m$ for these primers was determined to be 59°C, as implied by the higher DNA band intensity obtained (Figure 4.5).

No amplification was observed between 59.3–59.5°C. Therefore, in the next step, all GoIs were amplified by PCR at 59°C. The results of agarose GE showed expected product sizes (Table 3.6), confirming the specific amplification of the target regions (Figure 4.6).

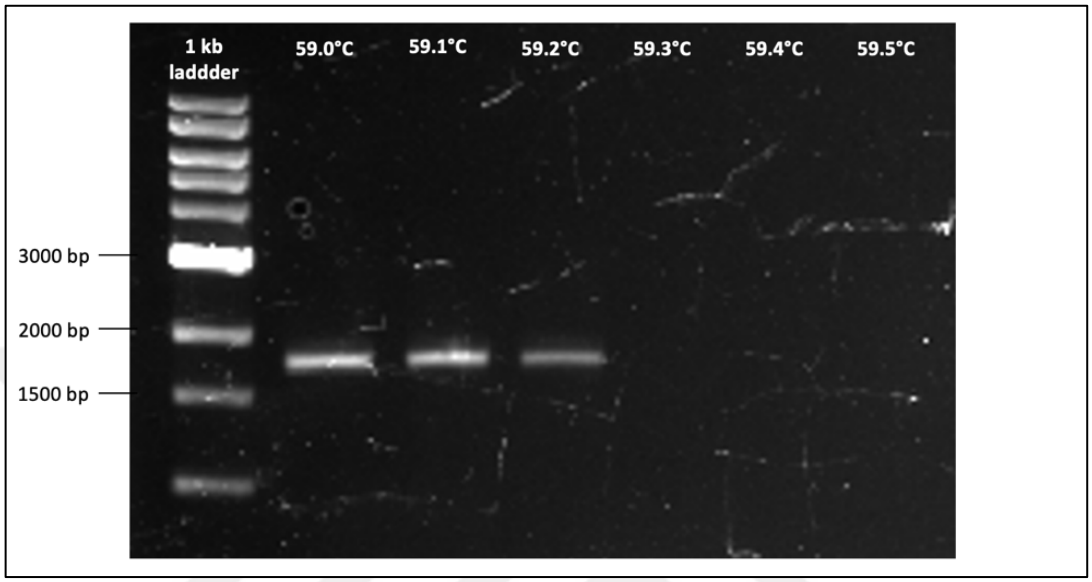



Figure 4.5. tTGv1 regions (2696 bp) amplified from the vector by gradient PCR. The DNA bands were visualized using the UV mode of the ChemiDoc XRS+ system.

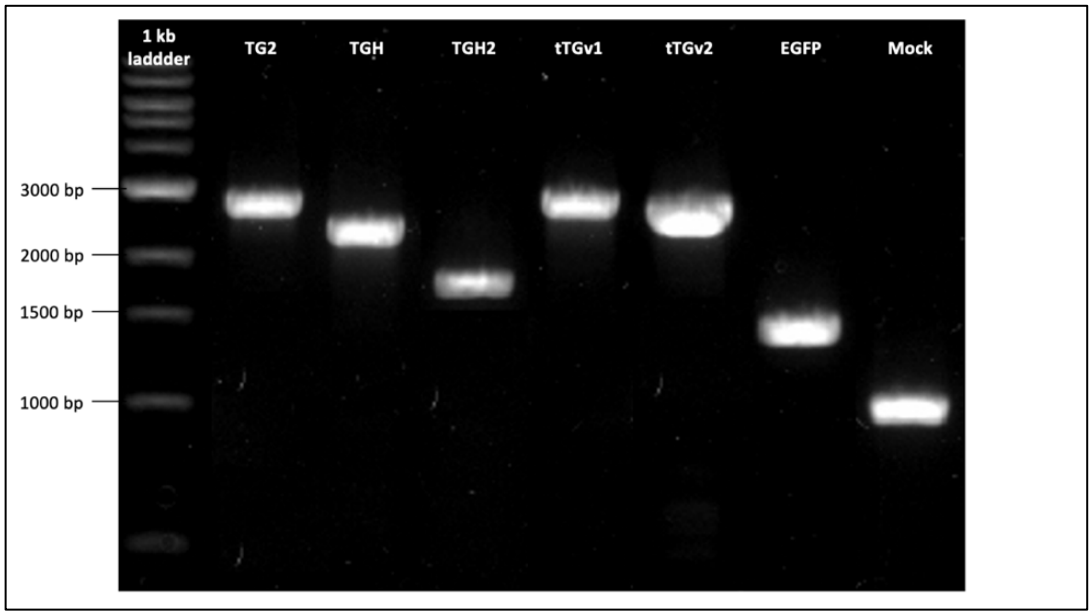



Figure 4.6. TG2 (2735 bp), TGH (2318 bp), TGH2 (1721 bp), tTGv1 (2696 bp), tTGv2 (2609 bp), EGFP (1391 bp), and stuffer DNA (Mock; 977 bp) regions amplified from the vectors by gradient PCR. DNA bands were visualized using the UV mode of the ChemiDoc XRS+ system.

The amplified PCR products were then analyzed using Sanger sequencing by outsourcing. Using the BLAST tool of NCBI, the similarities between the theoretical and experimental sequences were found between 97–100% for all isoforms (Table 4.2). The alignment quality of the sequences was confirmed by the high bit-scores and E values equal to zero.

Table 4.2. BLAST analysis results of the TG2 isoform sequences.

| Query | Bit-Score | E Value | Max Identity |
|---|---|---|---|
| TGM2 | 2383 | 0,0 | 98% |
| TGH | 2080 | 0,0 | 100% |
| TGH2 | 1986 | 0,0 | 100% |
| tTGv1 | 2353 | 0,0 | 97% |
| tTGv2 | 1823 | 0,0 | 99% |

## 1.15. TRANSFECTION EFFICIENCY

293-FT cells were transfected with lentiviral TG2, TGH, TGH2, tTGv1, tTGv2, EGFP, and Mock plasmids as described in Section 3.3.1. After the collection of viral particles released into the culture medium at 48 and 72 hours after transfection, cells transfected with the EGFP plasmid simultaneously treated with 1 µg/ml Dox were visualized under the fluorescent microscope. Reporter expression was detected using the filter with an excitation and emission wavelength of 489 and 509 nm, respectively (Figure 4.7), and the production of lentivirus in cells was confirmed.

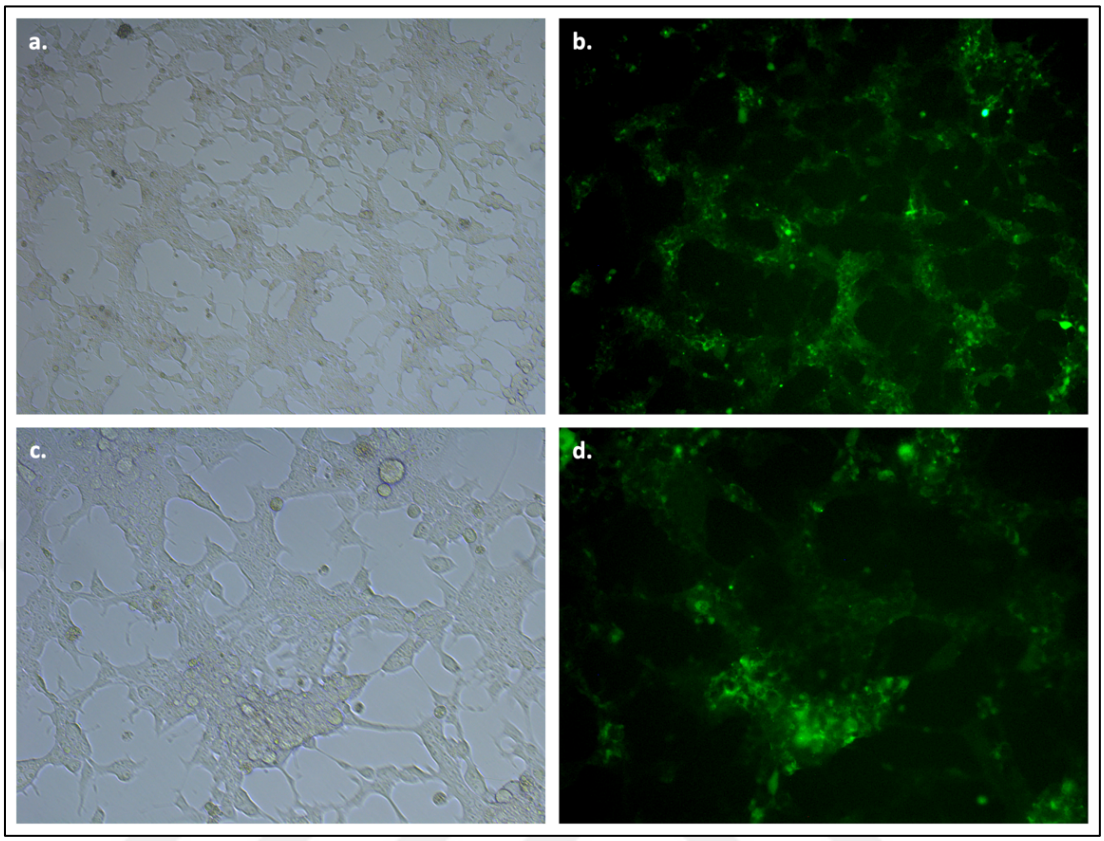



Figure 4.7. 293-FT cells transfected with the EGFP reporter plasmid. Gene expression was induced with 1 µg/ml Dox for 48 hours. (a) Brightfield and (b) GFP images under 10X objective; scale bar: 100 µm. (c) Brightfield and (d) GFP images under 20X objective; scale bar: 50 µm.

## 1.16. CHARACTERIZATION OF TRANSDUCED RENAL CELLS

### 1.16.1. Optimal RPTEC Transduction and Induction Conditions

Optimal conditions for RPTEC transduction and gene expression were determined as described in Section 3.2.2, using the EGFP lentiviral particles. Three different protamine sulfate concentrations were used in order to optimize the transduction efficiency, while Bsd and Dox concentration was set to 2.5 µg/ml and 1 µg/ml, respectively, in reference to the literature. A total of eight experimental conditions were set for the analysis: (i) non-transduced RPTECs treated with 2.5 µg/ml Bsd (Bsd control); (ii) non-transduced RPTECs treated with 1 µg/ml Dox (induced control); (iii) transduced RPTECs treated with Bsd and protamine sulfate (10 µg/ml) but not with Dox (PS-10$^{-}$); (iv) transduced RPTECs treated

with Bsd, protamine sulfate (10 µg/ml), and Dox (PS-10$^{+}$); (v) transduced RPTECs treated with Bsd and protamine sulfate (25 µg/ml) but not with Dox (PS-25$^{-}$); (vi) transduced RPTECs treated with Bsd, protamine sulfate (25 µg/ml), and Dox (PS-25$^{+}$); (vii) transduced RPTECs treated with Bsd and protamine sulfate (50 µg/ml) but not with Dox (PS-50$^{-}$); and (viii) transduced RPTECs treated with Bsd, protamine sulfate (50 µg/ml), and Dox (PS-50$^{+}$). The experimental groups and the related conditions are presented in Table 4.3.

Table 4.3. Experimental groups designed for the determination of optimal transduction conditions for RPTECs.

| Group | Protamine sulfate concentration | GoI in lentiviral particle | Bsd concentration | Dox concentration |
|---|---|---|---|---|
| Bsd control | - | - | 2.5 µg/ml | - |
| Induced control | - | - | - | 1 µg/ml |
| PS-10$^{-}$ | 10 µg/ml | EGFP | 2.5 µg/ml | - |
| PS-10$^{+}$ | 10 µg/ml | EGFP | 2.5 µg/ml | 1 µg/ml |
| PS-25$^{-}$ | 25 µg/ml | EGFP | 2.5 µg/ml | - |
| PS-25$^{+}$ | 25 µg/ml | EGFP | 2.5 µg/ml | 1 µg/ml |
| PS-50$^{-}$ | 50 µg/ml | EGFP | 2.5 µg/ml | - |
| PS-50$^{+}$ | 50 µg/ml | EGFP | 2.5 µg/ml | 1 µg/ml |

Bsd, blasticidin; Dox, doxycycline; EGFP, enhanced green fluorescent protein; PS, protamine sulfate.

Following the treatments, the cells were analyzed for EGFP expression using the Cytell cell imaging system. No reporter expression could be detected at 24 (Figure 4.8) or 48 hours (Figure 4.9) after the initiation of Dox induction.

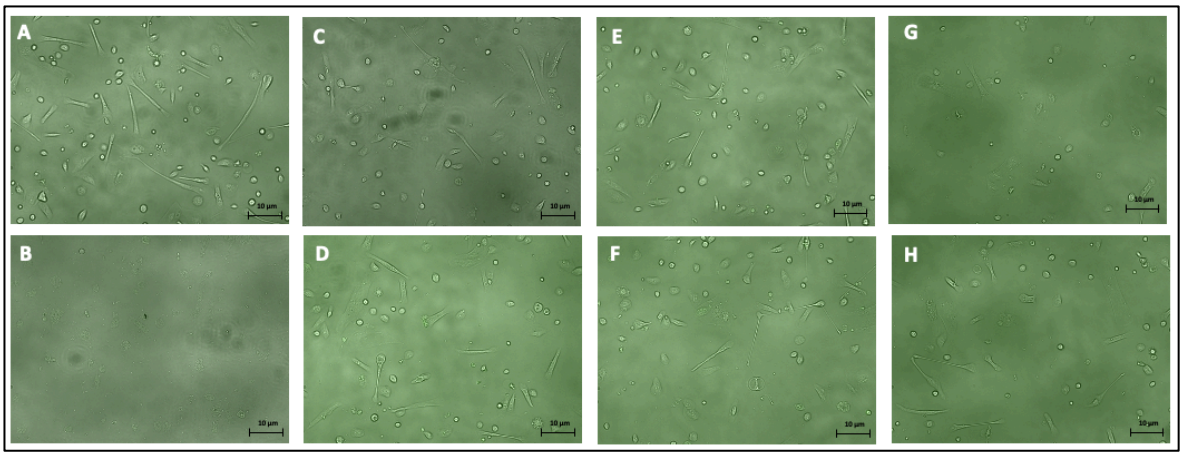



Figure 4.8. Optimization of optimal transduction and gene expression conditions for RPTECs (24 hours). EGFP expression in (a) Bsd control, (b) induced control; (c) PS-10$^{-}$, (d) PS-10$^{+}$, (e) PS-25$^{-}$, (f) PS-25$^{+}$, (g) PS-50$^{-}$, (h) PS-50$^{+}$ groups were analyzed at 24 hours following the initiation of Dox treatment. Scale bar: 10 µm.

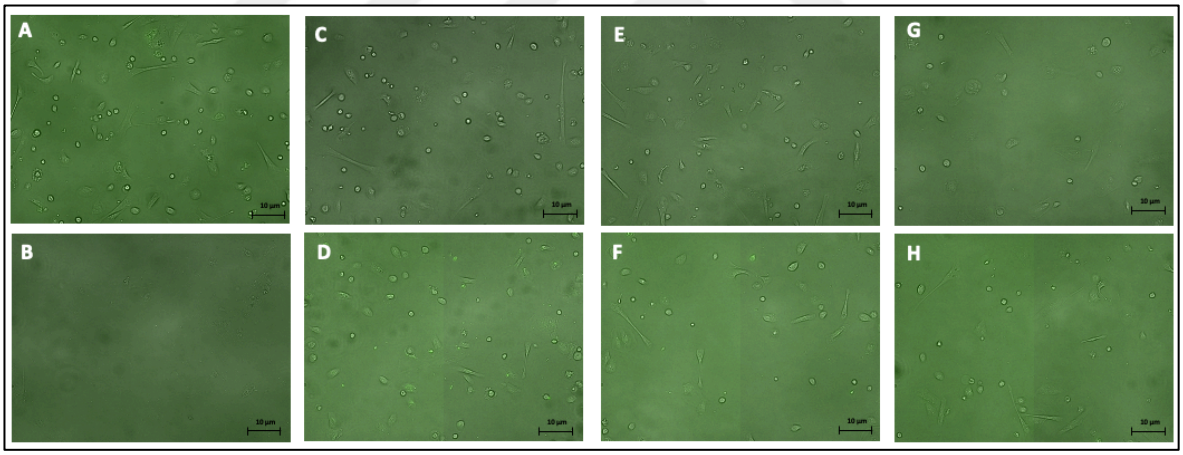



Figure 4.9. Optimization of optimal transduction and gene expression conditions for RPTECs (48 hours).EGFP expression in (a) Bsd control, (b) induced control; (c) PS-10$^{-}$, (d) PS-10$^{+}$, (e) PS-25$^{-}$, (f) PS-25$^{+}$, (g) PS-50$^{-}$, (h) PS-50$^{+}$ groups were analyzed at 48 hours following the initiation of Dox treatment. Scale bar: 10 µm.

At 72 hours, weak fluorescent signals were detected in Dox-induced RPTECs treated with protamine sulfate. There was no apparent difference between the signal intensities of cells treated with 10, 25, or 50 µg/ml protamine sulfate (Figure 4.10). Following 96 hours of Dox induction, RPTECs treated with protamine sulfate displayed a higher signal intensity compared to the 48 hour results. At this time point, an inverse correlation was observed

between protamine sulfate concentration and EGFP expression: RPTECs treated with 10 µg/ml protamine sulfate showed the highest signal intensity, while those treated with 50 µg/ml showed the lowest intensity (Figure 4.11).

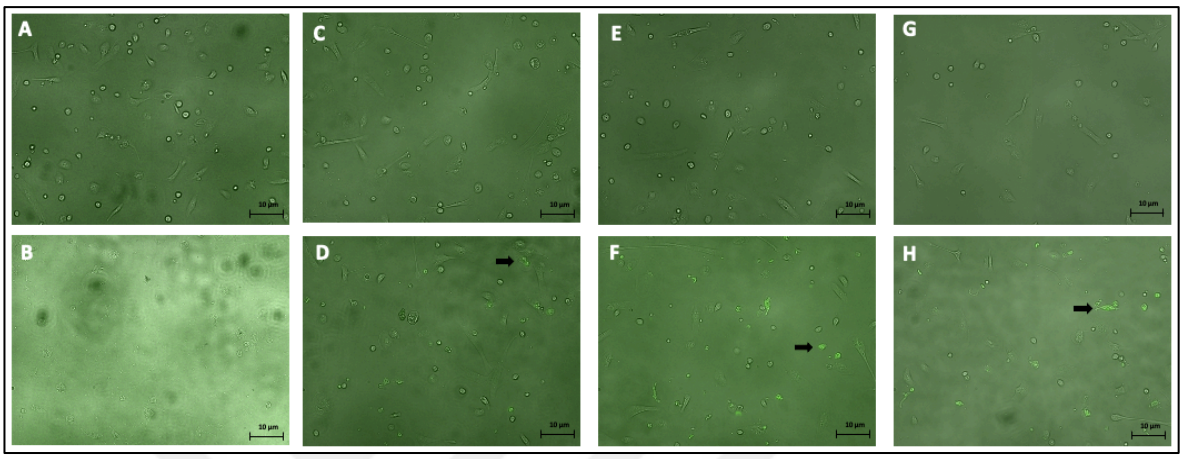



Figure 4.10. Optimization of optimal transduction and gene expression conditions for RPTECs (72 hours). EGFP expression in (a) Bsd control, (b) induced control; (c) PS-10$^{-}$, (d) PS-10$^{+}$, (e) PS-25$^{-}$, (f) PS-25$^{+}$, (g) PS-50$^{-}$, (h) PS-50$^{+}$ groups were analyzed at 72 hours following the initiation of Dox treatment. Scale bar: 10 µm. Black arrows show cells with detectable EGFP expression.

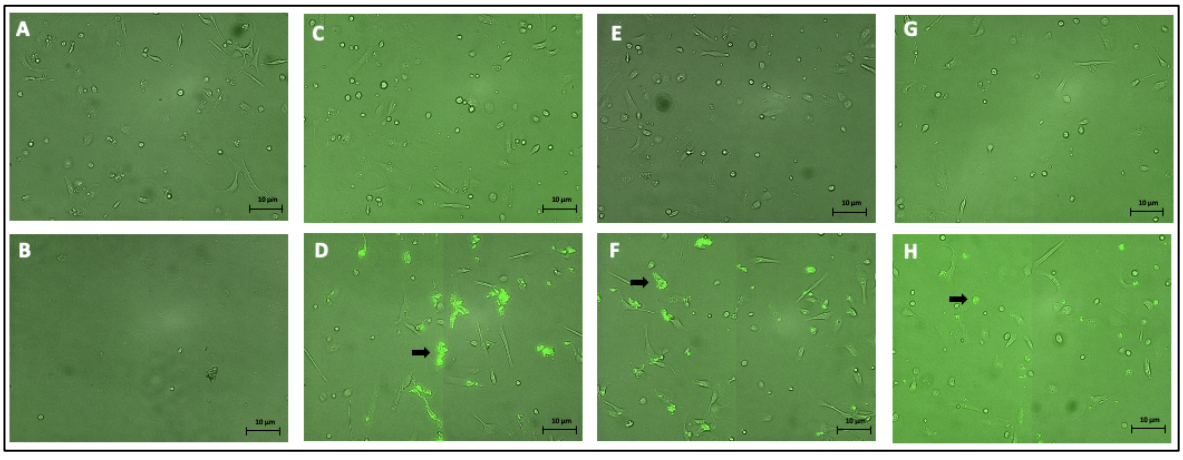



Figure 4.11. Optimization of optimal transduction and gene expression conditions for RPTECs (96 hours). EGFP expression in (a) Bsd control, (b) induced control; (c) PS-10$^{-}$, (d) PS-10$^{+}$, (e) PS-25$^{-}$, (f) PS-25$^{+}$, (g) PS-50$^{-}$, (h) PS-50$^{+}$ groups were analyzed at 96 hours following the initiation of Dox treatment. Scale bar: 10 µm. Black arrows show cells with detectable EGFP expression.

Overall, Cytell imaging results revealed that transduction efficiency of RPTECs was higher with low-dose (10 µg/ml) protamine sulfate pre-treatment. Therefore, this pre-treatment condition was applied in the following experiments. Moreover, since no reporter expression was detected in non-induced RPTECs transduced with EGFP, the absence of "leaky" target gene expression, i.e., uncontrolled activation of the TRE promoter by rtTS_M2 in the absence of Dox, was confirmed for the 2$^{nd}$ generation all-in-one Tet-On system employed in this study.

### 1.16.2. Induced Gene Expression in RPTECs

Gradient PCR was performed in order to detect the optimal $T_m$ for the TG2 isoform-specific primers. For this purpose, total RNA was isolated from Dox-induced RPTECs as described in Section 3.4.1, and cDNA synthesized from these samples was used as a template. PCR was performed at annealing temperatures set between 52.0–55.0°C. Based on the band intensities observed on agarose gels, the optimal annealing temperatures were detected as 55°C for TG2, tTGv1, and tTGv2, and 52°C for TGH and TGH2 (Figure 4.12).

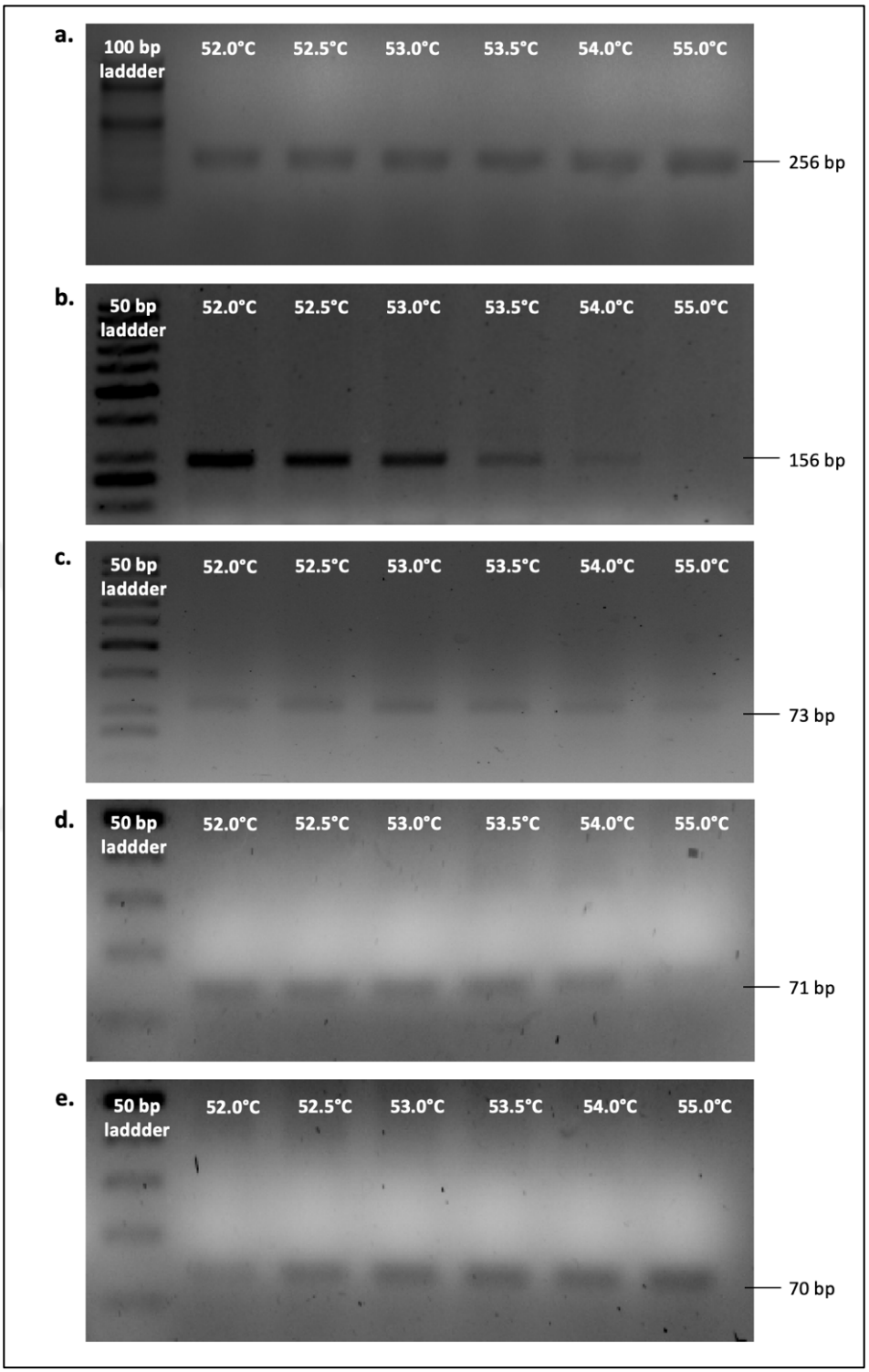



Figure 4.12. (a) TG2, (b) TGH, (c) TGH2, (d) tTGv1, and (e) tTGv2 regions amplified from Dox-induced RPTEC cDNA by gradient PCR. The DNA bands were visualized using the UV mode of the ChemiDoc XRS+ system.

Next, isoform expressions in Dox-induced (96 hours) and non-induced RPTECs were determined by qPCR, and it was found that all TG2 isoform mRNA were expressed at significantly higher levels in Dox-induced cells (Figure 4.13). TG2 and TGH expressions in Dox-induced RPTECs were 3.4-fold and 2.6-fold higher than those in non-induced RPTECs, respectively. Induced RPTEC-TGH2 cells displayed a 2.9-fold higher mRNA expression than the non-induced counterparts. Finally, tTGv1 and tTGv2 were increased by 2.3- and 1.9-fold upon Dox induction, respectively (Figure 4.13).

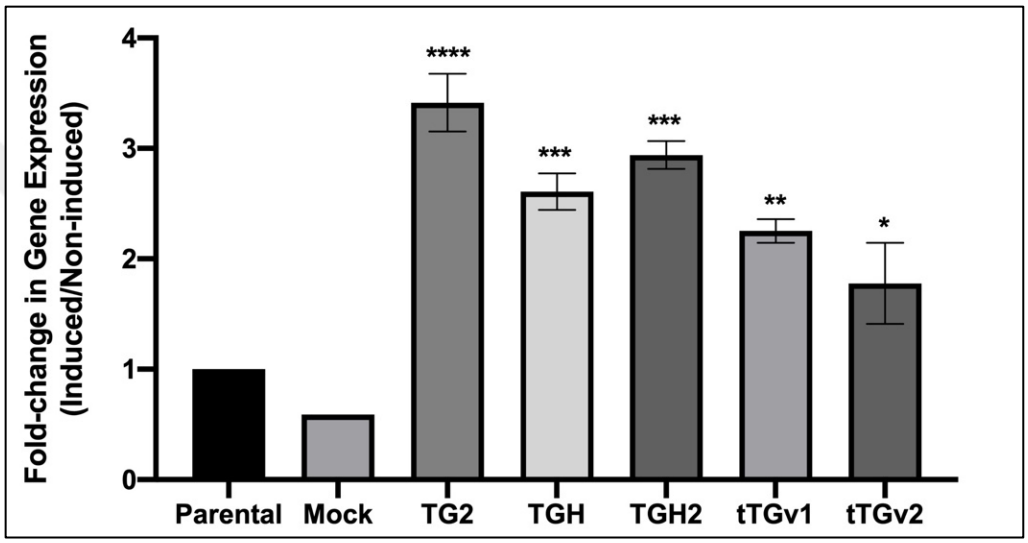



Figure 4.13. Isoform expression levels in transduced RPTECs. Cells were subjected to Dox treatment for 96 hours. mRNA expression levels in Dox-induced RPTECs relative to those in non-induced cells are presented. 18sRNA was used as the endogenous reference. *p<0.05, **p<0.01, ***p<0.005, ****p<0.001.

qPCR was also performed to analyze the time-dependent isoform expression status upon Dox treatment. In the analysis, the expression levels of all isoforms in transduced RPTECs were normalized to the levels in cells transduced with the mock vector (RPTEC-Mock). In other words, following the normalization of all expression levels to that of the endogenous 18S rRNA, fold-change in gene expression was presented as the levels relative to that in RPTEC-Mock cells, which was assumed as "1" (Figure 4.14).

After 24 hours of induction, TG2 expression was 3.5-fold higher in RPTEC-TG2 cells, compared with the levels in RPTEC-Mock cells (Figure 4.14). At this time point, no significant change was observed in the mRNA levels of other isoforms relative to RPTEC-Mock cells. Following 48 hours, the level of TG2 mRNA expression in RPTEC-TG2 cells

was 2.6-fold higher than that in RPTEC-Mock cells; even though the level of TG2 was decreased compared to that after 24 hours, it was still significantly higher than the levels in RPTEC-Mock cells. There was a prominent increase in TGH levels at 48 hours, with a 2.3-fold difference from the levels in RPTEC-Mock cells (Figure 4.14). While TG2 levels were sustained until 72 hours, the levels of TGH was slightly decreased at this time point, with 1.9-fold higher expression than RPTEC-Mock cells. TGH2 and tTGv1 showed a significant upregulation at 72 hours, with 2.1- and 2.7-fold higher expression levels than those in RPTEC-Mock cells, respectively. Furthermore, following 96 hours after the initiation of Dox treatment, both TG2 and TGH were dropped to the baseline levels. At this time point, TGH2, tTGv1, and tTGv2 were significantly upregulated in transduced cells with 1.8-, 1.6-, and 2.5-fold higher expression, respectively, compared to those in RPTEC-Mock cells (Figure 4.14).

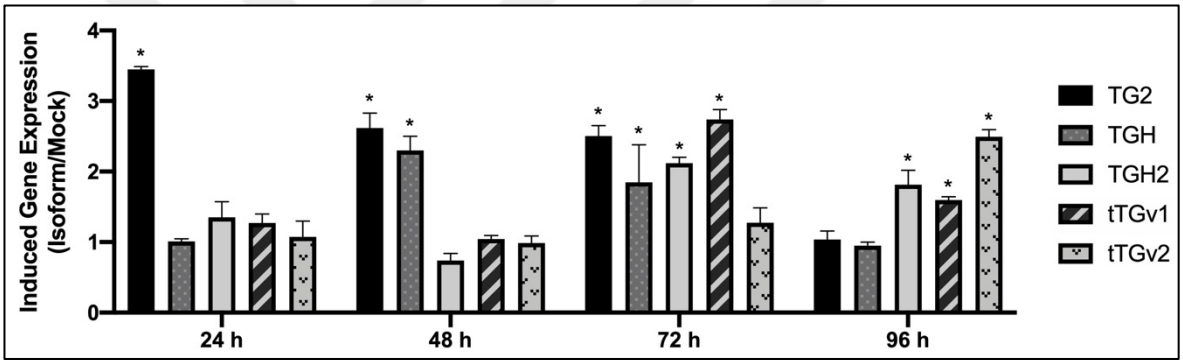



Figure 4.14. Time-dependent isoform expression levels in transduced RPTECs. Cells were subjected to Dox treatment for up to 96 hours, and RNA was isolated at every 24-hour interval. mRNA expression levels in Dox-induced RPTECs relative to those in RPTEC-Mock cells are presented. 18sRNA was used as the endogenous reference. *p<0.05, **p<0.01, ***p<0.005, ****p<0.001.

### 1.16.3. Cell Surface Localization of TG2 Isoforms in RPTECs

To determine the TG2 isoform levels on RPTEC membranes, Dox-induced cells were treated with an anti-Flag antibody conjugated with FITC, and the fluorescent signal intensities were analyzed by flow cytometry. The results showed that TG2, tTGv1, and tTGv2 were externalized onto the RPTEC membrane at similar levels (6.42, 5.55, and 6.44%, respectively). The levels of surface TGH (10.46%) and TGH2 (12.41%,) were higher than the other isoforms (Figure 4.15).

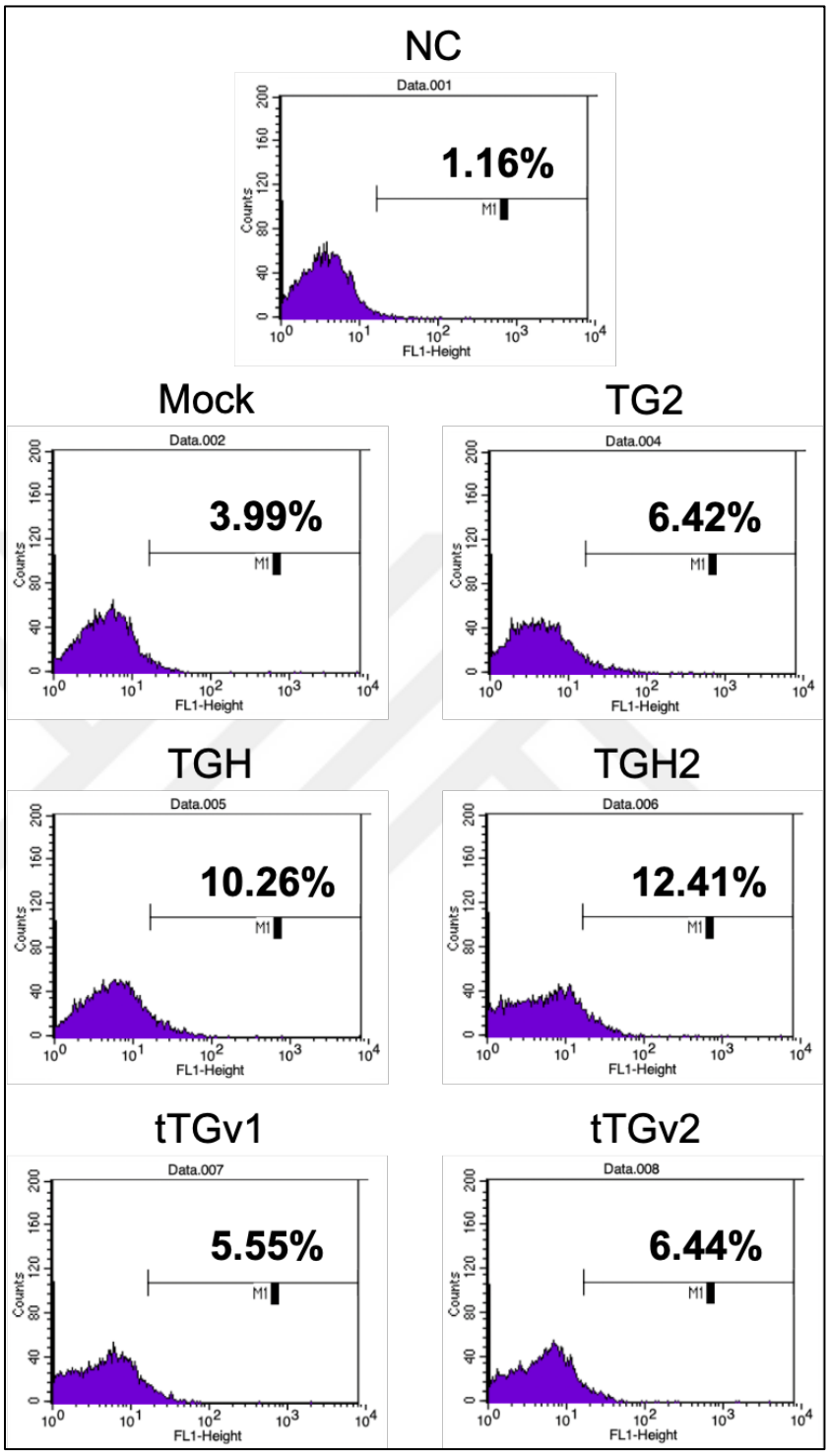



Figure 4.15. TG2 isoform levels on RPTEC surface determined by flow cytometry. The cells were incubated with the FITC-conjugated anti-Flag primary antibody for 1 hour at 4°C and an additional 30 minutes at 37°C. The percentage of FITC-positive cells was determined using BD FACSCalibur, and histogram plots were generated using the CellQuestPro software. NC, negative control (parental RPTECs).

## 1.17. EFFECTS OF TG2 ISOFORMS ON CELLULAR PROCESSES

### 1.17.1. Growth Profiles of Transduced RPTECs

In order to determine the effects of TG2 isoforms on the proliferation of RPTECs, a time-dependent cell proliferation analysis was performed. The initial number of RPTEC-TG2 cells (at 24 hours) was 1860, which was reached to 3986 at 72 h (Figure 4.16a), representing a 2-fold increase in cell proliferation (Figure 4.16b). At 96 hours, the number of RPTEC-TG2 cells reached 4810 (proliferation rate: 250%), which was 50% higher than the number of viable RPTEC-Mock cells at the same time point.

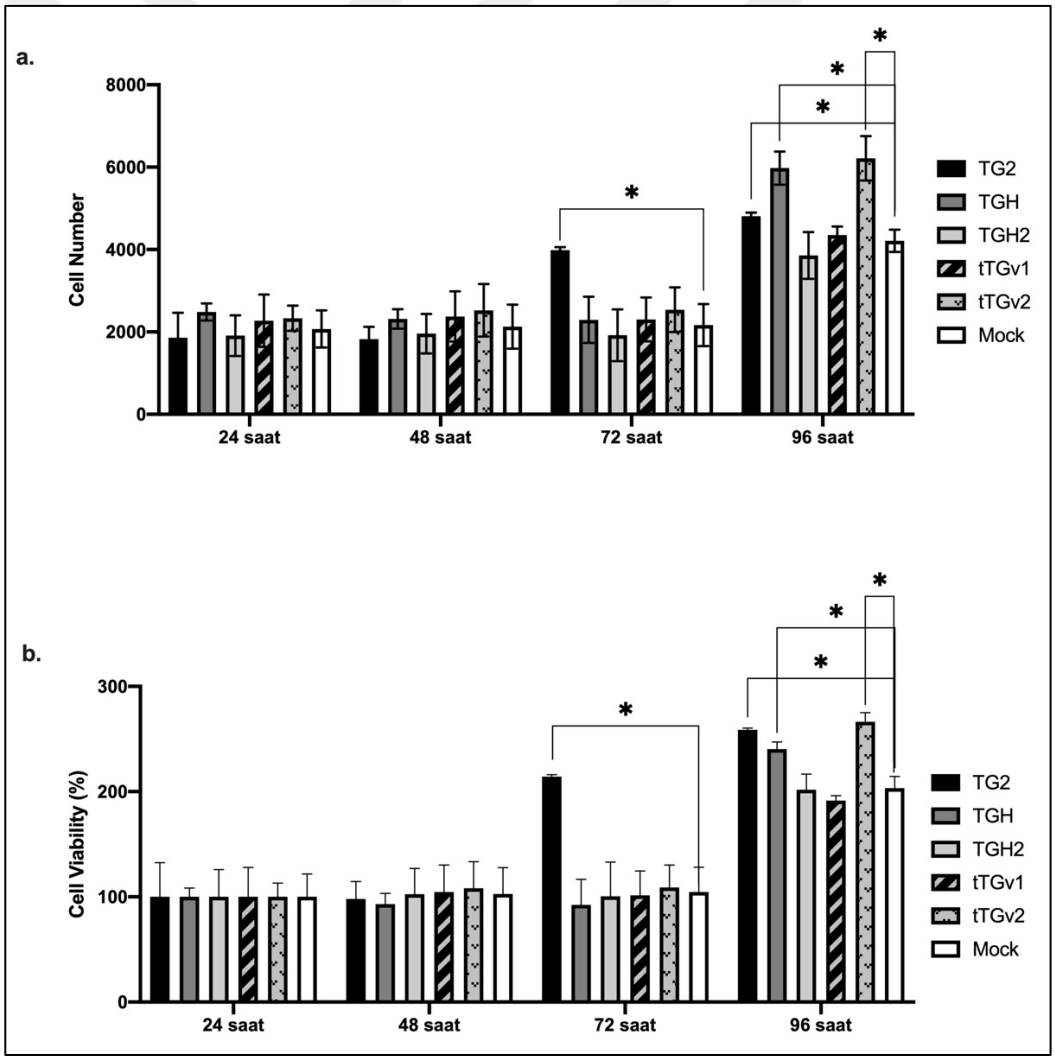



Figure 4.16. Time-dependent growth of transduced RPTECs. WST-1 cell proliferation assay was performed to determine (a) cell numbers and (b) percentage cell viability at 24, 48, 72, and 96 hours following the initiation of Dox treatment. *p<0.05.

Additionally, the population doubling-time of each cell line was calculated using the growth trend equations obtained: the doubling time of RPTEC-Mock cells was calculated as 95 hours, which was similar to the reported doubling-time of parental RPTECs (96 hours; Wieser et al., 2008), and that of RPTEC-TG2 was found as 75 h, which is significantly lower (Table 4.4).

The number of RPTEC-TGH cells at 24 hours was 2487; similar to RPTEC-TG2, these cells showed a significant increase at 72 hours, reaching a number of 5980, which accounted for a 40% higher proliferation rate than RPTEC-Mock cells (Figure 4.16). Moreover, the doubling-time of this cell line was calculated as 90 hours (Table 4.4).

Induction of the expressions of TGH2 and tTGv1 resulted in a respective 2.2-fold and 2.8-fold increase in cell proliferation. The number of RPTEC-TGH2 cells increased from 1912 to 3860 during the 96 hours of Dox induction, reaching a proliferation rate of 201% (Figure 4.16). The doubling-time of RPTEC-TGH2 cells was calculated as 95 hours, similar to that of RPTEC-Mock cells. Meanwhile, the number of RPTEC-tTGv1 cells increased from 2274 to 4352, accounting for 191% cell viability. The population doubling-time was calculated as 98 hours for these cells (Table 4.4).

Finally, RPTEC-tTGv2 cells showed a significant increase in proliferation from 72 to 96 hours of Dox treatment. The number of these cells increased from the initial number of 2333 to 6217, displaying a 270% cell viability (Figure 4.16). These cells also had a significantly shorter doubling-time than RPTEC-Mock cells (85 hours vs. 95 hours; Table 4.4).

Table 4.4. Calculated doubling time of TG2 isoform-transduced RPTECs.

| RPTEC cell line | Doubling-time |
|---|---|
| TG2 | 75 hours |
| TGH | 90 hours |
| TGH2 | 95 hours |
| tTGv1 | 98 hours |
| tTGv2 | 85 hours |
| Mock | 95 hours* |

*The doubling-time calculated for RPTEC-Mock cells is similar to the reported doubling-time of parental RPTECs (96 hours) [242].

To observe the long-term effects of TG2 isoforms on RPTEC viability, cell proliferation assay was also performed from 24 to 96 hours post-induction. Transduced RPTECs showed sustained proliferation during this period (Figure 4.17). At 72 hours post-induction, RPTECs transduced with TG2, TGH, TGH2, and tTGv2 showed a 2-fold increase, and tTGv1 showed a 1.5-fold increase in cell viability. At the end of 96 hours, the proliferation rate of cells expressing TG2, TGH, TGH2, and tTGv2 showed an approximate 60% increase, and RPTEC-tTGv2 showed 30% increase (Figure 4.17).

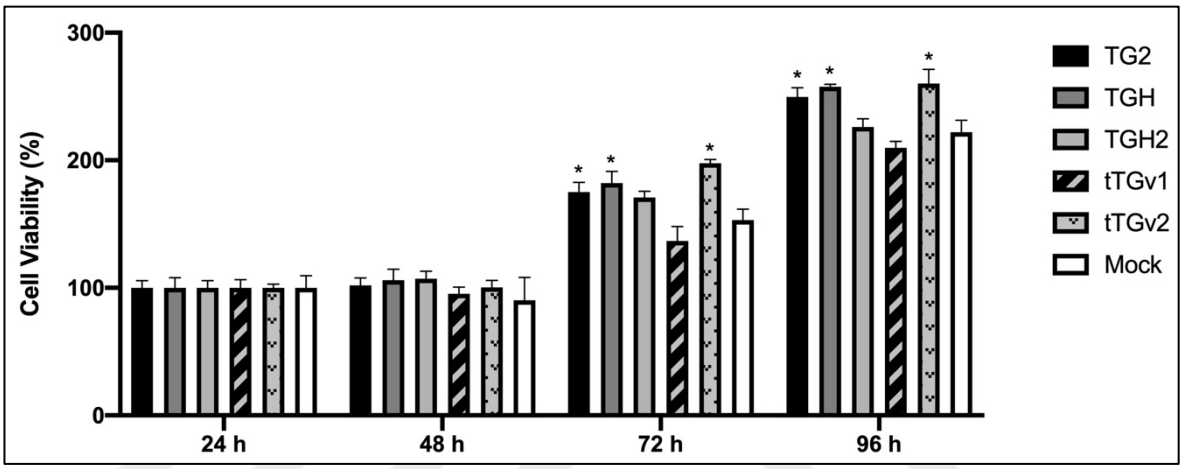



Figure 4.17. Time-dependent growth of transduced RPTECs during the 96 hours post-induction. WST-1 cell proliferation assay was performed to determine the percentage cell viability at every 24 hours. *p<0.05.

### 1.17.2. Cell Cycle Progression of Transduced RPTECs

Cell cycle profiles of transduced RPTECs were initially analyzed using the Cytell imaging system. According to the histograms obtained from the analysis, the majority of parental and RPTEC-Mock cells were at the G1 phase. At 96 hours following the Dox induction, 12% of RPTEC-TG2, 26% of RPTEC-TGH, 10% of RPTEC-tTGv1, and 8% of RPTEC-tTGv2 cells were at the G2/M phase, as opposed to RPTEC-Mock cells (0%), showing an increased proliferative potential (Figure 4.18, Table 4.5).

Higher proportions of the isoform-transduced cells were found in the S phase than the parental and RPTEC-Mock cells, except for TGH2 in that approximately 46% of RPTEC-TG2, 34% of RPTEC-TGH, 11% of RPTEC-TGH2, 48% of RPTEC-tTGv1, and 50% of

RPTEC-tTGv2 cells were at the S phase, as opposed to the 14% of parental and 2% of RPTEC-Mock cells being at the S phase of the cell cycle (Figure 4.18 and Table 4.5).

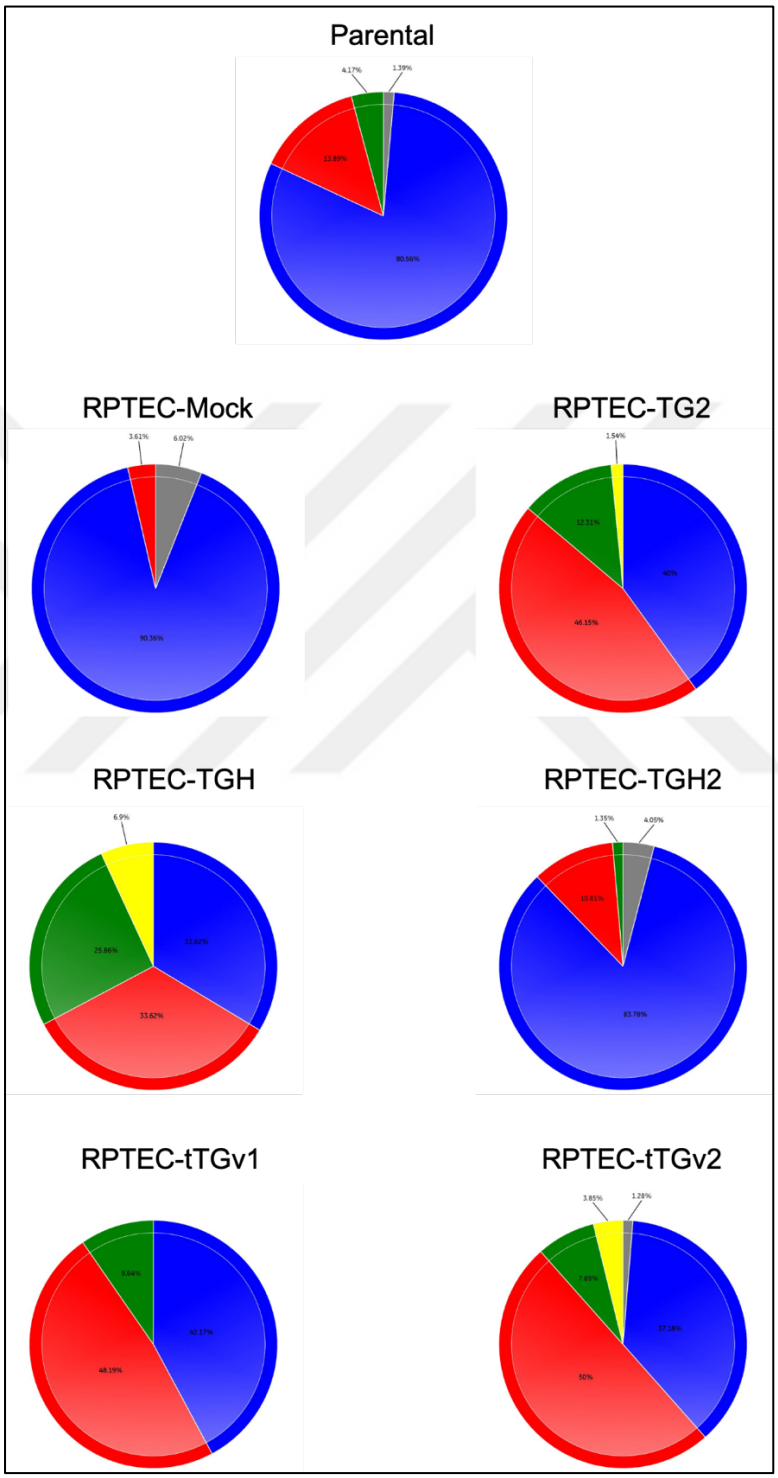



Figure 4.18. Cell cycle progression of transduced RPTECs at 96 hours upon Dox induction. The cells were fixed with paraformaldehyde and stained with PI, and imaging was performed using the orange filter of the Cytell imaging system.

Table 4.5. Cell cycle profiles of transduced RPTECs based on Cytell imaging results.

| RPTEC cell line | <2n (Sub-G0/G1) | G0/G1 | S | G2/M |
|---|---|---|---|---|
| **Parental** | 1,39% | 80,56% | 13,89% | 4,17% |
| **Mock** | 6,02% | 90,36% | 1,61% | 0% |
| **TG2** | 0% | 40% | 46,15% | 12,31% |
| **TGH** | 0% | 33,62% | 33,62% | 25,86% |
| **TGH2** | 4,05% | 83,78% | 10,81% | 1,35% |
| **tTGv1** | 0% | 42,17% | 48,19% | 9,64% |
| **tTGv2** | 1,28% | 37,18% | 50% | 7,69% |

Next, the cell cycle profiles were confirmed by flow cytometry analysis. Similar to the Cytell results, higher percentage (40 to 50%) of the isoform-transduced RPTECs were at the S or G2/M phase, with the full-length TG2 (80%) showing the most prominent effect on RPTEC cell cycle progression (Figure 4.19).

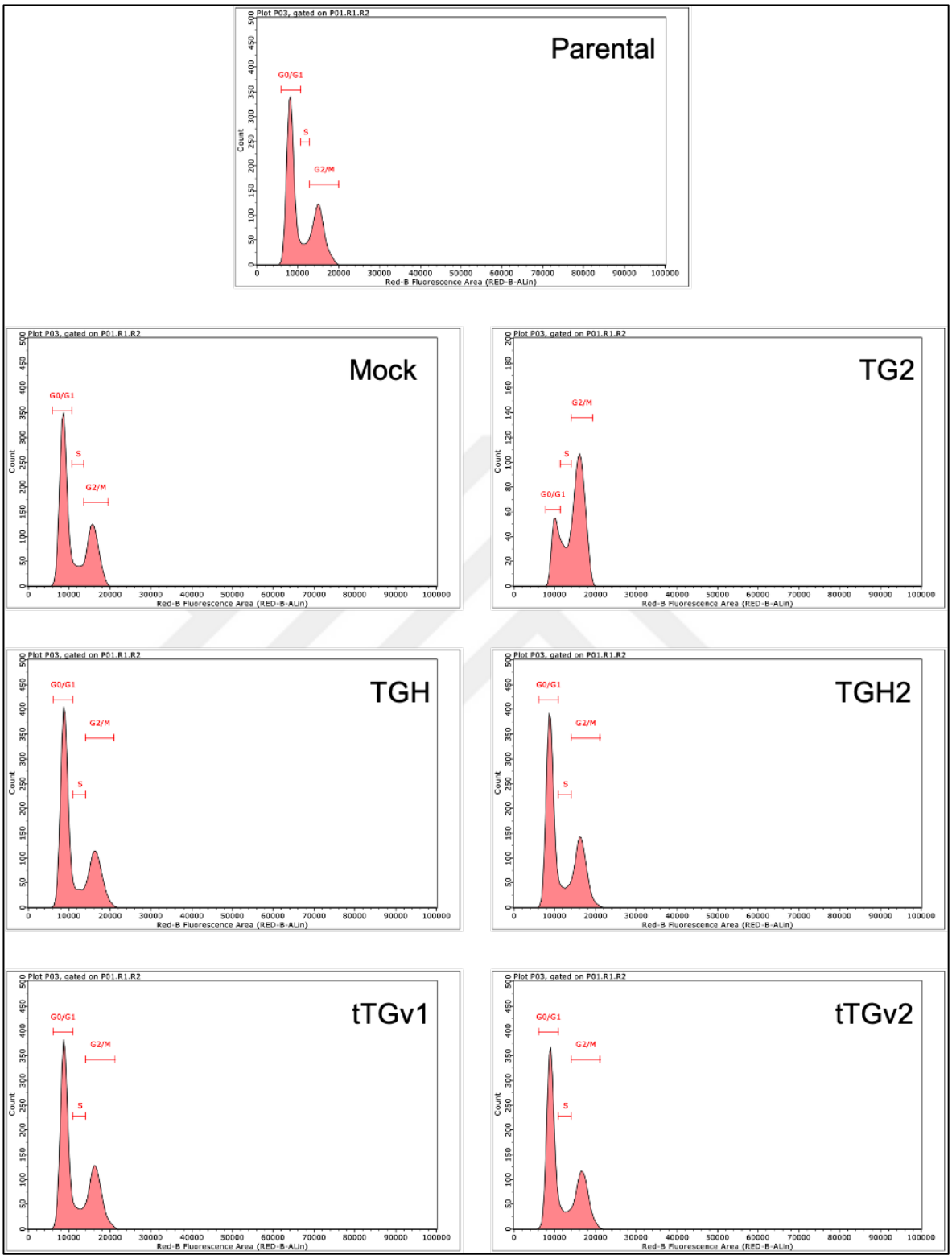



Figure 4.19. Cell cycle progression of transduced RPTECs at 96 hours upon Dox induction. The cells were fixed and stained with PI, and imaging was performed using the orange filter of the Cytell imaging system.

Finally, the levels of key proteins in cell cycle progression were analyzed by western blotting. Compared to the expression levels in parental RPTECs (Cnt), cyclin D1, cyclin D3, and CDK4 were upregulated in RPTEC-TG2 and RPTEC-TGH cells (Figure 4.20). Cyclin E1 and CDK2 were also slightly upregulated in RPTEC-TGH cells. These results were consistent with the high percentage of RPTEC-TG2 and RPTEC-TGH cells in the S and G2/M phases detected in the cell cycle analysis (Table 4.5). RPTEC-TGH2 cells also showed an upregulation in cyclin D1 and D3, albeit without concomitant CDK4 expression. Since cyclins D1 and D3 are associated with CDK4 to enable the progression of cells through the G1 phase, this result is consistent with the cell Cytell results showing a similar distribution for RPTEC-TGH2 and RPTEC-Mock cells. In addition, tTGv1 and tTGv2 expressions caused an increase in all cyclin and CDK protein levels, in line with the high percentages of the cells at the S and G2/M phases revealed by the Cytell analysis. A notable downregulation of p27 Kip1, an inhibitor of cyclin/CDK complexes, was observed in transduced RPTECs in comparison with the parental cells (Figure 4.20, Table 4.5).

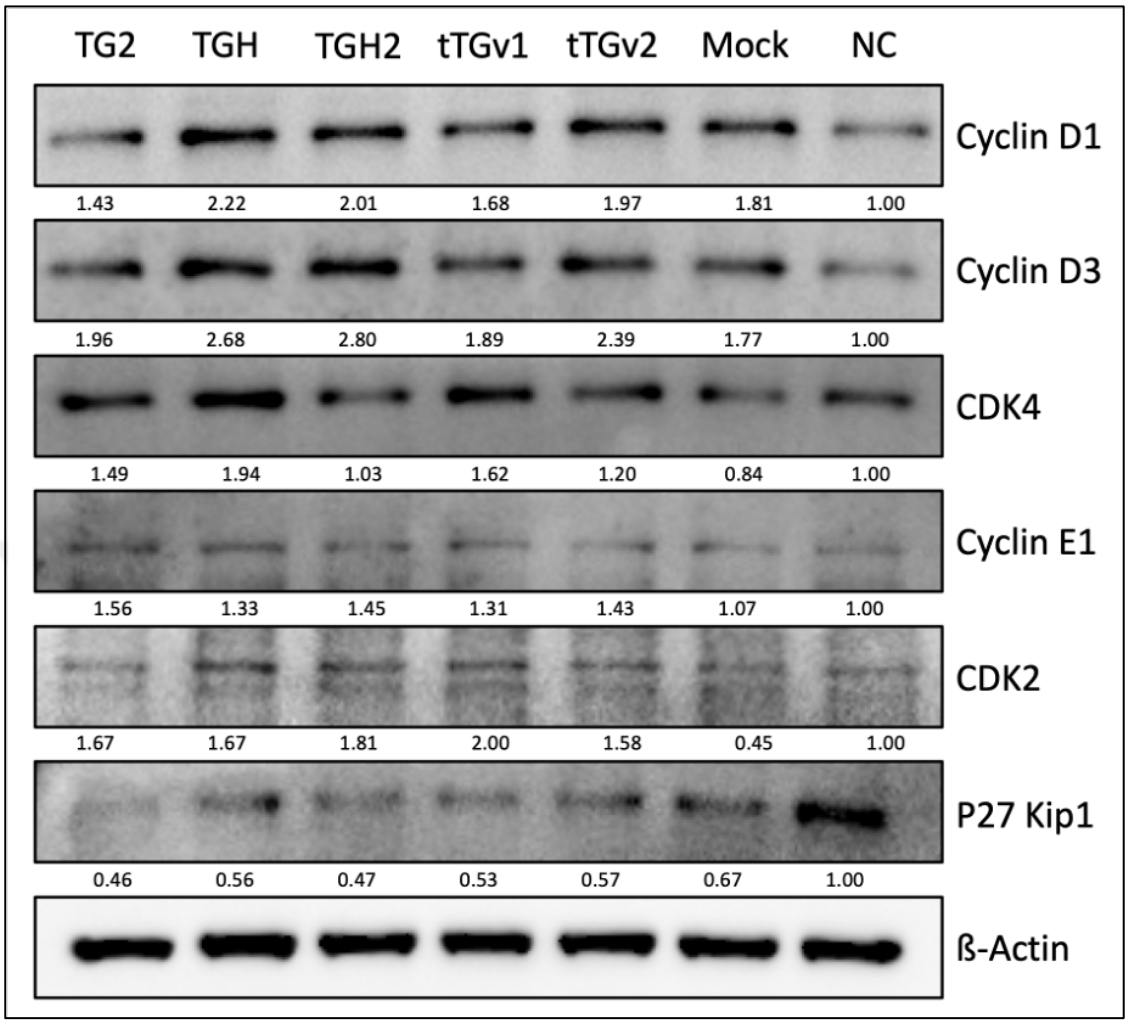



Figure 4.20. Protein levels of cyclins and CDKs in induced RPTECs determined by western blotting. The cells were incubated with the indicated primary antibodies overnight at 4°C, followed by secondary antibody incubation for 2 hours at room temperature. β-actin was used as the loading control. The protein bands were visualized using the ChemiDoc XRS+ imaging system. NC, parental RPTECs.

### 1.17.3. EMT and MMP Profiles of Transduced RPTECs

The potential effects of TG2 isoforms on the process of EMT was analyzed by qPCR at 72 and 96 hours following Dox treatment. The level of E-cadherin, an important epithelial cell marker, was significantly reduced in RPTECs expressing the TG2 isoforms, compared with that in RPTEC-Mock cells. A low but statistically significant increase in N-cadherin levels was observed in RPTEC-TGH and RPTEC-TGH2 cells (Figure 4.21a), while no significant

difference was observed in the mRNA expression levels of Zeb 1 and Zeb 2 for neither isoform (Figure 4.21b).

Twist 1 expression was increased by 8-fold in RPTEC-TG2 cells, and about 14-fold in RPTEC-TGH2, -tTGv1, and tTGv2 cells. Twist 2 was increased by 4-fold in RPTEC-TGH2 cells (Figure 4.21c). Although no significant difference in Snail 1 levels was found between RPTEC-Mock and isoform-transduced RPTECs, there was a significant 3.5-fold upregulation in the mRNA levels of Snail 2 in RPTEC-TG2 and -TGH cells (Figure 4.21d). In addition, a 2-fold increase in Snail 2 mRNA was observed in RPTEC-tTGv2 cells compared with that in RPTEC-Mock cells (Figure 4.21d). Vimentin upregulation was caused only by the induced expressions of TGH (3.2-fold) and TGH2 (10-fold) in RPTECs (Figure 4.21e).

At 96 hours, E-cadherin was significantly downregulated to undetectable levels in all transduced RPTECs following Dox-induction (Figure 4.22a). At this time point, a significant 1.8-fold increase in N-cadherin levels was observed in RPTEC-TG2 cells, which did not occur at 72 hours. The level of Zeb 1 was also increased (by 1.5-fold) at this time point in RPTECs-TG2 and -TGH cells (Figure 4.22b). Twist1 expression profiles of the cells at 96 hours was similar to those at 72 hours, with a marked 25-fold upregulation in RPTEC-tTGv2 cells (Figure 4.22c). Twist 2, Snail 1, and Snail 2 were dropped to the near-baseline levels at 96 hours (Figure 4.22c,d). Finally, vimentin levels were further increased at this time point in RPTEC-TGH2 cells (reaching 15-fold relative to the levels in RPTEC-Mock cells), while it was drastically diminished in RPTEC-TGH (Figure 4.22e).

Taken together, the results of the qPCR analysis suggest that the induction of TG2 isoform expression in RPTECs causes the loss of epithelial characteristics and enables the cells to adopt the mesenchymal features.

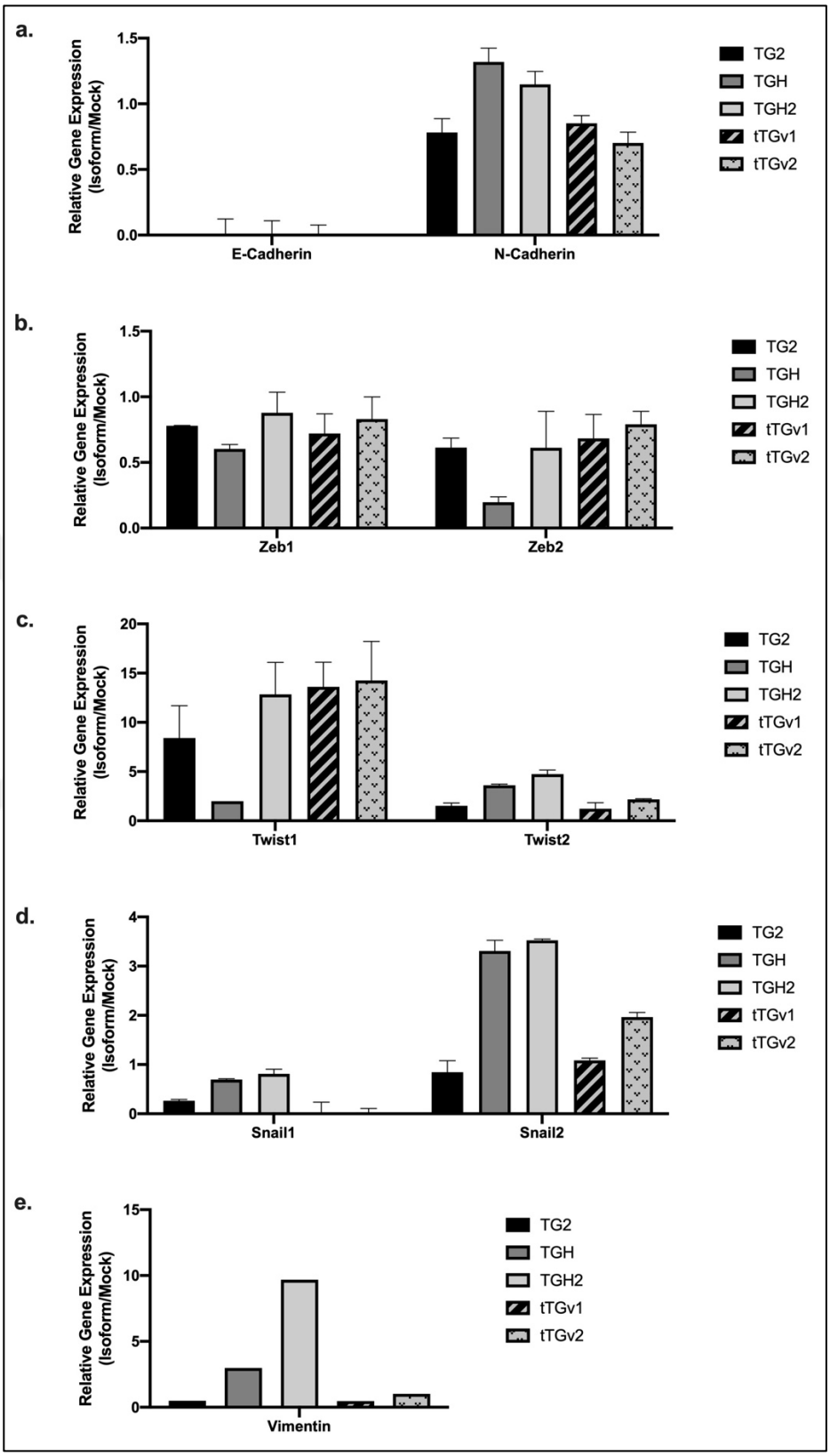



Figure 4.21. EMT marker levels in transduced RPTECs at 72 hours following Dox induction. mRNA expression levels in transduced RPTECs relative to those in RPTEC-Mock cells are presented. 18sRNA was used as the endogenous reference.

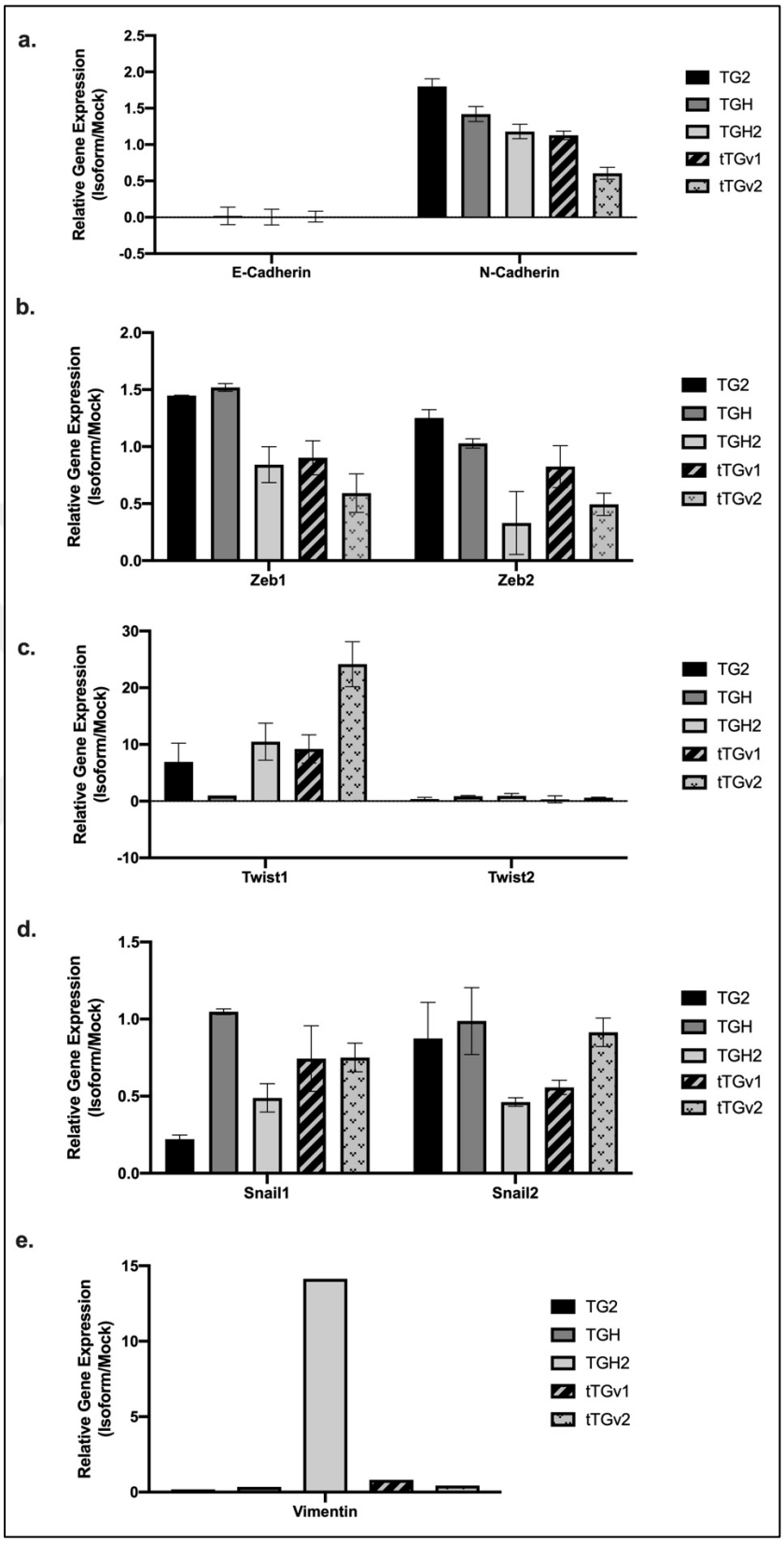



Figure 4.22. EMT marker levels in transduced RPTECs at 96 hours following Dox induction. mRNA expression levels in transduced RPTECs relative to those in RPTEC-Mock cells are presented. 18sRNA was used as the endogenous reference.

The levels of MMPs 1, 2, 9, and 13 were analyzed in transduced RPTECs to assess the possible effects of the isoforms on the invasion potential. At 72 hours following Dox induction, MMP-9 was upregulated in all RPTECs expressing TG2 isoforms (Figure 4.23a). In RPTEC-TG2 cells, MMP-1 and MMP-9 were upregulated by 1.5-fold and 5-fold, respectively, compared with the levels in RPTEC-Mock cells. RPTEC-TGH cells showed a 2-fold increase in MMP-1 and MMP-13, 2.5-fold in MMP-2, and 20-fold in MMP-9. Induction of TGH2 expression in RPTECs was accompanied by a 7.7-fold, 5-fold, and 2-fold increase in MMP-1, MMP-2, and MMP-9 levels, respectively. tTGv1 expression only influenced the levels of MMP-9, with a 7.6-fold increase with respect to RPTEC-Mock cells. MMP-2 and MMP-9 were upregulated by 2-fold and 20-fold, respectively, in RPTEC-tTGv2 cells (Figure 4.23a).

At 96 hours following Dox induction, MMP-9 mRNA expression was upregulated in all transduced RPTECs, compared with the levels in RPTEC-Mock cells (Figure 4.23b). MMP-1 and -2 were upregulated in RPTEC-TGH2 cells by 11.3-fold and 7.4-fold, respectively, while MMP-2 and -13 levels were 1.5-fold higher in RPTEC-tTGv1 cells than in RPTEC-Mock cells. MMP-9 was upregulated by 13.5-fold and 10.6-fold in RPTEC-tTGv1 and RPTEC-tTGv2 cells, respectively (Figure 4.23b).

Collectively, the data implicated that upregulation of TG2 isoforms had the potential the increase the invasion capacity of RPTECs.

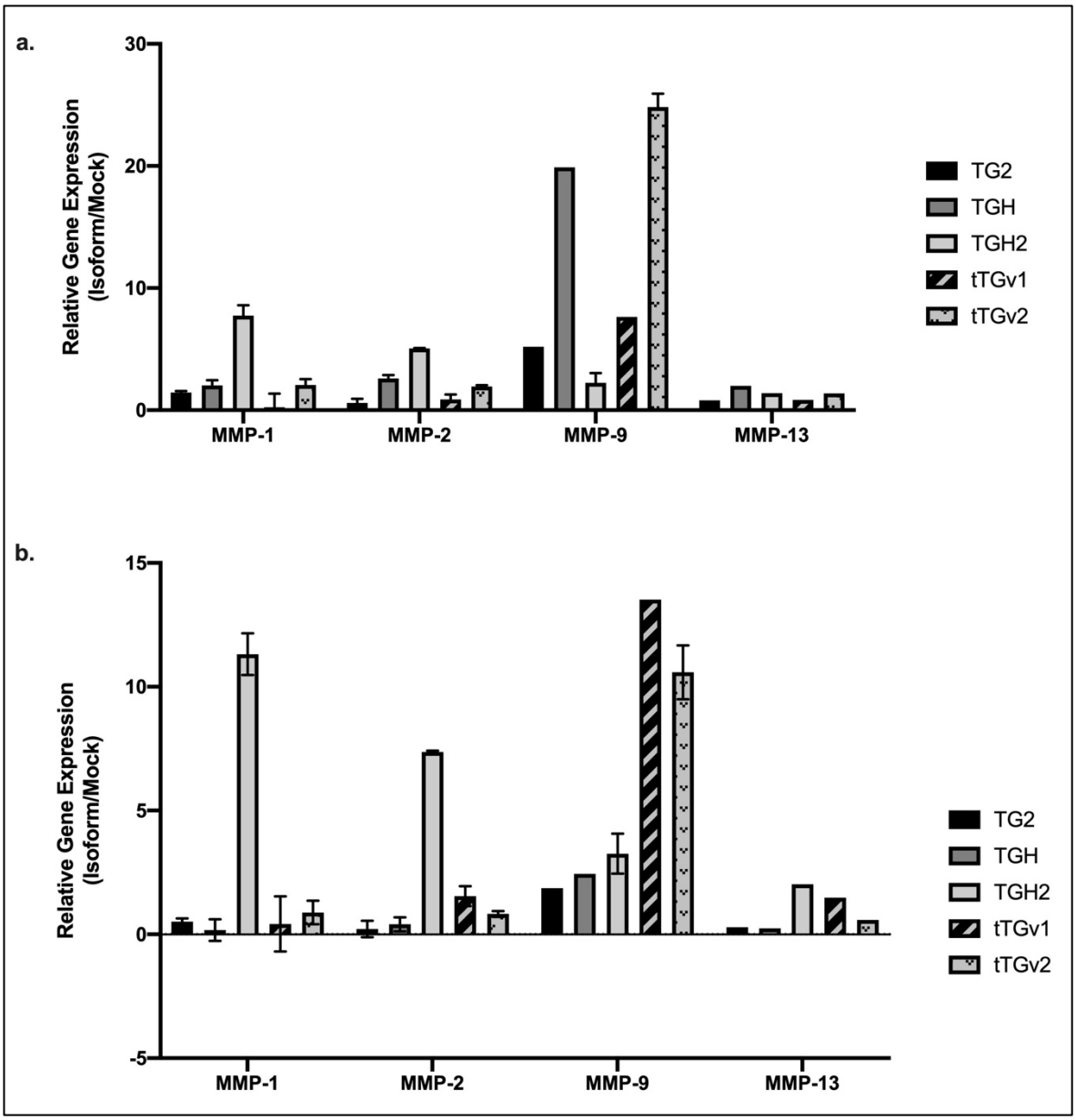



Figure 4.23. MMP levels in transduced RPTECs at (a) 72 and (b) 96 hours following Dox induction. mRNA expression levels in transduced RPTECs relative to those in RPTEC-Mock cells are presented. 18sRNA was used as the endogenous reference.

### 1.17.4. Migration Potential of Transduced RPTECs

A wound healing assay was performed to evaluate the migration potential of RPTECs transduced with TG2 isoforms. According to the analysis of cell density on the wound scratch area at 72 h, non-transduced (parental) RPTECs and RPTEC-Mock cells had a

similar wound healing capacity with approximately 65% of the scratched area being occupied by cells (Figure 4.24 and Figure 4.25).

RPTEC-TG2 cells closed 50% of the wound area at 24 h, and about 92% of the area was closed by the end of 72 h. Wound closure by RPTEC-TGH and RPTEC-TGH2 cells reached 81% and 83%, respectively, by the end of 72 h. Wound healing capacities of RPTEC-tTGv1 and RPTEC-tTGv2 cells were 74% and 58%, respectively. Among all isoforms, only tTGv2 did not show a significantly different wound healing capacity compared with those of parental and RPTEC-mock cells (Figure 4.24 and Figure 4.25).

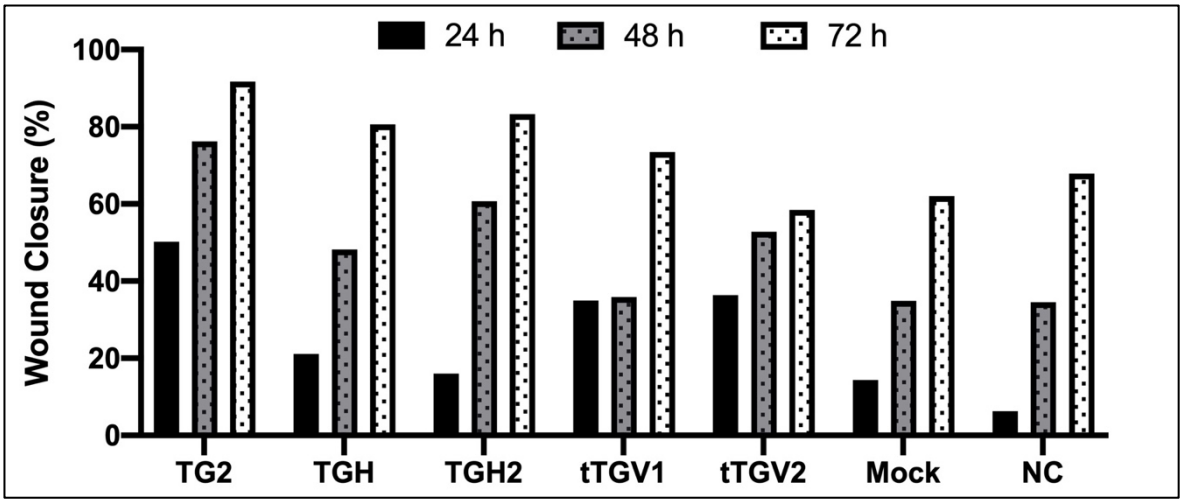



Figure 4.24. Wound healing capacities of transduced RPTECs. The scratched zones on 24-well plates were captured immediately after generating the wounds, and the area closed by cells were monitored at every 24 h until 72 h. Wound healing capacity is expressed as percentage closed area. ImageJ was used for the analyses.

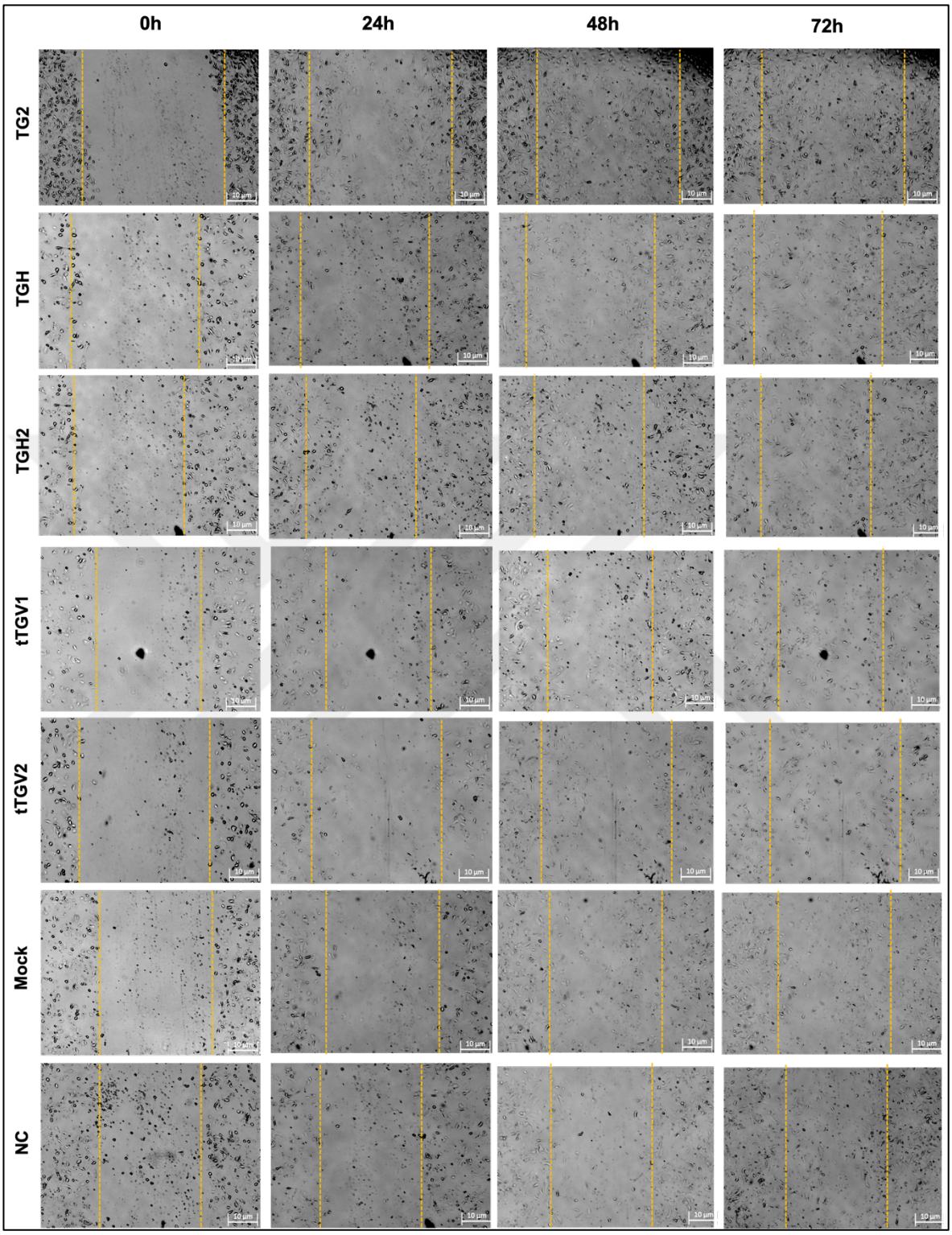



Figure 4.25. Monitoring of the wound healing capacities of transduced RPTECs. The scratched zones on 24-well plates were captured immediately after generating the wounds, and the area closed by cells were monitored at every 24 h until 72 h. The images were obtained using Cytell.

# 5. DISCUSSION

TG2 has long been considered an important mediator in cancer progression [70]. The identification of TG2 in pathogenic kidneys dates back to 1997, with the revelation that the crosslinking activity was involved in the occurrence of fibrosis and chronic renal insufficiency, which led to the proposal that the TG2-mediated crosslinking of ECM proteins resulted in ECM resistance to breakdown [243]. Later, TG2 was extensively characterized in kidney scarring and fibrosis, and mainly the tubular epithelial cells were responsible for TG2 production [244, 245]. More recently, our group and others have demonstrated the significance of TG2 in RCC from a prognostic point of view. While TG2 mRNA expression was reduced in the majority of primary RCC tumors regardless of the clinical parameters such as the stage and histopathological grading, TG2 upregulation with a concomitant increase in ITGB1 and SDC4 levels showed a significant association with metastasis, which was attributed to the induction of integrin-mediated outside-in survival signaling through the interactions of TG2 with these proteins [246]. In a follow-up study analyzing patients with RCC, increased expression of TG2 in primary tumors predicted metastasis and negatively correlated with the disease-free and cancer-specific survival [222]. Adding strength to these findings, high TG2 expression was associated with high nuclear grade and poor prognosis in a cohort of 638 patients with ccRCC [223]. Our group has also demonstrated the prominence of TG2 expression in cancer cell adhesion, migration, invasiveness, and stemness in four different RCC cell lines [224].

Since TG2 is a uniquely multifaceted enzyme within the TG family, displaying an additional GTP-binding/GTPase activity and protein-protein interactions, the relevance of each activity to different disease states became an important aspect of TG2-related research. Previous work by the prominent researchers in the field showed that the GTP-binding domain of TG2 was responsible for the transforming potential of TG2 in cancers such as breast, ovarian, and squamous skin cancer [70]. In agreement with these studies, investigating the effects of GTP-binding deficient (R580A), transamidase-deficient/GTP-binding-low (C277S), and transamidase-inactive (W241A) TG2 mutants in mouse RCC cells, our group was able to show that the GTP-binding/GTPase activity, rather than the transamidase activity of TG2 was also important for the maintenance of the mesenchymal and stem cell-like features in RCC [247]. Based on this crucial finding, we proposed that the alternatively spliced isoforms

of TG2, which display a higher GTPase activity than the canonical TG2 [94], might play an important role in RCC biology.

Cancer cells are known to acquire flexibility by deregulating many pathways important for the maintenance of homeostasis [248]. Many of these deregulated pathways promote the aberrant splicing, offering diverse outcomes through radical alterations in the functions of the protein product [202]. Much like the majority of apoptotic protein-coding genes giving rise to the production of anti-apoptotic isoforms through alternative splicing in cancer [249], alternative splicing of the *TGM2* gene in RCC might give rise to the production of these GTPase-potent isoforms in RCC. Indeed, a strong correlation was reported to exist between the expressions of the full-length TG2 and its alternatively spliced variants in normal human tissues, while a dysregulated expression profile arises in prostate, head and neck, melanoma, and breast cancer cells [203]. As a result, four TG2 isoforms with distinct C-termini are produced: these isoforms have residual (but GTP-regulation-insensitive) transamidase activity and higher GTPase activity than the full-length TG2 [94].

Given the influence of TG2 not only in the development and propagation but also in the mediation of the invasive and metastatic potential of RCC [193], this study initially focused on the TG2 isoform expression profiles in patients with RCC. According to our bioinformatic analysis of a previous study [240], four out of ten patients with ccRCC displayed irregular TG2 isoform expression patterns, while the fold-change in mRNA levels of TG2 in tumor tissues were comparable between each patient who displayed an upregulation [240, 241]. This observation was in line with the findings of Phatak et al. [203], suggesting that the changes in TG2 isoform levels might have different pathological implications in RCC. Aiming to validate these findings in a larger patient population, we further analyzed 40 patients with ccRCC for TG2 isoform expression levels, along with the full-length TG2, in normal and tumor specimens. In our patient population, upregulation of TG2, tTGv1, and tTGv2 in RCC tissues was significantly associated with high Fuhrman grades, while no such association was found for TGH and TGH2. These findings should be evaluated carefully since we stratified the patients into low-grade (G1-2) and high-grade (G3-4) groups, but only patients with non-metastatic RCC were included in the study, and among these, only three had G4 disease. In other words, the observed upregulation of tTGv1 and tTGv2 was more in association with G3 disease. In this setting, the prognostic value of TGH and TGH2 might be underestimated since we have yet to determine whether these two

isoforms are associated with G4 disease. Regarding the tumor stage, only TG2 showed significantly different expression levels between low and high T stages. We might have been unable to find an association between any of the TG2 isoforms and the T stage due to the limiting effect of our small sample size. Our studies will continue until a sample size of 100 patients is reached, aiming to reflect the true prognostic value of TG2 isoforms in RCC, as well as their association with additional clinical and demographic parameters.

As our findings suggested that TG2 isoforms might play a role in the development of ccRCC that originates from the cellular transformation of epithelial cells of the renal proximal tubule, we investigated the effects of TG2 isoforms on the proliferation, cell cycle progression, EMT status, and MMP profiles of RPTECs chosen as the model cell line. The importance of the selection of this cell line as the model underlies the following two key findings: (i) PDGFR and VEGFR signaling, along with mTOR, HIF-1, and MAPK activated in the downstream, constitute the key pathways in RCC development and progression [250], and TG2 is known to activate these pathways [193]; (ii) as aforementioned, TG2 is abundantly expressed in tubular epithelial cells under pathological conditions [244]. Importantly, we decided to avoid prior silencing of TG2 in RPTECs inducibly expressing the isoforms, given that all patients in our study showed an upregulation in TG2 isoforms with a concomitant upregulation of the full-length form (Figure 4.1). These findings suggested that the clinical significance of TG2 isoforms was not independent from the presence of the full-length TG2. Therefore, the only alteration in the established RPTECs was the induction of one TG2 isoform.

Prior to establishing RPTECs with exogenous TG2 isoform expression, we considered the contradicting reports regarding the roles of TG2 isoforms on cell survival and death. Since TGH has been implicated in several reports to induce apoptosis independent from its transamidase activity [121, 251], and not all isoforms have been characterized extensively, we intended to avoid untimely cell death by employing an inducible gene expression system [252]. The improved ‘all-in-one’ tetracycline-responsive gene expression system used in this study also offers the advantages of reduced oncogene activation caused by the integrated vector genome, increased transgene expression, and delivery of a single vector carrying all elements required for a successful transduction [252, 253]. Dox was used as an inducer due to its shorter serum half-life compared with other tetracycline analogs (22 vs. 48 hours), which ensures the suppression of transgene expression in a shorter period [254]. Successful

production of Tet-on lentiviral particles in this study was confirmed by the detection of fluorescent signals in 293FT cells transfected with the EGFP vector.

Transgene delivery to primary cells is often difficult due to their surface characteristics and strong immune responses, and lentiviral vectors are often preferred for the transduction of such cells owing to their ability to transduce both dividing and non-dividing cells and allow stable transgene expression [255]. In addition, polycations have been widely used in mammalian cell transduction since they can reverse the negative charges on cellular and viral membranes, preventing their repulsion [256]. Among the polycation agents widely used to increase the transduction efficiency, we selected protamine sulfate due to its well-characterized efficiency and low toxicity on a range of cells [257–259], including primary cells [259–261]. In addition, based on our previous study comparing the efficacy of cell transduction using viral pellets with that of viral suspensions (98.65% vs. 99.56%), we decided to transduce RPTECs directly with the viral suspensions collected from 293FT cells [261]. Our results showed a significant improvement in the transduction efficiency of RPTECs when 10 μg/ml protamine sulfate was used. Higher doses of the agent neither increased the transduction efficiency nor showed alterations in cell morphology, indicating that protamine sulfate at the tested doses did not exert marked toxicity on RPTECs.

We characterized the transduced RPTECs in terms of ‘leaky’ mRNA expression, i.e., a residual transgene expression occurring without Dox induction [262]. To this end, we performed a qPCR analysis using a forward primer specific to a *TGM2* region common for all isoforms and a reverse primer specific to the Flag tag region. Using the Flag-specific primer for this analysis eliminated the possibility of detecting any possible endogenous TG2 isoform expressions. As expected, no detectable target region amplification was observed for most replicates of the parental cells (lacking the Flag tag region) and RPTEC-Mock cells (lacking the common *TGM2* region). The ratios of isoform mRNA expression in Dox-induced RPTECs to those in non-induced cells showed that a significant Dox-dependent transgene upregulation could be achieved in each case, with at least a 2-fold increase in the TG2 isoform mRNA levels.

The time-dependent analysis of TG2 isoform expression in response to Dox treatment showed that the full-length TG2 was the first isoform to be upregulated, with a significant 3.5-fold increase at 24 hours after the initiation of induction. A significant upregulation was observed in TGH mRNA at 48 hours, TGH2 and tTGv1 mRNAs at 72 hours, and tTGv2

mRNA at 96 hours. One possible reason for the upregulation of each TG2 isoform mRNA at a distinct time point is the potential differences in their miRNA regulations in RPTECs [263, 264]. The differences in the mRNA sequences might not only affect the number of miRNA binding regions on each isoform but also allow their regulation by different miRNAs. For example, miRNAs regulating the level of the full-length TG2 mRNA by binding to a 3' UTR region that is absent in other isoforms cannot be expected to regulate the mRNA expression of these isoforms [265]. Additionally, the unique sequences at the 3' ends of the alternatively spliced isoforms [192] might comprise target sites for miRNAs that do not normally regulate TG2 mRNA levels. A supporting insight into this phenomenon was obtained by the study reporting a higher protein level of TGH in contrast to its decreased mRNA levels [266]. In the study, the authors identified miR-19a/b as a potential miRNA regulator of TG2 by *in silico* analysis of the 3'-UTR regions. miR-19a expression was significantly upregulated in liver metastasis sections of colorectal cancer patients, compared with primary tumor sections. Correspondingly, TG2 was downregulated in colorectal cancer cells derived from the metastatic site. However, TGH escaped this regulation, potentially compensating for the miR-19-induced reduction of TG2 in metastatic cells to maintain the adhesive and migratory functions [266]. Therefore, it is plausible to assume that a similar regulation exists for the other splice variants of TG2, and future *in silico* analyses focusing on this aspect will be key to dissecting the characteristics of TG2 isoforms. Another factor that might contribute to the dissimilarities in isoform induction profiles is the potential variability in the integrated copy numbers. The viral genome insertion process might be affected by the cellular and environmental conditions at the time of the experiment, resulting in the transfection of different proportions of cells in a population and multiple integrations into the host genome [267]. The copy numbers in transduced cells can be identified using lentiviral standards and high-specificity detection methods such as digital droplet PCR, allowing the systematical analysis of potential cellular responses and a more accurate interpretation of the obtained results [268].

Despite the contradicting reports on the role of TG2 in cell survival and death, the induction of TG2 splice variants in RPTECs did not cause cell death within the given time frame of 96 hours. In 2015, Fraij characterized a transamidase-active 55-kDa truncated form (TG-55kDa) produced *in vitro* and *in vivo* by proteolytic cleavage of the full-length TG2, which is a common phenomenon for members of the TG family [120, 269]. An increase in $Ca^{2+}$

concentration usually accompanied the activation of TG2 through this mechanism, followed by cell death. The author explained the distinctions of the TG2 isoforms from TG-55kDa, clarifying the potential reasons underlying the contradicting findings in the literature [269]. According to our observations in this study, none of the TG2 isoforms seemed to possess the same activities as the TG-55kDa form.

Since the full-length TG2 is known to be present in cellular membranes [4, 70], we used a flow cytometry analysis to determine the externalization potential of each isoform. The highest RPTEC-membrane association was recorded for the TGH2 variant. Among the most important roles of TG2 on the cell surface are the activation of integrin signaling and ECM crosslinking; however, TGH and TGH2 are known to lack some residues involved in the interaction of TG2 with ITGB1 [32] and FN [270]. Therefore, it was suggested that these two shortest variants cannot be involved in cell migration through the adhesive functions [271], and the significance of the residual transamidase activity level is yet to be elucidated. The abundance of TGH2 on the RPTEC membrane might be associated with its lacking GTPase and constant transamidase activities, promoting the selective accumulation of this protein to compensate for the downregulation of TG2, especially in primary tumor lesions [246]. Meanwhile, TGH, tTGv1, and tTGv2 are likely to compensate for the GTPase activity-dependent transforming functions of TG2 under these circumstances [175]. Notably, TGH mRNA showed significantly higher expression in the epithelial compartment of paraffin-embedded breast cancer tissue samples, while TG2 mRNA levels were comparable in the epithelial and stromal compartments [272]. Moreover, among the triple-negative breast cancer cell lines analyzed, those derived from primary tumors were not significantly different in TGH expression than those isolated from metastatic pleural effusions [272], supporting the idea of a compensation mechanism for this isoform.

This study demonstrated the proliferative effect of TG2 isoforms in renal tubular epithelial cells for the first time. In the literature, the doubling time of parental RPTECs has been reported as 96 hours [242]. Our population doubling time analysis showed that the induction of TG2 in RPTECs reduced their doubling time to 75 hours. These results were in line with previous studies reporting a TG2-dependent increase in the cell proliferation rate [273].

TGH was found to hydrolyze GTP three to four-fold faster than TG2 [194], and, in hepatic cells, the GTPase-active form of the full-length TG2 was found to be responsible for the activation of PLCδ signaling as a component of α1-adrenergic receptor complexes,

promoting cell growth [251]. Of note, α1-adrenergic receptors are found in the kidney cortex, pelvis, calyces, blood vessels, and tubules, and receptor antagonists targeting α1-adrenergic receptors are known to reduce vascularity and impair renal tumor growth by inducing apoptosis and overcoming resistance to anoikis [274], a mechanism likely involving the GTPase-active TG2. RPTEC-TGH cells initially displayed a growth profile similar to that of RPTEC-Mock cells, with a prominent increase in the proliferation rate only at 72 hours after the termination of Dox induction. This slower response of RPTECs to the induction of TGH compared with TG2 can be explained by the delayed upregulation of its mRNA (24 hours vs. 48 hours following the initiation of Dox treatment). Nevertheless, by the end of 96 hours, the induction of TGH resulted in a 40% higher proliferation rate compared with RPTEC-Mock cells, reducing the doubling time of RPTECs to 90 hours. In line with these findings, a recent study reported that TGH accumulates in triple-negative MDA-MB-231 breast cancer cells, being actively transcribed with the increased cell proliferation rate [272]. Further, demonstrating that the levels of the TGH isoform was not significantly different between the primary and metastatic site-derived cells, the authors inferred that the TG2/TGH ratio might be an important feature of the actively proliferating and aggressive cancer cells [272].

Despite the significant upregulation of TGH2 and tTGv1 mRNA levels in RPTECs at 72 hours after the termination of Dox induction, RPTEC-TGH2 and RPTEC-tTGv1 cells displayed a proliferation rate comparable to that of RPTEC-Mock cells, with population doubling times of 95 and 98 hours, respectively. For TGH2, this profile might be associated with the complete lack of its GTP-binding domain [94, 192], which might implicate transforming functions other than GTPase-dependent signaling for this isoform [175]. However, the reasons underlying the inability of the tTGv1 isoform to take part in similar cellular processes are expected to be elucidated in future studies focusing on their crystal structures and protein-protein interactions.

A notable increase in proliferation was observed in RPTECs following the induction of the tTGv2 isoform, resulting in a 70% increase in the cell doubling compared with RPTEC-Mock cells. The doubling time of RPTEC-tTGv2 cells was calculated as 85 hours, making this isoform the second most effective inducer of cell proliferation after the full-length TG2. This result is plausible given the approximate 7-fold higher GTPase activity of tTGv2 compared with the canonical isoform [94].

Following the analysis of cell proliferation rate, we examined the influence of TG2 isoforms on cell cycle progression. We found that expression of TG2, TGH, tTGv1, and tTGv2 shifted approximately 60% and TGH2 shifted 12% of the transduced RPTECs to the S and G2/M phases, compared with RPTEC-Mock cells. TG2-mediated regulation of cell cycle proteins have been reported previously [275]. Consistently, cyclin D and CDK4 proteins were upregulated in RPTEC-TG2 cells, promoting their progression through the G1 restriction point. RPTEC-TGH cells showed the upregulation of cyclin D, CDK4, cyclin E, and CDK2, indicating progression into the S and G2/M phases. Expression of TGH2 caused an increase in cyclin D protein levels albeit without an accommodating upregulation in CDK4, which explained the lower percentage of cells at the S-G2/M phase since the complex formed by these proteins is required for the progression through the G1 checkpoint [276]. Expressions of tTGv1 and tTGv2 caused an upregulation to some extent in all cell cycle proteins investigated, in line with the high cell cycle progression rate observed for RPTECs transduced with these isoforms.

Overall, the results of the cell proliferation and cell cycle analyses support our previous finding that the GTPase activity is tightly associated with RCC progression [247]. Future studies investigating the activation of cellular signaling pathways depending on the GTPase activity of the isoforms will provide detailed insight into the molecular mechanisms underlying the effects observed in this work.

EMT is a well-known phenomenon in cancer, and NF-κB is crucial for the induction and maintenance of this process in transformed cells [277]. NF-κB activates the expression of EMT transcription factors in the nucleus, including Zeb1, Zeb2, Snail and Twist. Since TG2 activates NF-κB both through the crosslinking-dependent and independent degradation of IκB molecules [164], and the GTP-binding/GTPase activity of TG2 was necessary for the induction of EMT and the acquisition of the cancer stem cell phenotype in RCC [247], we investigated the EMT profile of RPTECs transduced with TG2 isoforms. Notably, the levels of E-cadherin mRNA (*CDH1*), an important epithelial cell adhesion protein and EMT marker [278], was dropped to undetectable levels upon induction of each TG2 isoform in RPTECs.

Out of eight mesenchymal markers investigated, four (N-cadherin, Zeb 1, Zeb 2, Twist 1) showed a significant upregulation in RPTEC-TG2 cells. Although nearly all these markers were reported to be upregulated in correlation with TG2 levels, the difference in our findings

might be explained in part by the timing of the experiment. As described in the results section, TG2 was highly upregulated at 24 hours after Dox induction, but reduced to levels comparable to that of RPTEC-Mock cells by the end of 96 hours. Our qPCR analysis was performed at late time points, at which several EMT markers might have been already downregulated. For example, Snail transcription factors are known to bind the *CDH1* promoter and suppress E-cadherin expression [279]. Considering the low E-cadherin and Snail 1/2 levels at the analyzed time points, Snail upregulation might have occurred early upon Dox-induction to suppress *CDH1* expression. This hypothesis should be tested with further experiments showing the mRNA as well as protein expression levels. Moreover, four EMT markers (N-cadherin, Twist 2, Snail 2, vimentin) in RPTEC-TGH, three (Twist 1/2, Snail 2, vimentin) in RPTEC-TGH2, two (Twist 1 and vimentin) in RPTEC-tTGv1, and two (Twist 1 and Snail 2) in RPTEC-tTGv2 cells were significantly upregulated. An important factor in interpreting these results is that the EMT markers are usually tissue-specific and even the transcription factors of the same family might have antagonistic roles [280]. For example, the Snail transcription factors induce metastasis in breast cancer but have no effect on pancreatic cancer [281]. Further, the Zeb 1 transcription factor was shown to promote the development of melanoma, while Zeb 2 was associated with a reduction in aggressive tumor profile [282, 283]. Finally, the complete activation of EMT in cancer is rare, and some of the final players in the activation sequence, such as vimentin, are often undetected [280]. Therefore, our results showing the upregulation of vimentin only in TGH- and TGH2-transduced RPTECs might be attributed to this partial activation mechanism, especially considering that these are normal tubular epithelial cells and do not possess the aberrant genetic/epigenetic alterations found in transformed cells, which could have a substantial effect on the outcomes. Upregulation in several EMT markers actually indicates a tremendous effect of the isoforms on the malignant transformation potential of RPTECs, considering that the induction of a TG2 isoform was the only dysregulation in these cells. Whether the observed changes in EMT markers can be associated with the activation of the NF-κB pathway in RPTECs is yet to be determined.

Our group has previously demonstrated the TG2-dependent increase in MMP expression and activation [179, 284]. Based on our key study showing that the association of TG2-induced MMP expression with the invasive potential of RCC was dependent on the GTP-binding/GTPase activity [247], we assessed the MMP profiles of isoform-transduced

RPTECs and found that the mRNA levels of gelatinases (*MMP2* and *MMP9*) and collagenases (*MMP1* and *MMP13*) were increased in response to the induction of TG2 isoforms in RPTECs. High MMP-9 expression was found in human cancer tissues, and this profile was associated with invasion and metastasis through the downregulation of E-cadherin [285]. Moreover, the protein levels of MMP-2 and MMP-9 were upregulated by Zeb 1/2 transcription factors [279]. Additionally, Snail 1 initiated the EMT process by promoting the expression of MMPs, the levels of which were then maintained by both Snail 1 and 2 [286]. Crosstalk between MMP-13 and Twist 1 has also been reported [287]. Therefore, a tight relationship exists between the induction of cancer-associated EMT and MMPs. From this perspective, our results suggest that the invasive potential of renal epithelial cells can be increased by the expression of TG2 isoforms. However, we only demonstrated the changes in mRNA levels. Since MMPs are produced as inactive zymogens and require proteolytic cleavage to exert their functions, the activation of the enzymes should be confirmed with further experiments such as zymography.

EMT induction and MMP activity on the ECM components are followed by a migratory movement in oncogenic transformation. Acording to our wound healing data, induction of all isoforms in RPTECs except tTGv2 resulted in an improved wound healing capacity. Although tTGv2 was present on the membrane at equal levels to TG2 and tTGv1 and several EMT markers, as well as MMPs, were upregulated at the transcriptional level, RPTECs expressing the tTGv2 variant did not show any difference from the parental RPTECs in terms of migration potential. Possible explanations for this case might be explained in part by the future experiments showing MMP activation profiles.

# 6. CONCLUSIONS AND FUTURE WORK

The work presented in this thesis show the clinical significance of TG2 and its alternatively spliced variants in RCC, as well as the successful establishment of renal tubular epithelial cells inducibly expressing the TG2 isoforms and the potential transforming effects of these isoforms exerted on the modulation of cell proliferation, cell cycle, EMT, and invasion potential in these cells. Our immediate future efforts will be directed at determining (i) the activities of MMPs to better elucidate the effects of TG2 isoforms on the invasion capacity, (ii) the cell scattering potential to demonstrate isoform-induced RPTEC mobility, and (iii) the activation of growth factor signaling axes, including the VEGFR and PDGFR pathways, to provide a strong molecular basis for the TG2 isoform-dependent transformation of RPTECs. Unraveling the mechanisms underlying the preferential expression of alternatively spliced mRNA variants in cancer cells due to the intracellular and extracellular factors in the tumor microenvironment is an indisputable challenge in cancer research, and the findings presented in this thesis have a guiding significance for the future efforts of developing new and effective therapeutic approaches against RCC, considering the novel contributions of TG2 isoforms to the process.

# REFERENCES


1. Duarte L, Matte CR, Bizarro CV, Ayub MAZ (2020) Transglutaminases: part I—origins, sources, and biotechnological characteristics. World Journal of Microbiology and Biotechnology 2020 36:1 36:1–18

2. Lerner A, Ramesh A, Matthias T (2020) The temperature and pH repertoire of the transglutaminase family is expanding. FEBS Open Bio 10:492–494

3. Ohtsuka T, Ota M, Nio N, Motoki M (2000) Comparison of Substrate Specificities of Transglutaminases Using Synthetic Peptides as Acyl donors. Biosci Biotechnol Biochem 64:2608–2613

4. Eckert RL, Kaartinen MT, Nurminskaya M, Belkin AM, Colak G, Johnson GVW, Mehta K (2014) Transglutaminase regulation of cell function. Physiol Rev 94:383–417

5. Sarkar NK, Clarke DD, Waelsch H (1957) An enzymically catalyzed incorporation of amines into proteins. Biochim Biophys Acta 25:451–452

6. Esposito C, Caputo I (2005) Mammalian transglutaminases. FEBS J 272:615–631

7. Martins IM, Choupina A (2018) Protein-Glutamine Gamma-Glutamyltransferase. Encyclopedia of Signaling Molecules 4253–4257

8. Griffin M, Casadio R, Bergamini CM (2002) Transglutaminases: nature's biological glues. Biochem J 368:377–396

9. Yokoyama K, Nio N, Kikuchi Y (2004) Properties and applications of microbial transglutaminase. Appl Microbiol Biotechnol 64:447–454

10. Clarke DD, Mycek MJ, Neidle A, Waelsch H (1959) The incorporation of amines into protein. Arch Biochem Biophys 79:338–354

11. Folk JE, Cole PW (1967) Mechanism of action of guinea pig liver transglutaminase. 3. The metal-dependent hydrolysis of p-nitrophenyl acetate; further observations on

the role of metal in enzyme activation. Journal of Biological Chemistry 242:2615–2621

12. Lorand L, Graham RM (2003) Transglutaminases: crosslinking enzymes with pleiotropic functions. Nature Reviews Molecular Cell Biology 2003 4:2 4:140–156

13. Lorand L, Iismaa SE (2019) Transglutaminase diseases: from biochemistry to the bedside. FASEB J 33:3–12

14. Makarova KS, Aravind L, Koonin E V (1999) A superfamily of archaeal, bacterial, and eukaryotic proteins homologous to animal transglutaminases.

15. Plácido D, Fernandes CG, Isidro A, Carrondo MA, Henriques AO, Archer M (2008) Auto-induction and purification of a Bacillus subtilis transglutaminase (Tgl) and its preliminary crystallographic characterization. Protein Expr Purif 59:1–8

16. Lai TS, Lin CJ, Greenberg CS (2016) Role of tissue transglutaminase-2 (TG2)-mediated aminylation in biological processes. Amino Acids 2016 49:3 49:501–515

17. Gundemir S, Colak G, Tucholski J, Johnson GVW (2012) Transglutaminase 2: A molecular Swiss army knife. Biochimica et Biophysica Acta (BBA) - Molecular Cell Research 1823:406–419

18. Yang M Te, Chang CH, Wang JM, Wu TK, Wang YK, Chang CY, Li THT (2011) Crystal structure and inhibition studies of transglutaminase from Streptomyces mobaraense. J Biol Chem 286:7301–7307

19. Shi YG, Qian L, Zhang N, Han CR, Liu Y, Zhang YF, Ma YQ (2011) Changes in morphology and activity of transglutaminase following cross-linking and immobilization on a polypropylene microporous membrane. Molecules 16:10046–10058

20. Aufenvenne K, Larcher F, Hausser I, Duarte B, Oji V, Nikolenko H, Del Rio M, Dathe M, Traupe H (2013) Topical enzyme-replacement therapy restores transglutaminase 1 activity and corrects architecture of transglutaminase-1-deficient skin grafts. Am J Hum Genet 93:620–630

21. Cserhalmi-Friedman PB, Milstone LM, Christiano AM (2001) Diagnosis of autosomal recessive lamellar ichthyosis with mutations in the TGM1 gene. British Journal of Dermatology 144:726–730

22. Huber M, Rettler I, Bernasconi K, Frenk E, Lavrijsen SPM, Ponec M, Bon A, Lautenschlager S, Schorderet DF, Hohl D (1995) Mutations of keratinocyte transglutaminase in lamellar ichthyosis. Science 267:525–528

23. Matsuki M, Yamashita F, Ishida-Yamamoto A, et al (1998) Defective stratum corneum and early neonatal death in mice lacking the gene for transglutaminase 1 (keratinocyte transglutaminase). Proc Natl Acad Sci U S A 95:1044–1049

24. Diaz-Hidalgo L, Altuntas S, Rossin F, D'Eletto M, Marsella C, Farrace MG, Falasca L, Antonioli M, Fimia GM, Piacentini M (2016) Transglutaminase type 2-dependent selective recruitment of proteins into exosomes under stressful cellular conditions. Biochim Biophys Acta 1863:2084–2092

25. Antonyak MA, Li B, Boroughs LK, Johnson JL, Druso JE, Bryant KL, Holowka DA, Cerione RA (2011) Cancer cell-derived microvesicles induce transformation by transferring tissue transglutaminase and fibronectin to recipient cells. Proc Natl Acad Sci U S A 108:4852–4857

26. Nurminskaya M V., Belkin AM (2012) Cellular functions of tissue transglutaminase. Int Rev Cell Mol Biol 294:1–97

27. Nakaoka H, Perez DM, Baek KJ, Das T, Husain A, Misono K, Im MJ, Graham RM (1994) Gh: a GTP-binding protein with transglutaminase activity and receptor signaling function. Science 264:1593–1596

28. Mishra S, Murphy LJ (2006) Phosphorylation of transglutaminase 2 by PKA at Ser216 creates 14-3-3 binding sites. Biochem Biophys Res Commun 347:1166–1170

29. Mishra S, Murphy LJ (2006) The p53 oncoprotein is a substrate for tissue transglutaminase kinase activity. Biochem Biophys Res Commun 339:726–730

30. Mishra S, Melino G, Murphy LJ (2007) Transglutaminase 2 kinase activity facilitates protein kinase A-induced phosphorylation of retinoblastoma protein. Journal of Biological Chemistry 282:18108–18115

31. Hasegawa G, Suwa M, Ichikawa Y, Ohtsuka T, Kumagai S, Kikuchi M, Sato Y, Saito Y (2003) A novel function of tissue-type transglutaminase: protein disulphide isomerase. Biochemical Journal 373:793–803

32. Akimov SS, Krylov D, Fleischmana LF, Belkin AM (2000) Tissue Transglutaminase Is an Integrin-Binding Adhesion Coreceptor for Fibronectin. Journal of Cell Biology 148:825–838

33. Katt WP, Antonyak MA, Cerione RA (2018) The diamond anniversary of tissue transglutaminase: a protein of many talents. Drug Discov Today 23:575–591

34. Nanda N, Iismaa SE, Owens WA, Husain A, Mackay F, Graham RM (2001) Targeted inactivation of Gh/tissue transglutaminase II. J Biol Chem 276:20673–20678

35. Haroon ZA, Hettasch JM, Lai T, Dewhirst MW, Greenberg CS (1999) Tissue transglutaminase is expressed, active, and directly involved in rat dermal wound healing and angiogenesis. FASEB J 13:1787–1795

36. Mearns B, Nanda N, Michaelicek J, Iismaa S, Graham R (2002) Impaired wound healing and altered fibroblast cytoskeletal dynamics in G(h) knockout mice. Minerva Biotecnol 14:218

37. Hitomi K, Horio Y, Ikura K, Yamanishi K, Maki M (2001) Analysis of epidermal-type transglutaminase (TGase 3) expression in mouse tissues and cell lines. Int J Biochem Cell Biol 33:491–498

38. Hitomi K, Presland RB, Nakayama T, Fleckman P, Dale BA, Maki M (2003) Analysis of epidermal-type transglutaminase (transglutaminase 3) in human stratified epithelia and cultured keratinocytes using monoclonal antibodies. J Dermatol Sci 32:95–103

39. Hitomi K, Kanehiro S, Ikura K, Maki M (1999) Characterization of recombinant mouse epidermal-type transglutaminase (TGase 3): regulation of its activity by proteolysis and guanine nucleotides. J Biochem 125:1048–1054

40. Bognar P, Nemeth I, Mayer B, et al (2014) Reduced Inflammatory Threshold Indicates Skin Barrier Defect in Transglutaminase 3 Knockout Mice. Journal of Investigative Dermatology 134:105–111

41. John S, Thiebach L, Frie C, Mokkapati S, Bechtel M, Nischt R, Rosser-Davies S, Paulsson M, Smyth N (2012) Epidermal transglutaminase (TGase 3) is required for proper hair development, but not the formation of the epidermal barrier. PLoS One. https://doi.org/10.1371/JOURNAL.PONE.0034252

42. Uemura N, Nakanishi Y, Kato H, Saito S, Nagino M, Hirohashi S, Kondo T (2009) Transglutaminase 3 as a prognostic biomarker in esophageal cancer revealed by proteomics. Int J Cancer 124:2106–2115

43. Negishi A, Masuda M, Ono M, et al (2009) Quantitative proteomics using formalin-fixed paraffin-embedded tissues of oral squamous cell carcinoma. Cancer Sci 100:1605–1611

44. Jiang WG, Ablin RJ (2011) Prostate transglutaminase: a unique transglutaminase and its role in prostate cancer. http://dx.doi.org/102217/bmm1136 5:285–291

45. Dean MD (2013) Genetic Disruption of the Copulatory Plug in Mice Leads to Severely Reduced Fertility. PLoS Genet 9:e1003185

46. Ablin RJ, Owen S, Jiang WG (2017) Prostate Transglutaminase (TGase-4) Induces Epithelial-to-Mesenchymal Transition in Prostate Cancer Cells. Anticancer Res 37:481–488

47. Candi E, Oddi S, Paradisi A, Terrinoni A, Ranalli M, Teofoli P, Citro G, Scarpato S, Puddu P, Melino G (2002) Expression of transglutaminase 5 in normal and pathologic human epidermis. J Invest Dermatol 119:670–677

48. Candi E, Paradisi A, Terrinoni A, et al (2004) Transglutaminase 5 is regulated by guanine–adenine nucleotides. Biochemical Journal 381:313–319

49. Cassidy AJ, Van Steensel MAM, Steijlen PM, Van Geel M, Van Der Velden J, Morley SM, Terrinoni A, Melino G, Candi E, McLean WHI (2005) A homozygous missense mutation in TGM5 abolishes epidermal transglutaminase 5 activity and causes acral peeling skin syndrome. Am J Hum Genet 77:909–917

50. Cangkrama M, Darido C, Georgy SR, Partridge D, Auden A, Srivastava S, Wilanowski T, Jane SM (2016) Two Ancient Gene Families Are Critical for

Maintenance of the Mammalian Skin Barrier in Postnatal Life. Journal of Investigative Dermatology 136:1438–1448

51. Mehta K (2005) Mammalian transglutaminases: a family portrait. Prog Exp Tumor Res 38:1–18

52. Liu YT, Tang BS, Lan W, et al (2013) Distribution of transglutaminase 6 in the central nervous system of adult mice. Anat Rec (Hoboken) 296:1576–1587

53. Thomas H, Beck K, Adamczyk M, Aeschlimann P, Langley M, Oita RC, Thiebach L, Hils M, Aeschlimann D (2013) Transglutaminase 6: A protein associated with central nervous system development and motor function. Amino Acids 44:161–177

54. Wang J, Wang JL, Yang X, et al (2010) TGM6 identified as a novel causative gene of spinocerebellar ataxias using exome sequencing. Brain 133:3510–3518

55. Pan LL, Huang YM, Wang M, Zhuang XE, Luo DF, Guo SC, Zhang ZS, Huang Q, Lin SL, Wang SY (2014) Positional cloning and next-generation sequencing identified a TGM6 mutation in a large Chinese pedigree with acute myeloid leukaemia. European Journal of Human Genetics 2015 23:2 23:218–223

56. Zheng R, Li Z, He F, et al (2018) Genome-wide association study identifies two risk loci for tuberculosis in Han Chinese. Nature Communications 2018 9:1 9:1–9

57. Tatsukawa H, Otsu R, Tani Y, Wakita R, Hitomi K (2018) Isozyme-specific comprehensive characterization of transglutaminase-crosslinked substrates in kidney fibrosis. Scientific Reports 2018 8:1 8:1–18

58. Tahlan A, Ahluwalia J (2014) Factor XIII: congenital deficiency factor XIII, acquired deficiency, factor XIII A-subunit, and factor XIII B-subunit. Arch Pathol Lab Med 138:278–281

59. Nurminskaya M, Magee C, Nurminsky D, Linsenmayer TF (1998) Plasma Transglutaminase in Hypertrophic Chondrocytes: Expression and Cell-specific Intracellular Activation Produce Cell Death and Externalization. J Cell Biol 142:1135

60. Dardik R, Leor J, Skutelsky E, Castel D, Holbova R, Schiby G, Shaish A, Dickneite G, Loscalzo J, Inbal A (2006) Evaluation of the pro-angiogenic effect of factor XIII

in heterotopic mouse heart allografts and FXIII-deficient mice. Thromb Haemost 95:546–550

61. Koseki-Kuno S, Yamakawa M, Dickneite G, Ichinose A (2003) Factor XIII A subunit-deficient mice developed severe uterine bleeding events and subsequent spontaneous miscarriages. Blood 102:4410–4412

62. Nahrendorf M, Hu K, Frantz S, et al (2006) Factor XIII deficiency causes cardiac rupture, impairs wound healing, and aggravates cardiac remodeling in mice with myocardial infarction. Circulation 113:1196–1202

63. Peters LL, Jindel HK, Gwynn B, et al (1999) Mild spherocytosis and altered red cell ion transport in protein 4.2–null mice. Journal of Clinical Investigation 103:1527

64. Hayashi S, Koomoto R, Yano A, Ishigami S, Tsujino G, Saeki S, Tanaka T (1974) Abnormality in a specific protein of the erythrocyte membrane in hereditary spherocytosis. Biochem Biophys Res Commun 57:1038–1044

65. Gentile V, Saydak M, Chioccas EA, Akandes O, Birckbichlerq PJ, Lees KN, Steinsv JP, Davies PJA (1991) Isolation and Characterization of cDNA Clones to Mouse Macrophage and Human Endothelial Cell Tissue Transglutaminases. J Biol Chem 266:478–483

66. Fraij BM, Gonzales RA (1997) Organization and structure of the human tissue transglutaminase gene. Biochim Biophys Acta 1354:65–71

67. Liu S, Cerione RA, Clardy J (2002) Structural basis for the guanine nucleotide-binding activity of tissue transglutaminase and its regulation of transamidation activity. Proc Natl Acad Sci U S A 99:2743–2747

68. Csosz E, Bagossi P, Nagy Z, Dosztanyi Z, Simon I, Fesus L (2008) Substrate Preference of Transglutaminase 2 Revealed by Logistic Regression Analysis and Intrinsic Disorder Examination. J Mol Biol 383:390–402

69. Facchiano A, Facchiano F (2009) Transglutaminases and their substrates in biology and human diseases: 50 Years of growing. Amino Acids 36:599–614

70. Sima LE, Matei D, Condello S (2022) The Outside-In Journey of Tissue Transglutaminase in Cancer. 11:1779

71. Baek KJ, Kwon NS, Lee HS, Kim MS, Muralidhar P, Im MJ (1996) Oxytocin receptor couples to the 80 kDa Gh alpha family protein in human myometrium. Biochemical Journal 315:739

72. Vezza R, Habib A, FitzGerald GA (1999) Differential signaling by the thromboxane receptor isoforms via the novel GTP-binding protein, Gh. J Biol Chem 274:12774–12779

73. Lin YF, Tseng MJ, Hsu HL, Wu YW, Lee YH, Tsai YH (2006) A novel follicle-stimulating hormone-induced G alpha h/phospholipase C-delta1 signaling pathway mediating rat sertoli cell Ca2+-influx. Mol Endocrinol 20:2514–2527

74. Antonyak M, Cerione RA (2010) Tissue Transglutaminase: A Unique GTP-Binding/GTPase. Handbook of Cell Signaling, Second Edition 2:1795–1802

75. Iismaa SE, Wu MJ, Nanda N, Church WB, Graham RM (2000) GTP binding and signaling by G(h)/transglutaminase II involves distinct residues in a unique GTP-binding pocket. Journal of Biological Chemistry 275:18259–18265

76. Mishra S, Murphy LJ (2004) Tissue Transglutaminase Has Intrinsic Kinase Activity. Journal of Biological Chemistry 279:23863–23868

77. Mishra S, Saleh A, Espino PS, Davie JR, Murphy LJ (2006) Phosphorylation of histones by tissue transglutaminase. Journal of Biological Chemistry 281:5532–5538

78. Jung SH, Kong DH, Jeon HY, Ji SH, Han ET, Park WS, Hong SH, Kim MS, Kim YM, Ha KS (2016) Identification of transglutaminase 2 kinase substrates using a novel on-chip activity assay. Biosens Bioelectron 82:40–48

79. Malorni W, Farrace MG, Matarrese P, et al (2009) The adenine nucleotide translocator 1 acts as a type 2 transglutaminase substrate: implications for mitochondrial-dependent apoptosis. Cell Death & Differentiation 2009 16:11 16:1480–1492

80. Mastroberardino PG, Farrace MG, Viti I, Pavone F, Fimia GM, Melino G, Rodolfo C, Piacentini M (2006) “Tissue” transglutaminase contributes to the formation of disulphide bridges in proteins of mitochondrial respiratory complexes. Biochimica et Biophysica Acta (BBA) - Bioenergetics 1757:1357–1365

81. Rossin F, Villella VR, D’Eletto M, et al (2018) TG2 regulates the heat-shock response by the post-translational modification of HSF1. EMBO Rep 19:e45067

82. Wang Z, Collighan RJ, Gross SR, Danen EHJ, Orend G, Telci D, Griffin M (2010) RGD-independent cell adhesion via a tissue transglutaminase-fibronectin matrix promotes fibronectin fibril deposition and requires syndecan-4/2 α5β1 integrin co-signaling. J Biol Chem 285:40212–40229

83. Zemskov EA, Mikhailenko I, Smith EP, Belkin AM (2012) Tissue transglutaminase promotes PDGF/PDGFR-mediated signaling and responses in vascular smooth muscle cells. J Cell Physiol 227:2089–2096

84. Zemskov EA, Loukinova E, Mikhailenko I, Coleman RA, Strickland DK, Belkin AM (2009) Regulation of platelet-derived growth factor receptor function by integrin-associated cell surface transglutaminase. J Biol Chem 284:16693–16703

85. Tempest R, Guarnerio S, Maani R, Cooper J, Peake N (2021) The Biological and Biomechanical Role of Transglutaminase-2 in the Tumour Microenvironment. Cancers (Basel). https://doi.org/10.3390/CANCERS13112788

86. Lee CS, Park HH (2017) Structural aspects of transglutaminase 2: functional, structural, and regulatory diversity. Apoptosis 22:1057–1068

87. Kim GE, Park HH (2020) Structures of Human Transglutaminase 2: Finding Clues for Interference in Cross-linking Mediated Activity. Int J Mol Sci. https://doi.org/10.3390/IJMS21062225

88. Han BG, Cho JW, Cho YD, Jeong KC, Kim SY, Lee B Il (2010) Crystal structure of human transglutaminase 2 in complex with adenosine triphosphate. Int J Biol Macromol 47:190–195

89. Pinkas DM, Strop P, Brunger AT, Khosla C (2007) Transglutaminase 2 Undergoes a Large Conformational Change upon Activation. PLoS Biol 5:e327

90. Begg GE, Holman SR, Stokes PH, Matthews JM, Graham RM, Iismaa SE (2006) Mutation of a critical arginine in the GTP-binding site of transglutaminase 2 disinhibits intracellular cross-linking activity. Journal of Biological Chemistry 281:12603–12609

91. Begg GE, Carrington L, Stokes PH, Matthews JM, Wouters MA, Husain A, Lorand L, Iismaa SE, Graham RM (2006) Mechanism of allosteric regulation of transglutaminase 2 by GTP. Proc Natl Acad Sci U S A 103:19683–19688

92. Casadio R, Polverini E, Mariani P, Spinozzi F, Carsughi F, Fontana A, De Laureto PP, Matteucci G, Bergamini CM (1999) The structural basis for the regulation of tissue transglutaminase by calcium ions. Eur J Biochem 262:672–679

93. Di Venere A, Rossi A, De Matteis F, Rosato N, Finazzi Agrò A, Mei G (2000) Opposite effects of Ca2+ and GTP binding on tissue transglutaminase tertiary structure. Journal of Biological Chemistry 275:3915–3921

94. Király R, Demény MÁ, Fésüs L (2011) Protein transamidation by transglutaminase 2 in cells: a disputed Ca2+-dependent action of a multifunctional protein. FEBS J 278:4717–4739

95. Monsonego A, Friedmann I, Shani Y, Eisenstein M, Schwartz M (1998) GTP-dependent conformational changes associated with the functional switch between Gα and cross-linking activities in brain-derived tissue transglutaminase. J Mol Biol 282:713–720

96. Zhang J, Lesort M, Guttmann RP, Johnson GVW (1998) Modulation of the in situ activity of tissue transglutaminase by calcium and GTP. Journal of Biological Chemistry 273:2288–2295

97. Achyuthan KE, Greenberg CS (1987) Identification of a guanosine triphosphate-binding site on guinea pig liver transglutaminase. Role of GTP and calcium ions in modulating activity. Journal of Biological Chemistry 262:1901–1906

98. Jang TH, Lee DS, Choi K, Jeong EM, Kim IG, Kim YW, Chun JN, Jeon JH, Park HH (2014) Crystal structure of transglutaminase 2 with GTP complex and amino acid

sequence evidence of evolution of GTP binding site. PLoS One. https://doi.org/10.1371/JOURNAL.PONE.0107005

99. Feng JF, Gray CD, Im MJ (1999) α1B-Adrenoceptor Interacts with Multiple Sites of Transglutaminase II: Characteristics of the Interaction in Binding and Activation. Biochemistry 38:2224–2232

100. Feng JF, Readon M, Yadav SP, Im MJ (1999) Calreticulin Down-Regulates both GTP Binding and Transglutaminase Activities of Transglutaminase II. Biochemistry 38:10743–10749

101. Iismaa SE, Chung L, Wu MJ, Teller DC, Yee VC, Graham RM (1997) The Core Domain of the Tissue Transglutaminase Gh Hydrolyzes GTP and ATP. Biochemistry 36:11655–11664

102. Lai T-S, Slaughter TF, Peoples KA, Hettasch JM, Greenberg CS (1998) Regulation of Human Tissue Transglutaminase Function by Magnesium-Nucleotide Complexes. Journal of Biological Chemistry 273:1776–1781

103. Siegel M, Strnad P, Watts RE, Choi K, Jabri B, Omary MB, Khosla C (2008) Extracellular Transglutaminase 2 Is Catalytically Inactive, but Is Transiently Activated upon Tissue Injury. PLoS One 3:e1861

104. Stamnaes J, Pinkas DM, Fleckenstein B, Khosla C, Sollid LM (2010) Redox regulation of transglutaminase 2 activity. Journal of Biological Chemistry 285:25402–25409

105. Turano C, Coppari S, Altieri F, Ferraro A (2002) Proteins of the PDI family: unpredicted non-ER locations and functions. J Cell Physiol 193:154–163

106. Yi MC, Melkonian A V, Ousey JA, Khosla C (2018) Endoplasmic reticulumâ€“resident protein 57 (ERp57) oxidatively inactivates human transglutaminase 2. https://doi.org/10.1074/jbc.RA117.001382

107. Lai TS, Slaughter TF, Koropchak CM, Haroon ZA, Greenberg CS (1996) C-terminal deletion of human tissue transglutaminase enhances magnesium-dependent GTP/ATPase activity. J Biol Chem 271:31191–31195

108. Jeong EM, Lee KB, Kim GE, Kim CM, Lee JH, Kim HJ, Shin JW, Kwon MA, Park HH, Kim IG (2020) Competitive Binding of Magnesium to Calcium Binding Sites Reciprocally Regulates Transamidase and GTP Hydrolysis Activity of Transglutaminase 2. Int J Mol Sci. https://doi.org/10.3390/IJMS21030791

109. Jeitner TM, Delikatny EJ, Ahlqvist J, Capper H, Cooper AJL (2005) Mechanism for the inhibition of transglutaminase 2 by cystamine. Biochem Pharmacol 69:961–970

110. Karpuj M V., Becher MW, Springer JE, Chabas D, Youssef S, Pedotti R, Mitchell D, Steinman L (2002) Prolonged survival and decreased abnormal movements in transgenic model of Huntington disease, with administration of the transglutaminase inhibitor cystamine. Nature Medicine 2002 8:2 8:143–149

111. Lorand L, Conrad SM (1984) Transglutaminases. Mol Cell Biochem 58:9–35

112. DiRaimondo TR, Klöck C, Khosla C (2012) Interferon-γ activates transglutaminase 2 via a phosphatidylinositol-3-kinase-dependent pathway: implications for celiac sprue therapy. J Pharmacol Exp Ther 341:104–114

113. Shin D-M, Jeon J-H, Kim C-W, et al (2008) TGFbeta mediates activation of transglutaminase 2 in response to oxidative stress that leads to protein aggregation. FASEB J 22:2498–2507

114. Jeong EM, Kim CW, Cho SY, Jang GY, Shin DM, Jeon JH, Kim IG (2009) Degradation of transglutaminase 2 by calcium-mediated ubiquitination responding to high oxidative stress. FEBS Lett 583:648–654

115. Király R, Cssz É, Kurtán T, Antus S, Szigeti K, Simon-Vecsei Z, Korponay-Szabó IR, Keresztessy Z, Fésüs L (2009) Functional significance of five noncanonical Ca2+-binding sites of human transglutaminase 2 characterized by site-directed mutagenesis. FEBS J 276:7083–7096

116. Lai TS, Hausladen A, Slaughter TF, Eu JP, Stamler JS, Greenberg CS (2001) Calcium Regulates S-Nitrosylation, Denitrosylation, and Activity of Tissue Transglutaminase†. Biochemistry 40:4904–4910

117. Harsfalvi J, Arato G, Fesus L (1987) Lipids associated with tissue transglutaminase. Biochimica et Biophysica Acta (BBA) - General Subjects 923:42–45

118. Zemskov EA, Mikhailenko I, Hsia RC, Zaritskaya L, Belkin AM (2011) Unconventional Secretion of Tissue Transglutaminase Involves Phospholipid-Dependent Delivery into Recycling Endosomes. PLoS One 6:e19414

119. Singh US, Kunar MT, Kao YL, Baker KM (2001) Role of transglutaminase II in retinoic acid-induced activation of RhoA-associated kinase-2. EMBO J 20:2413–2423

120. Fraij BM (2011) "Activation of tissue tranglutsaminase by removal of carboxyl-terminal peptides." J Cell Biochem 112:3469–3481

121. Antonyak MA, Jansen JM, Miller AM, Ly TK, Endo M, Cerione RA (2006) Two isoforms of tissue transglutaminase mediate opposing cellular fates. Proc Natl Acad Sci U S A 103:18609–18614

122. Festoff BW, Santa Cruz K, Arnold PM, Sebastian CT, Davies PJA, Citron BA (2002) Injury-induced 'switch' from GTP-regulated to novel GTP-independent isoform of tissue transglutaminase in the rat spinal cord. J Neurochem 81:708–718

123. Fraij BM, Birckbichler PJ, Patterson MK, Lee KN, Gonzales RA (1992) A Retinoic Acid-inducible mRNA from Human Erythroleukemia Cells Encodes a Novel Tissue Transglutaminase Homologue. J Biol Chem 267:22616–22623

124. Lai T, Liu Y, Li W, Greenberg CS (2007) Identification of two GTP-independent alternatively spliced forms of tissue transglutaminase in human leukocytes, vascular smooth muscle, and endothelial cells. The FASEB Journal 21:4131–4143

125. Tee AEL, Marshall GM, Liu PY, Xu N, Haber M, Norris MD, Iismaa SE, Liu T (2010) Opposing effects of two tissue transglutaminase protein isoforms in neuroblastoma cell differentiation. Journal of Biological Chemistry 285:3561–3567

126. Lesort M, Attanavanich K, Zhang J, Johnson GVW (1998) Distinct nuclear localization and activity of tissue transglutaminase. J Biol Chem 273:11991–11994

127. Piacentini M, D'Eletto M, Farrace MG, Rodolfo C, Del Nonno F, Ippolito G, Falasca L (2014) Characterization of distinct sub-cellular location of transglutaminase type II: changes in intracellular distribution in physiological and pathological states. Cell Tissue Res 358:793

128. Tatsukawa H, Fukaya Y, Frampton G, et al (2009) Role of transglutaminase 2 in liver injury via cross-linking and silencing of transcription factor Sp1. Gastroenterology. https://doi.org/10.1053/J.GASTRO.2009.01.007

129. Mann AP, Verma A, Sethi G, Manavathi B, Wang H, Fok JY, Kunnumakkara AB, Kumar R, Aggarwal BB, Mehta K (2006) Overexpression of tissue transglutaminase leads to constitutive activation of nuclear factor-kappaB in cancer cells: delineation of a novel pathway. Cancer Res 66:8788–8795

130. Xu D, Bai J, Duan Q, Costa M, Dai W (2009) Covalent modifications of histones during mitosis and meiosis. Cell Cycle 8:3688–3694

131. Caccamo D, Currò M, Ferlazzo N, Condello S, Ientile R (2012) Monitoring of transglutaminase 2 under different oxidative stress conditions. Amino Acids 42:1037–1043

132. Piacentini M, Farrace MG, Piredda L, et al (2002) Transglutaminase overexpression sensitizes neuronal cell lines to apoptosis by increasing mitochondrial membrane potential and cellular oxidative stress. J Neurochem 81:1061–1072

133. D'Eletto M, Rossin F, Occhigrossi L, et al (2018) Transglutaminase Type 2 Regulates ER-Mitochondria Contact Sites by Interacting with GRP75. Cell Rep 25:3573-3581.e4

134. Jones RA, Kotsakis P, Johnson TS, Chau DYS, Ali S, Melino G, Griffin M (2005) Matrix changes induced by transglutaminase 2 lead to inhibition of angiogenesis and tumor growth. Cell Death & Differentiation 2006 13:9 13:1442–1453

135. Aeschlimann D, Paulsson M (1991) Cross-linking of laminin-nidogen complexes by tissue transglutaminase: A novel mechanism for basement membrane stabilization. Journal of Biological Chemistry 266:15308–15317

136. Akimov SS, Belkin AM (2001) Cell-surface transglutaminase promotes fibronectin assembly via interaction with the gelatin-binding domain of fibronectin: a role in TGFbeta-dependent matrix deposition. J Cell Sci 114:2989–3000

137. Van Den Akker J, Van Weert A, Afink G, Bakker ENTP, Van Der Pol E, Böing AN, Nieuwland R, VanBavel E (2012) Transglutaminase 2 is secreted from smooth muscle cells by transamidation-dependent microparticle formation. Amino Acids 42:961

138. Furini G, Burhan I, Huang L, Savoca MP, Atobatele A, Johnson T, Verderio EAM (2020) Insights into the heparan sulphate-dependent externalisation of transglutaminase-2 (TG2) in glucose-stimulated proximal-like tubular epithelial cells. Anal Biochem 603:113628

139. Furini G, Schroeder N, Huang L, et al (2018) Proteomic profiling reveals the transglutaminase-2 externalization pathway in kidneys after unilateral ureteric obstruction. Journal of the American Society of Nephrology 29:880–905

140. Chou CY, Streets AJ, Watson PF, Huang L, Verderio EAM, Johnson TS (2011) A crucial sequence for transglutaminase type 2 extracellular trafficking in renal tubular epithelial cells lies in its N-terminal β-sandwich domain. Journal of Biological Chemistry 286:27825–27835

141. Adamczyk M, Griffiths R, Dewitt S, Knäuper V, Aeschlimann D (2015) P2X7 receptor activation regulates rapid unconventional export of transglutaminase-2. J Cell Sci 128:4615–4628

142. Agnihotri N, Mehta K (2016) Transglutaminase-2: evolution from pedestrian protein to a promising therapeutic target. Amino Acids 2016 49:3 49:425–439

143. Yuan L, Siegel M, Choi K, Khosla C, Miller CR, Jackson EN, Piwnica-Worms D, Rich KM (2006) Transglutaminase 2 inhibitor, KCC009, disrupts fibronectin assembly in the extracellular matrix and sensitizes orthotopic glioblastomas to chemotherapy. Oncogene 2007 26:18 26:2563–2573

144. Satpathy M, Cao L, Pincheira R, Emerson R, Bigsby R, Nakshatri H, Matei D (2007) Enhanced peritoneal ovarian tumor dissemination by tissue transglutaminase. Cancer Res 67:7194–7202

145. Shao M, Cao L, Shen C, Satpathy M, Chelladurai B, Bigsby RM, Nakshatri H, Matei D (2009) Epithelial-to-mesenchymal transition and ovarian tumor progression induced by tissue transglutaminase. Cancer Res 69:9192–9201

146. Iacobuzio-Donahue CA, Maitra A, Shen-Ong GL, et al (2002) Discovery of novel tumor markers of pancreatic cancer using global gene expression technology. American Journal of Pathology 160:1239–1249

147. Martinet N, Bonnard L, Regnault V, Picard E, Burke L, Siat J, Grosdidier G, Martinet Y, Vignaud JM (2003) In vivo transglutaminase type 1 expression in normal lung, preinvasive bronchial lesions, and lung cancer. Am J Respir Cell Mol Biol 28:428–435

148. Grigoriev; M Y, Suspitsin; E N, Togo; A V, Pozharisski; K M, Ivanova; O A, Nardacci; R, Falasca; L, Piacentini; M, Imyanitov; E N, Hanson; K P (2001) Tissue transglutaminase expression in breast carcinomas. Journal of Experimental & Clinical Cancer Research 20:265–268

149. Verma A, Guha S, Wang H, Fok JY, Koul D, Abbruzzese J, Mehta K (2008) Tissue Transglutaminase Regulates Focal Adhesion Kinase/AKT Activation by Modulating PTEN Expression in Pancreatic Cancer Cells. Clinical Cancer Research 14:1997–2005

150. Janiak A, Zemskov EA, Belkin AM (2006) Cell surface transglutaminase promotes RhoA activation via integrin clustering and suppression of the Src-p190RhoGAP signaling pathway. Mol Biol Cell 17:1606–1619

151. Fisher ML, Kerr C, Adhikary G, Grun D, Xu W, Keillor JW, Eckert RL (2016) Transglutaminase Interaction with α6/β4-Integrin Stimulates YAP1-Dependent ΔNp63α Stabilization and Leads to Enhanced Cancer Stem Cell Survival and Tumor Formation. Cancer Res 76:7265–7276

152. Condello S, Cao L, Matei D (2013) Tissue transglutaminase regulates β-catenin signaling through a c-Src-dependent mechanism. FASEB J 27:3100–3112

153. Verma A, Wang H, Manavathi B, Fok JY, Mann AP, Kumar R, Mehta K (2006) Increased Expression of Tissue Transglutaminase in Pancreatic Ductal Adenocarcinoma and Its Implications in Drug Resistance and Metastasis. Cancer Res 66:10525–10533

154. Kumar A, Gao H, Xu J, Reuben J, Yu D, Mehta K (2011) Evidence That Aberrant Expression of Tissue Transglutaminase Promotes Stem Cell Characteristics in Mammary Epithelial Cells. PLoS One 6:e20701

155. Mantovani A, Allavena P, Sica A, Balkwill F (2008) Cancer-related inflammation. Nature 2008 454:7203 454:436–444

156. Grivennikov SI, Greten FR, Karin M (2010) Immunity, Inflammation, and Cancer. Cell 140:883–899

157. Balkwill F, Mantovani A (2001) Inflammation and cancer: Back to Virchow? Lancet 357:539–545

158. Bertout J, Thomas-Tikhonenko A (2006) Infection & neoplastic growth 101: The required reading for microbial pathogens aspiring to cause cancer. Cancer Treat Res 130:167–197

159. Verderio EAM, Johnson TS, Griffin M (2005) Transglutaminases in wound healing and inflammation. Prog Exp Tumor Res 38:89–114

160. Verderio EAM, Johnson T, Griffin M (2004) Tissue transglutaminase in normal and abnormal wound healing: Review article. Amino Acids 26:387–404

161. Mehta K, Kumar A, Kim HI (2010) Transglutaminase 2: A multi-tasking protein in the complex circuitry of inflammation and cancer. Biochem Pharmacol 80:1921–1929

162. Quan G, Choi JY, Lee DS, Lee SC (2005) TGF-β1 up-regulates transglutaminase two and fibronectin in dermal fibroblasts: A possible mechanism for the stabilization of tissue inflammation. Arch Dermatol Res 297:84–90

163. Suto N, Ikuras K, Sasaki R (1993) Expression Induced by Interleukin-6 of Tissue-type Transglutaminase in Human Hepatoblastoma HepG2 Cells*. J Biol Chem 268:7469–7473

164. Kumar S, Mehta K (2012) Tissue transglutaminase constitutively activates HIF-1α promoter and nuclear factor-κB via a non-canonical pathway. PLoS One. https://doi.org/10.1371/JOURNAL.PONE.0049321

165. Cordella-Miele E, Miele L, Mukherjee AB (1990) A novel transglutaminase-mediated post-translational modification of phospholipase A2 dramatically increases its catalytic activity. J Biol Chem 265:17180–17188

166. Peng Z, Chang Y, Fan J, Ji W, Su C (2021) Phospholipase A2 superfamily in cancer. Cancer Lett 497:165–177

167. Kumar S, Mehta K (2013) Tissue transglutaminase, inflammation, and cancer: How intimate is the relationship? Amino Acids 44:81–88

168. Kalluri R, Neilson EG (2003) Epithelial-mesenchymal transition and its implications for fibrosis. J Clin Invest 112:1776–1784

169. Thiery JP (2002) Epithelial–mesenchymal transitions in tumour progression. Nature Reviews Cancer 2002 2:6 2:442–454

170. Kalluri R, Zeisberg M (2006) Fibroblasts in cancer. Nature Reviews Cancer 2006 6:5 6:392–401

171. Kumar A, Xu J, Brady S, Gao H, Yu D, Reuben J, Mehta K (2010) Tissue Transglutaminase Promotes Drug Resistance and Invasion by Inducing Mesenchymal Transition in Mammary Epithelial Cells. PLoS One 5:e13390

172. Jeanes A, Gottardi CJ, Yap AS (2008) Cadherins and cancer: how does cadherin dysfunction promote tumor progression? Oncogene 2008 27:55 27:6920–6929

173. Yang J, Weinberg RA (2008) Epithelial-mesenchymal transition: at the crossroads of development and tumor metastasis. Dev Cell 14:818–829

174. Nunes I, Gleizes PE, Metz CN, Rifkin DB (1997) Latent transforming growth factor-beta binding protein domains involved in activation and transglutaminase-dependent cross-linking of latent transforming growth factor-beta. J Cell Biol 136:1151–1163

175. Lai TS, Greenberg CS (2013) TGM2 and implications for human disease: role of alternative splicing. Front Biosci (Landmark Ed) 18:504–519

176. Stetler-Stevenson WG (1996) Dynamics of matrix turnover during pathologic remodeling of the extracellular matrix. Am J Pathol 148:1345

177. Satpathy M, Shao M, Emerson R, Donner DB, Matei D (2009) Tissue transglutaminase regulates matrix metalloproteinase-2 in ovarian cancer by modulating cAMP-response element-binding protein activity. Journal of Biological Chemistry 284:15390–15399

178. Chen S-H, Lin C-Y, Lee L-T, Chang G-D, Lee P-P, Hung C-C, Kao W-T, Tsai P-H, Schally A V, Lee M-T Up-regulation of Fibronectin and Tissue Transglutaminase Promotes Cell Invasion Involving Increased Association with Integrin and MMP Expression in A431 Cells.

179. Kurt-Celep İ, Nihan Kilinc A, Griffin M, Telci D (2022) Nitrosylation of tissue transglutaminase enhances fibroblast migration and regulates MMP activation. Matrix Biology 105:1–16

180. Bose S, Zhang C, Le A (2021) Glucose Metabolism in Cancer: The Warburg Effect and Beyond. Adv Exp Med Biol 1311:3–15

181. Lunt SY, Vander Heiden MG (2011) Aerobic glycolysis: meeting the metabolic requirements of cell proliferation. Annu Rev Cell Dev Biol 27:441–464

182. Yamada K, Miyamoto K (2005) Basic helix-loop-helix transcription factors, BHLHB2 and BHLHB3; their gene expressions are regulated by multiple extracellular stimuli. Front Biosci 10:3151–3171

183. Al-Nedawi K, Meehan B, Micallef J, Lhotak V, May L, Guha A, Rak J (2008) Intercellular transfer of the oncogenic receptor EGFRvIII by microvesicles derived from tumour cells. Nat Cell Biol 10:619–624

184. Nolte'T Hoen ENM, Buermans HPJ, Waasdorp M, Stoorvogel W, Wauben MHM, 'T Hoen PAC (2012) Deep sequencing of RNA from immune cell-derived vesicles uncovers the selective incorporation of small non-coding RNA biotypes with potential regulatory functions. Nucleic Acids Res 40:9272

185. Valadi H, Ekström K, Bossios A, Sjöstrand M, Lee JJ, Lötvall JO (2007) Exosome-mediated transfer of mRNAs and microRNAs is a novel mechanism of genetic exchange between cells. Nature Cell Biology 2007 9:6 9:654–659

186. Skog J, Würdinger T, van Rijn S, Meijer DH, Gainche L, Curry WT, Carter BS, Krichevsky AM, Breakefield XO (2008) Glioblastoma microvesicles transport RNA and proteins that promote tumour growth and provide diagnostic biomarkers. Nat Cell Biol 10:1470–1476

187. Baj-Krzyworzeka M, Szatanek R, Węglarczyk K, Baran J, Urbanowicz B, Brański P, Ratajczak MZ, Zembala M (2006) Tumour-derived microvesicles carry several surface determinants and mRNA of tumour cells and transfer some of these determinants to monocytes. Cancer Immunol Immunother 55:808–818

188. Ratajczak J, Wysoczynski M, Hayek F, Janowska-Wieczorek A, Ratajczak MZ (2006) Membrane-derived microvesicles: important and underappreciated mediators of cell-to-cell communication. Leukemia 2006 20:9 20:1487–1495

189. Paget; S (1989) The distribution of secondary growths in cancer of the breast. Cancer Metastasis Rev 8:98–101

190. Hoshino A, Costa-Silva B, Shen TL, et al (2015) Tumour exosome integrins determine organotropic metastasis. Nature 2015 527:7578 527:329–335

191. Fraij BM, Gonzales RA (1996) A third human tissue transglutaminase homologue as a result of alternative gene transcripts. Biochimica et Biophysica Acta (BBA) - Gene Structure and Expression 1306:63–74

192. Bianchi N, Beninati S, Bergamini CM (2018) Spotlight on the transglutaminase 2 gene: a focus on genomic and transcriptional aspects. Biochem J 475:1643–1667

193. Nezir AE, Ulukan B, Telci D (2019) Transglutaminase 2: The Maestro of the Oncogenic Mediators in Renal Cell Carcinoma. Med Sci (Basel) 7:24

194. Fraij BM (1996) GTP hydrolysis by human tissue transglutaminase homologue. Biochem Biophys Res Commun 218:45–49

195. Yong C, Arnold PM, Zoubine MN, Citron BA, Watanabe I, Berman NEJ, Festoff BW (1998) Apoptosis in cellular compartments of rat spinal cord after severe contusion injury. J Neurotrauma 15:459–472

196. Kojima S, Kuo TF, Tatsukawa H (2012) Regulation of transglutaminase-mediated hepatic cell death in alcoholic steatohepatitis and non-alcoholic steatohepatitis. Journal of Gastroenterology and Hepatology (Australia) 27:52–57

197. Tee AEL, Marshall GM, Liu PY, Xu N, Haber M, Norris MD, Iismaa SE, Liu T (2010) Opposing effects of two tissue transglutaminase protein isoforms in neuroblastoma cell differentiation. J Biol Chem 285:3561–3567

198. Citron BA, Suo Z, SantaCruz K, Davies PJA, Qin F, Festoff BW (2002) Protein crosslinking, tissue transglutaminase, alternative splicing and neurodegeneration. Neurochem Int 40:69–78

199. Sestito C, Brevé JJP, Killestein J, Teunissen CE, Wilhelmus MMM, Drukarch B, van Dam AM (2018) Differential Expression of Tissue Transglutaminase Splice Variants in Peripheral Blood Mononuclear Cells of Primary Progressive Multiple Sclerosis Patients. Med Sci (Basel). https://doi.org/10.3390/MEDSCI6040108

200. Currò M, Ferlazzo N, Risitano R, Condello S, Vecchio M, Caccamo D, Ientile R (2014) Transglutaminase 2 and phospholipase $A_2$ interactions in the inflammatory response in human Thp-1 monocytes. Amino Acids 46:759–766

201. Kalyvas A, David S (2004) Cytosolic Phospholipase A2 Plays a Key Role in the Pathogenesis of Multiple Sclerosis-like Disease. Neuron 41:323–335

202. David CJ, Manley JL (2010) Alternative pre-mRNA splicing regulation in cancer: pathways and programs unhinged. Genes Dev 24:2343

203. Phatak VM, Croft SM, Rameshaiah Setty SG, Scarpellini A, Hughes DC, Rees R, McArdle S, Verderio EAM (2013) Expression of transglutaminase-2 isoforms in normal human tissues and cancer cell lines: Dysregulation of alternative splicing in cancer. Amino Acids 44:33–44

204. Kumar A, Xu J, Sung B, Kumar S, Yu D, Aggarwal BB, Mehta K (2012) Evidence that GTP-binding domain but not catalytic domain of transglutaminase 2 is essential for epithelial-to-mesenchymal transition in mammary epithelial cells. Breast Cancer Res. https://doi.org/10.1186/BCR3085

205. Calvert NWJ; D;, Gates EWJ, Calvert ND, et al (2023) Cell-Impermeable Inhibitors Confirm That Intracellular Human Transglutaminase 2 Is Responsible for the Transglutaminase-Associated Cancer Phenotype. International Journal of Molecular Sciences 2023, Vol 24, Page 12546 24:12546

206. Verma A, Mehta K (2007) Tissue transglutaminase-mediated chemoresistance in cancer cells. Drug Resistance Updates 10:144–151

207. Siegel RL, Miller KD, Wagle NS, Jemal A (2023) Cancer statistics, 2023. CA Cancer J Clin 73:17–48

208. Ferlay J, Soerjomataram I, Dikshit R, Eser S, Mathers C, Rebelo M, Parkin DM, Forman D, Bray F (2015) Cancer incidence and mortality worldwide: Sources, methods and major patterns in GLOBOCAN 2012. Int J Cancer 136:E359–E386

209. Montironi R, Cheng L, Scarpelli M, Lopez-Beltran A (2016) Pathology and Genetics: Tumours of the Urinary System and Male Genital System: Clinical Implications of the 4th Edition of the WHO Classification and Beyond. Eur Urol 70:120–123

210. JN E, G S, J E, I S (eds) (2004) Pathology and Genetics of Tumours of the Urinary System and Male Genital Organs. IARC

211. Li M, Li L, Zheng J, Li Z, Li S, Wang K, Chen X (2023) Liquid biopsy at the frontier in renal cell carcinoma: recent analysis of techniques and clinical application. Molecular Cancer 2023 22:1 22:1–51

212. Rini BI, Campbell SC, Escudier B (2009) Renal cell carcinoma. The Lancet 373:1119–1132

213. Hsieh JJ, Manley BJ, Khan N, Gao JJ, Carlo MI, Cheng EH (2017) Overcome tumor heterogeneity-imposed therapeutic barriers through convergent genomic biomarker discovery: A braided cancer river model of kidney cancer. Semin Cell Dev Biol 64:98–106

214. Meskawi M, Sun M, Trinh QD, et al (2012) A review of integrated staging systems for renal cell carcinoma. Eur Urol 62:303–314

215. Thun MJ, Linet MS, Cerhan JR, Haiman C, Schottenfeld D (2017) Cancer Epidemiology and Prevention. Schottenfeld and Fraumeni Cancer Epidemiology and Prevention, Fourth Edition 1–1308

216. Haas NB, Nathanson KL (2014) Hereditary Kidney Cancer Syndromes. Adv Chronic Kidney Dis 21:81–90

217. Karami S, Schwartz K, Purdue MP, Davis FG, Ruterbusch JJ, Munuo SS, Wacholder S, Graubard BI, Colt JS, Chow WH (2010) Family history of cancer and renal cell cancer risk in Caucasians and African Americans. British Journal of Cancer 2010 102:11 102:1676–1680

218. Gnarra JR, Tory K, Weng Y, et al (1994) Mutations of the VHL tumour suppressor gene in renal carcinoma. Nature Genetics 1994 7:1 7:85–90

219. Lee CH, Hötker AM, Voss MH, Feldman DR, Woo KM, Patil S, Coskey DT, Akin O, Hsieh JJ, Motzer RJ (2016) Bevacizumab Monotherapy as Salvage Therapy for Advanced Clear Cell Renal Cell Carcinoma Pretreated with Targeted Drugs. Clin Genitourin Cancer 14:56–62

220. Battelli C, Cho DC (2011) mTOR inhibitors in renal cell carcinoma. Therapy 8:359

221. Hidaka H, Seki N, Yoshino H, Yamasaki T, Yamada Y, Nohata N, Fuse M, Nakagawa M, Enokida H (2012) Tumor suppressive microRNA-1285 regulates novel molecular targets: aberrant expression and functional significance in renal cell carcinoma. Oncotarget 3:44–57

222. Erdem S, Yegen G, Telci D, Yildiz I, Tefik T, Issever H, Kilicaslan I, Sanli O (2015) The increased transglutaminase 2 expression levels during initial tumorigenesis predict increased risk of metastasis and decreased disease-free and cancer-specific survivals in renal cell carcinoma. World J Urol 33:1553–1560

223. Jee Park M, Baek HW, Rhee YY, Lee C, Park JW, Kim HW, Moon KC (2015) Transglutaminase 2 Expression and Its Prognostic Significance in Clear Cell Renal Cell Carcinoma. J Pathol Transl Med 49:37

224. Bagatur Y, Ilter Akulke AZ, Bihorac A, Erdem M, Telci D (2018) Tissue transglutaminase expression is necessary for adhesion, metastatic potential and cancer stemness of renal cell carcinoma. Cell Adh Migr 12:138–151

225. Ku BM, Kim DS, Kim KH, Yoo BC, Kim SH, Gong YD, Kim SY (2013) Transglutaminase 2 inhibition found to induce p53 mediated apoptosis in renal cell carcinoma. FASEB J 27:3487–3495

226. Fuhrman SA, Lasky LC, Limas C (1982) Prognostic significance of morphologic parameters in renal cell carcinoma. Am J Surg Pathol 6:655–663

227. Delahunt B, Eble JN, Egevad L, Samaratunga H (2019) Grading of renal cell carcinoma. Histopathology 74:4–17

228. Dagher J, Delahunt B, Rioux-Leclercq N, et al (2017) Clear cell renal cell carcinoma: validation of World Health Organization/International Society of Urological Pathology grading. Histopathology 71:918–925

229. Delahunt B, Egevad L, Samaratunga H, Martignoni G, Nacey JN, Srigley JR (2016) Gleason and Fuhrman no longer make the grade. Histopathology 68:475–481

230. Delahunt B, Sika-Paotonu D, Bethwaite PB, McCredie MRE, Martignoni G, Eble JN, William Jordan T (2007) Fuhrman grading is not appropriate for chromophobe renal cell carcinoma. Am J Surg Pathol 31:957–960

231. Sika-Paotonu D, Bethwaite PB, McCredie MRE, William Jordan T, Delahunt B (2006) Nucleolar grade but not Fuhrman grade is applicable to papillary renal cell carcinoma. Am J Surg Pathol 30:1091–1096

232. Delahunt B, Sika-Paotonu D, Bethwaite PB, William Jordan T, Magi-Galluzzi C, Zhou M, Samaratunga H, Srigley JR (2011) Grading of clear cell renal cell carcinoma should be based on nucleolar prominence. Am J Surg Pathol 35:1134–1139

233. Humphrey PA, Moch H, Cubilla AL, Ulbright TM, Reuter VE (2016) The 2016 WHO Classification of Tumours of the Urinary System and Male Genital Organs-Part B: Prostate and Bladder Tumours. Eur Urol 70:106–119

234. Moch H, Amin MB, Berney DM, et al (2022) The 2022 World Health Organization Classification of Tumours of the Urinary System and Male Genital Organs-Part A: Renal, Penile, and Testicular Tumours. Eur Urol 82:458–468

235. Delahunt B, McKenney JK, Lohse CM, Leibovich BC, Thompson RH, Boorjian SA, Cheville JC (2013) A novel grading system for clear cell renal cell carcinoma incorporating tumor necrosis. Am J Surg Pathol 37:311–322

236. Rosen R, Sapra A (2023) TNM Classification. StatPearls. https://doi.org/10.1016/B978-0-323-66127-0.00047-8

237. Ridge CA, Pua BB, Madoff DC (2014) Epidemiology and staging of renal cell carcinoma. Semin Intervent Radiol 31:3–8

238. Sun R, Zhao S, Jiang H, Jiang H, Dai Y, Zhang C, Wang S (2021) Imaging Tool for Predicting Renal Clear Cell Carcinoma Fuhrman Grade: Comparing R.E.N.A.L. Nephrometry Score and CT Texture Analysis. Biomed Res Int. https://doi.org/10.1155/2021/1821876

239. Cohen HT, McGovern FJ (2005) Renal-Cell Carcinoma. https://doi.org/101056/NEJMra043172 353:2477–2490

240. Minotti L, Baldassari F, Galasso M, Volinia S, Bergamini CM, Bianchi N (2018) A long non-coding RNA inside the type 2 transglutaminase gene tightly correlates with the expression of its transcriptional variants. Amino Acids 50:421–438

241. Valletti A, Gigante M, Palumbo O, et al (2013) Genome-Wide Analysis of Differentially Expressed Genes and Splicing Isoforms in Clear Cell Renal Cell Carcinoma. PLoS One 8:e78452

242. Wieser M, Stadler G, Jennings P, Streubel B, Pfaller W, Ambros P, Riedl C, Katinger H, Grillari J, Grillari-Voglauer R (2008) hTERT alone immortalizes epithelial cells of renal proximal tubules without changing their functional characteristics. Am J Physiol Renal Physiol. https://doi.org/10.1152/AJPRENAL.90405.2008

243. Johnson TS, Griffin M, Thomas GL, et al (1997) The Role of Transglutaminase in the Rat Subtotal Nephrectomy Model of Renal Fibrosis glutamyl) lysine • tubule • scarring • subtotal nephrectomy. J Clin Invest 99:2950–2960

244. Johnson TS, El-Koraie AF, Skill NJ, Baddour NM, El Nahas AM, Njloma M, Adam AG, Griffin M (2003) Tissue transglutaminase and the progression of human renal scarring. Journal of the American Society of Nephrology 14:2052–2062

245. Johnson TS, Fisher M, Haylor JL, et al (2007) Transglutaminase inhibition reduces fibrosis and preserves function in experimental chronic kidney disease. Journal of the American Society of Nephrology 18:3078–3088

246. Erdem M, Erdem S, Sanli O, Sak H, Kilicaslan I, Sahin F, Telci D (2014) Up-regulation of TGM2 with ITGB1 and SDC4 is important in the development and metastasis of renal cell carcinoma. Urologic Oncology: Seminars and Original Investigations 32:25.e13-25.e20

247. Ulukan B, Bihorac A, Sipahioglu T, Kiraly R, Fesus L, Telci D (2020) Role of tissue transglutaminase catalytic and guanosine triphosphate-binding domains in renal cell carcinoma progression. ACS Omega 5:28273–28284

248. Hanahan D (2022) Hallmarks of Cancer: New Dimensions. Cancer Discov 12:31–46

249. Schwerk C, Schulze-Osthoff K (2005) Regulation of apoptosis by alternative pre-mRNA splicing. Mol Cell 19:1–13

250. Mihaly Z, Sztupinszki Z, Surowiak P, Gyorffy B (2012) A Comprehensive Overview of Targeted Therapy in Metastatic Renal Cell Carcinoma. Curr Cancer Drug Targets 12:857

251. Tatsukawa H, Furutani Y, Hitomi K, Kojima S (2016) Transglutaminase 2 has opposing roles in the regulation of cellular functions as well as cell growth and death. Cell Death & Disease 2016 7:6 7:e2244–e2244

252. Vogel R, Amar L, Thi A Do, Saillour P, Mallet J (2004) A single lentivirus vector mediates doxycycline-regulated expression of transgenes in the brain. Hum Gene Ther 15:157–165

253. Benabdellah K, Cobo M, Muñoz P, Toscano MG, Martin F (2011) Development of an All-in-One Lentiviral Vector System Based on the Original TetR for the Easy Generation of Tet-ON Cell Lines. PLoS One 6:e23734

254. Cunha; Burke A, Sibley; Carol M, Ristuccia; Angela M (1982) Doxycycline. Ther Drug Monit 4:115–135

255. Kalidasan V, Ng WH, Ishola OA, Ravichantar N, Tan JJ, Das KT (2021) A guide in lentiviral vector production for hard-to-transfect cells, using cardiac-derived c-kit expressing cells as a model system. Scientific Reports 2021 11:1 11:1–11

256. Wurm M, Schambach A, Lindemann D, Hanenberg H, Ständker L, Forssmann W-G, Blasczyk R, Horn PA (2010) The influence of semen-derived enhancer of virus infection on the efficiency of retroviral gene transfer. J Gene Med 12:137–146

257. Cornetta K, Anderson WF (1989) Protamine sulfate as an effective alternative to polybrene in retroviral-mediated gene-transfer: implications for human gene therapy. J Virol Methods 23:187–194

258. Lin P, Lin Y, Lennon DP, Correa D, Schluchter M, Caplan AI (2012) Efficient Lentiviral Transduction of Human Mesenchymal Stem Cells That Preserves Proliferation and Differentiation Capabilities. Stem Cells Transl Med 1:886

259. Balak JRA, de Graaf N, Zaldumbide A, Rabelink TJ, Hoeben RC, de Koning EJP, Carlotti F (2019) Highly efficient ex vivo lentiviral transduction of primary human pancreatic exocrine cells. Scientific Reports 2019 9:1 9:1–10

260. Pay SL, Qi X, Willard JF, et al (2018) Improving the Transduction of Bone Marrow-Derived Cells with an Integrase-Defective Lentiviral Vector. Hum Gene Ther Methods 29:44–59

261. Calikoglu Koyuncu AC, Nayman AH, Telci D, Torun Kose G (2020) Tissue transglutaminase_variant 2-transduced mesenchymal stem cells and their chondrogenic potential. Biotechnol Bioeng 117:1839–1852

262. Elegheert J, Behiels E, Bishop B, et al (2018) Lentiviral transduction of mammalian cells for fast, scalable and high-level production of soluble and membrane proteins. Nat Protoc 13:2991–3017

263. de Campos RP, Wink MR, Lenz G (2021) ENTPD5: identification of splicing variants and their impact on cancer survival. Purinergic Signal 17:467–480

264. Shi J (2014) Regulatory networks between neurotrophins and miRNAs in brain diseases and cancers. Acta Pharmacologica Sinica 2015 36:2 36:149–157

265. Wei W, Ji L, Duan W, Zhu J (2021) Circular RNA circ_0081001 knockdown enhances methotrexate sensitivity in osteosarcoma cells by regulating miR-494-3p/TGM2 axis. J Orthop Surg Res 16:1–12

266. Cellura D, Pickard K, Quaratino S, Parker H, Strefford JC, Thomas GJ, Mitter R, Mirnezami AH, Peake NJ (2015) miR-19-Mediated Inhibition of Transglutaminase-2 Leads to Enhanced Invasion and Metastasis in Colorectal Cancer. Mol Cancer Res 13:1095–1105

267. Charrier S, Ferrand M, Zerbato M, Précigout G, Viornery A, Bucher-Laurent S, Benkhelifa-Ziyyat S, Merten OW, Perea J, Galy A (2010) Quantification of lentiviral vector copy numbers in individual hematopoietic colony-forming cells shows vector dose-dependent effects on the frequency and level of transduction. Gene Therapy 2011 18:5 18:479–487

268. Corre G, Seye A, Frin S, Ferrand M, Winkler K, Luc C, Dorange F, Rocca CJ, Galy A (2022) Lentiviral standards to determine the sensitivity of assays that quantify lentiviral vector copy numbers and genomic insertion sites in cells. Gene Therapy 2022 29:9 29:536–543

269. Fraij BM (2015) The 55 kDa tissue transglutaminase cross-linking active isoform TG induces cell death. Mol Carcinog 54:720–729

270. Cardoso I, Østerlund EC, Stamnaes J, Iversen R, Andersen JT, Jørgensen TJD, Sollid LM (2017) Dissecting the interaction between transglutaminase 2 and fibronectin. Amino Acids 49:489–500

271. Arbildi P, Rodríguez-Camejo C, Perelmuter K, Bollati-Fogolín M, Sóñora C, Hernández A (2022) Hypoxia and inflammation conditions differentially affect the expression of tissue transglutaminase spliced variants and functional properties of extravillous trophoblast cells. Am J Reprod Immunol. https://doi.org/10.1111/AJI.13534

272. Aguiari G, Crudele F, Taccioli C, et al (2022) Dysregulation of Transglutaminase type 2 through GATA3 defines aggressiveness and Doxorubicin sensitivity in breast cancer. Int J Biol Sci 18:1–14

273. Li B, Antonyak MA, Druso JE, Cheng L, Nikitin AY, Cerione RA (2010) EGF potentiated oncogenesis requires a tissue transglutaminase-dependent signaling pathway leading to Src activation. Proc Natl Acad Sci U S A 107:1408–1413

274. Mihalopoulos M, Dovey Z, Archer MR, et al (2020) Repurposing of α1-Adrenoceptor Antagonists: Impact in Renal Cancer. Cancers (Basel) 12:1–11

275. Nadalutti C, Viiri KM, Kaukinen K, Mäki M, Lindfors K (2011) Extracellular transglutaminase 2 has a role in cell adhesion, whereas intracellular transglutaminase 2 is involved in regulation of endothelial cell proliferation and apoptosis. Cell Prolif 44:49–58

276. de Carcer G, Perez de Castro I, Malumbres M (2007) Targeting Cell Cycle Kinases for Cancer Therapy. Curr Med Chem 14:969–985

277. Huber MA, Azoitei N, Baumann B, Grünert S, Sommer A, Pehamberger H, Kraut N, Beug H, Wirth T (2004) NF-kappaB is essential for epithelial-mesenchymal transition and metastasis in a model of breast cancer progression. J Clin Invest 114:569–581

278. Van Roy F, Berx G (2008) The cell-cell adhesion molecule E-cadherin. Cellular and Molecular Life Sciences 65:3756–3788

279. Gonzalez DM, Medici D (2014) Signaling mechanisms of the epithelial-mesenchymal transition. Sci Signal 7:re8

280. Brabletz T, Kalluri R, Nieto MA, Weinberg RA (2018) EMT in cancer. Nat Rev Cancer 18:128–134

281. Zheng X, Carstens JL, Kim J, Scheible M, Kaye J, Sugimoto H, Wu CC, Lebleu VS, Kalluri R (2015) Epithelial-to-mesenchymal transition is dispensable for metastasis but induces chemoresistance in pancreatic cancer. Nature 527:525–530

282. Caramel J, Papadogeorgakis E, Hill L, et al (2013) A switch in the expression of embryonic EMT-inducers drives the development of malignant melanoma. Cancer Cell 24:466–480

283. Denecker G, Vandamme N, Akay Ö, et al (2014) Identification of a ZEB2-MITF-ZEB1 transcriptional network that controls melanogenesis and melanoma progression. Cell Death Differ 21:1250–1261

284. Telci D, Collighan RJ, Basaga H, Griffin M (2009) Increased TG2 expression can result in induction of transforming growth factor beta1, causing increased synthesis and deposition of matrix proteins, which can be regulated by nitric oxide. J Biol Chem 284:29547–29558

285. Zuo JH, Zhu W, Li MY, et al (2011) Activation of EGFR promotes squamous carcinoma SCC10A cell migration and invasion via inducing EMT-like phenotype change and MMP-9-mediated degradation of E-cadherin. J Cell Biochem 112:2508–2517

286. Dong C, Wu Y, Yao J, Wang Y, Yu Y, Rychahou PG, Evers BM, Zhou BP (2012) G9a interacts with Snail and is critical for Snail-mediated E-cadherin repression in human breast cancer. J Clin Invest 122:1469–1486

287. Mahmoudian RA, Gharaie ML, Abbaszadegan MR, Alasti A, Forghanifard MM, Mansouri A, Gholamin M (2021) Crosstalk between MMP-13, CD44, and TWIST1 and its role in regulation of EMT in patients with esophageal squamous cell carcinoma. Mol Cell Biochem 476:2465–2478

# APPENDIX A: ETHICAL APPROVAL FORM

**S.B. İSTANBUL MEDENİYET ÜNİVERSİTESİ GÖZTEPE EĞİTİM VE ARAŞTIRMA HASTANESİ**
**KLİNİK ARAŞTIRMALARI ETİK KURULU (2013-KAEK-64)**
**KARAR FORMU**

Tarih: 01.07.2020

SAYI:

KONU: Etik Kurulu Kararı

| | |
|---|---|
| ARAŞTIRMANIN AÇIK ADI | Yüksek ve Düşük Evreli Renal Hücreli Karsinomda Doku Transglutaminazı İzoformlarının İfadesi |
| VARSA ARAŞTIRMANIN PROTOKOL KODU | |

| ETİK KURUL BİLGİLERİ | | |
|---|---|---|
| | ETİK KURULUN ADI | S.B. İstanbul Medeniyet Üniversitesi Göztepe Eğitim ve Araştırma Hastanesi Klinik Araştırmalar Etik Kurulu |
| | AÇIK ADRESİ: | Doktor Erkin Cad. İstanbul Medeniyet Üniversitesi Göztepe Eğitim ve Araştırma Hastanesi |
| | TELEFON | 216 570 91 90 |
| | FAKS | 216 565 55 26 |
| | E-POSTA | etik@sbgoztepehastanesi.gov.tr |

| BAŞVURU BİLGİLERİ | | |
|---|---|---|
| | KOORDİNATÖR/SORUMLU ARAŞTIRMACI UNVANI/ADI/SOYADI | Prof. Dr. Asıf Yıldırım- Prof. Dr. Dilek Telci Temeltaş |
| | KOORDİNATÖR/SORUMLU ARAŞTIRMACININ UZMANLIK ALANI | Üroloji-Moleküler Hücre Biyolojisi |
| | KOORDİNATÖR/SORUMLU ARAŞTIRMACININ BULUNDUĞU MERKEZ | İstanbul Medeniyet Üniversitesi Göztepe Eğitim ve Araştırma Hastanesi<br>Yeditepe Üniversitesi |
| | VARSA İDARİ SORUMLU UNVANI/ADI/SOYADI | |
| | DESTEKLEYİCİ | |
| | PROJE YÜRÜTÜCÜSÜ UNVANI/ADI/SOYADI (TÜBİTAK vb. gibi kaynaklardan destek alanlar için) | |
| | DESTEKLEYİCİNİN YASAL TEMSİLCİSİ | |
| | ARAŞTIRMANIN FAZI VE TÜRÜ | FAZ 1 ☐<br>FAZ 2 ☐<br>FAZ 3 ☐<br>FAZ 4 ☐<br>Gözlemsel ilaç çalışması ☐<br>Tıbbi cihaz klinik araştırması ☐<br>İn vitro tıbbi tanı cihazları ile yapılan performans değerlendirme çalışmaları ☐<br>İlaç dışı klinik araştırma ☒<br>Retrospektif ☐ |
| | ARAŞTIRMAYA KATILAN MERKEZLER | TEK MERKEZ ☐ ÇOK MERKEZLİ ☒ ULUSAL ☐ ULUSLARARASI ☐ |

| DEĞERLENDİRİLEN BELGELER | Belge Adı | Tarihi | Versiyon Numarası | Dili |
|---|---|---|---|---|
| | ARAŞTIRMA PROTOKOLÜ | | | Türkçe ☐ İngilizce ☐ Diğer ☐ |
| | BİLGİLENDİRİLMİŞ GÖNÜLLÜ OLUR FORMU | | | Türkçe ☒ İngilizce ☐ Diğer ☐ |
| | OLGU RAPOR FORMU | | | Türkçe ☐ İngilizce ☐ Diğer ☐ |
| | ARAŞTIRMA BROŞÜRÜ | | | Türkçe ☐ İngilizce ☐ Diğer ☐ |

| DEĞERLENDİRİLEN DİĞER BELGELER | Belge Adı | | Açıklama |
|---|---|---|---|
| | SİGORTA | ☐ | |
| | ARAŞTIRMA BÜTÇESİ | ☐ | |
| | BİYOLOJİK MATERYEL TRANSFER FORMU | ☐ | |
| | İLAN | ☐ | |
| | YILLIK BİLDİRİM | ☐ | |
| | SONUÇ RAPORU | ☐ | |
| | GÜVENLİLİK BİLDİRİMLERİ | ☐ | |
| | DİĞER: | ☐ | |

| KARAR BİLGİLERİ | | |
|---|---|---|
| | **Karar No: 2020/0423** | **Tarih: 01.07.2020** |
| | Yukarıda bilgileri verilen başvuru dosyası ile ilgili belgeler araştırmanın/çalışmanın gerekçe, amaç, yaklaşım ve yöntemleri dikkate alınarak incelenmiş ve uygun bulunmuş olup araştırmanın/çalışmanın başvuru dosyasında belirtilen merkezlerde gerçekleştirilmesinde etik ve bilimsel sakınca bulunmadığına toplantıya katılan etik kurul üye tam sayısının salt çoğunluğu ile karar verilmiştir.<br>İlaç ve Biyolojik Ürünlerin Klinik Araştırmaları Hakkında Yönetmelik kapsamında yer alan araştırmalar/çalışmalar için Türkiye İlaç ve Tıbbi Cihaz Kurumu'ndan izin alınması gerekmektedir. | |

Etik Kurul Başkanı
Unvanı/Adı/Soyadı
İmza:

**S.B. İSTANBUL MEDENİYET ÜNİVERSİTESİ GÖZTEPE EĞİTİM VE ARAŞTIRMA HASTANESİ**
**KLİNİK ARAŞTIRMALARI ETİK KURULU (2013-KAEK-64)**
**KARAR FORMU**

SAYI: Tarih: 01.07.2020

KONU: Etik Kurulu Kararı

| | |
|---|---|
| ARAŞTIRMANIN AÇIK ADI | Yüksek ve Düşük Evreli Renal Hücreli Karsinomda Doku Transglutaminazı İzoformlarının İfadesi |
| VARSA ARAŞTIRMANIN PROTOKOL KODU | |

| KLİNİK ARAŞTIRMALAR ETİK KURULU | |
|---|---|
| **ETİK KURULUN ÇALIŞMA ESASI** | İlaç ve Biyolojik Ürünlerin Klinik Araştırmaları Hakkında Yönetmelik, İyi Klinik Uygulamaları Kılavuzu |
| **BAŞKANIN UNVANI / ADI / SOYADI:** | |

| Unvanı/Adı/Soyadı | Uzmanlık Alanı | Kurumu | Cinsiyet | | Araştırma ile ilişki | | Katılım * | | İmza |
|---|---|---|---|---|---|---|---|---|---|
| Doç. Dr. Şükrü Sadık ÖNER | Tıbbi Farmakoloji | S.B. İstanbul Medeniyet Üniversitesi Göztepe Eğitim ve Araştırma Hastanesi | E☐ | K☐ | E☐ | H☐ | E☐ | H☐ | |
| Prof. Dr. Aytekin OĞUZ | İç Hastalıkları Anabilim Dalı | S.B. İstanbul Medeniyet Üniversitesi Göztepe Eğitim ve Araştırma Hastanesi | E☐ | K☐ | E☐ | H☐ | E☐ | H☐ | |
| Prof. Dr. Işıl MARAL | Halk Sağlığı Anabilim Dalı | S.B. İstanbul Medeniyet Üniversitesi Göztepe Eğitim ve Araştırma Hastanesi | E☐ | K☐ | E☐ | H☐ | E☐ | H☐ | |
| Prof. Dr. Asıf Yıldırım | Üroloji | S.B. İstanbul Medeniyet Üniversitesi Göztepe Eğitim ve Araştırma Hastanesi | E☐ | K☐ | E☐ | H☐ | E☐ | H☐ | |
| Prof. Dr. Süleyman Daşdağ | Biyofizik | S.B. İstanbul Medeniyet Üniversitesi Göztepe Eğitim ve Araştırma Hastanesi | E☐ | K☐ | E☐ | H☐ | E☐ | H☐ | |
| Prof. Dr. Derya Büyükkayhan | Çocuk Sağlığı ve Hastalıkları Anabilim Dalı | T.C. Sağlık Bakanlığı Zeynep Kamil Kadın ve Çocuk Hastalıkları Eğitim ve Araştırma Hastanesi | E☐ | K☐ | E☐ | H☐ | E☐ | H☐ | |
| Doç. Dr. Asiye KANBAY | Göğüs Hastalıkları Anabilim Dalı | S.B. İstanbul Medeniyet Üniversitesi Göztepe Eğitim ve Araştırma Hastanesi | E☐ | K☐ | E☐ | H☐ | E☐ | H☐ | |
| Doç. Dr. Sıdıka Şeyma ÖZKANLI | Tıbbi Patoloji | S.B. İstanbul Medeniyet Üniversitesi Göztepe Eğitim ve Araştırma Hastanesi | E☐ | K☐ | E☐ | H☐ | E☐ | H☐ | |
| Dr. Öğr. Üyesi Hacer Hicran Mutlu | Aile Hekimliği | S.B. İstanbul Medeniyet Üniversitesi Göztepe Eğitim ve Araştırma Hastanesi | E☐ | K☐ | E☐ | H☐ | E☐ | H☐ | |
| Uzm. Dr. Ergül Demirçivi Bör | Kadın Hastalıkları ve Doğum | S.B. İstanbul Medeniyet Üniversitesi Göztepe Eğitim ve Araştırma Hastanesi | E☐ | K☐ | E☐ | H☐ | E☐ | H☐ | |
| Avukat Mahmut ÇELİK | Avukat | Çelik Hukuk Bürosu | E☐ | K☐ | E☐ | H☐ | E☐ | H☐ | |
| Saliha Şahin | İşçi | | E☐ | K☐ | E☐ | H☐ | E☐ | H☐ | |

*:Toplantıda Bulunma

**Karar:** ☒ Onaylandı ☐ Reddedildi

Etik Kurul Başkanının
Unvanı/Adı/Soyadı:
İmza: